The Advancement of Palladium-Catalyzed Decarboxylative and Desulfinative Cross-Couplings

Daniel Mangel

A Thesis

in

The Department

of

Chemistry and Biochemistry

Presented in Partial Fulfillment of the Requirements

for the Degree of Master of Science (Chemistry) at

Concordia University

Montreal, Quebec, Canada

May, 2016

©Daniel Mangel

CONCORDIA UNIVERSITY

School of Graduate Studies School of Graduate Studies

This is to certify that the thesis prepared

By: Daniel Mangel

Entitled: The Advancement of Palladium-Catalyzed Decarboylative and Desulfinative Cross-Couplings

and submitted in partial fulfillment of the requirements for the degree of

Master of Science (Chemistry)

complies with the regulations of the University and meets the accepted standards with

respect to originality and quality.

Signed by the final examining committee:

       (Chair) Dr. Gilles Peslherbe

       (Examiner) Dr. John Capobianco

       (Examiner) Dr. Xavier Ottenwaelder

       (Supervisor) Dr. Pat Forgione

Approved by

_____

Chair of Department or Graduate Program Director

_____

Dean of Faculty

Date 08-30-2016

Abstract

The Advancement of Palladium-Catalyzed Decarboxylative and Desulfinative Cross-Couplings

Daniel Mangel

Concordia University, 2016
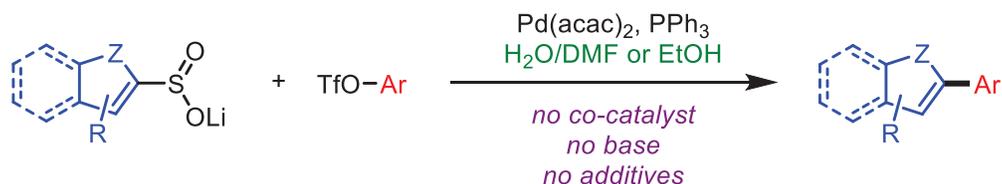
Aryl-substituted heteroaromatics play a key role in medicinal chemistry, natural products, advanced materials, and the agrochemical industry. Therefore, developing novel methods to access these scaffolds is of the upmost importance. The most common methods to access these scaffolds are through palladium-catalyzed cross-coupling reactions. Classically, these methods used harsh conditions and dangerous organometallic compounds; however, more recently an emphasis on using less harsh conditions and environmentally safe compounds has pushed towards developing novel methodologies. Palladium-catalyzed desulfinative and decarboxylative cross-couplings have emerged as powerful alternatives to the classical methods, yielding environmentally benign by-products with high atom economy and great efficiency. These methods use carboxylic acids and sulfonates as nucleophilic coupling partners with aryl-halides as the electrophilic partner.

To expand the desulfinative methodology, synthetically versatile aryl triflates have been employed as electrophilic coupling partners. Good yields were obtained in aqueous and alcoholic media without the use of base, additives, or co-catalysts. Furthermore, mechanistic studies on the decarboxylative cross-coupling have been investigated using computational methods. Density

functional theory (DFT) was used to determine the complete reaction profile as well as transition states. It was determined that the key decarboxylation step occurs via an electrophilic aromatic substitution reaction. These results are important for the development of alternative methods and the advancement of our current understanding of these methodologies.
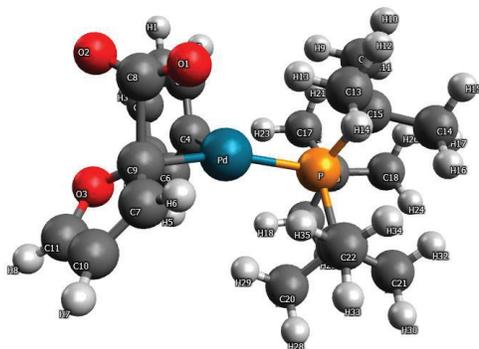
Acknowledgements

First and foremost, I would like to thank Dr. Pat Forgione for all the help and guidance he has giving me over the last few years. You have not only taught me how to be a professional in the organic chemistry world but you have taught me many valuable life lessons. Pat you have been a great mentor and I will never forget my time at the Forgione lab.

I would like to also thank my committee members Dr. John Capobianco and Dr. Xavier Ottenwaelder for all the advice and help you have given me.

I also greatly appreciate the help of Fei Chen and Franklin Chacon Huete for helping me proof read this document. It has been a tremendous pleasure working will all the members, past and present of the Forgione group.

I have spent many years at Concordia and I am greatly appreciative of all the faculty and staff of the chemistry and biochemistry department. You all have been amazing and I will be eternally grateful.

Contributions of Authors

The contribution of authors for chapter two of this thesis which was publish in Heterocycles (DOI: 10.3987/COM-14-S(K)104) is listed below:

Efficient Desulfinative Cross-Coupling of Heteroaromatic Sulfinates with Aryl Triflate in Environmentally Friendly Protic Solvents

Daniel Mangel	Synthesis, optimization, purification, and charactorization of compounds. Writing of manuscript, references, and revision.
Cindy Buonomano	Synthesis of precursors and characterization. Revision.
Stephan Sevigny	Optimization using DMF.
Gianna Di Censo and Gowsic Thevendran	Preliminary Results.
Pat Forgione	Supervisor. Revision.

Table of Contents

Index of Tables

Chapter 1 – Introduction

1.1 Importance of Aryl Substituted Heteroaromatics

X = NR, O, S
Y = N, CH
Z = N, CH
n = 1, 2

Figure 1 - Aryl-Substituted Heteroaromatics

The aryl substituted heteroaromatic moiety (**Figure 1**) has had a great impact on variety of research areas and industries such as pharmaceutical, material, and the fine chemical industry (**Figure 2**).[1] The heteroaromic motif consists of two components, a conjugated ring system and the presence of at least one heteroatom in the ring. Oxygen, nitrogen, or sulfur are the heteroatoms that most commonly participate in these.

1
QUINAP
(Fine Chemical)

2
Lipitor
(Top Selling Pharmaceutical)

3
A photochromatic DTE system
(photoswitch)

4
Ambien CR
(Top Selling Pharmaceutical)
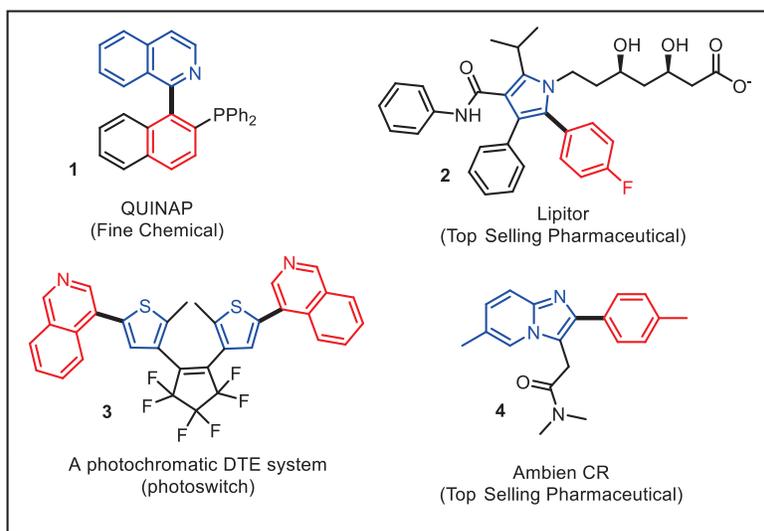
Figure 2 - Examples of Aryl-Substituted Heteroaromatics in Industry

Arguably, the area that has had the greatest impact by these motifs is the multibillion dollar industry of pharmaceuticals.[2] Certain properties of the aryl-substituted heteroaromatic seem to

have a great effect on this industry, for example, the aromatic cores of these compounds provide a flat rigid backbone that can be fine-tuned and interact *via* many interactions with a biological system.[3] Heteroatoms are also known to participate in a wide range of interactions, from the hydrogen bond to dipole interactions. In addition, the synthesis of biaryl compounds is greatly facilitated by the incorporation of a heteroatom into one of the aromatic system. In many cases thiophene may act as a bioisostere of benzene, that is, both compounds have similar activity in a biological system, and therefore the replacement of benzene with thiophene not only improves the synthetic ease of developing a molecule, but also mimics its role in a biological system.[4]

A study performed by Njardarson highlights the importance of aryl-substituted heteroaromatics in the pharmaceutical industry as these motifs are found in four of the top fifty prescribed drugs in the USA.[5] Another example that illustrates the importance of these aryl-substituted heteroaromatic motifs is related to the pharmaceutical Lipitor (**2**), a drug that is used to treat high levels of cholesterol contains this motif. This pharmaceutical is considered the world's top selling drug of all time with a gross revenue of over $140B.[6] Therefore it can be seen that development of the chemistry involved in the synthesis of these compounds is of the upmost importance. The most common method of accessing these motifs is via palladium-catalyzed cross-coupling reactions.

1.2 Palladium-catalyzed Cross-Coupling Reactions

Palladium-catalyzed cross-coupling reactions have emerged as some of the most important tools in the organic chemist's 'toolbox'. It is of no surprise that the robust and powerful nature of these reactions have transformed them into one of the preferred strategies for the formation of carbon-carbon bonds between (hetero)-aromatics. The importance of these reactions can be demonstrated by a survey performed by Carey *et al*., where he classified several reactions used in

the synthesis of 128 compounds by three major pharmaceutical companies, GlaxoSmithKline, AstraZeneca, and Pfizer (**Figure 3**).[7] Of all the reactions performed, 11% were for the formation of carbon-carbon bonds.
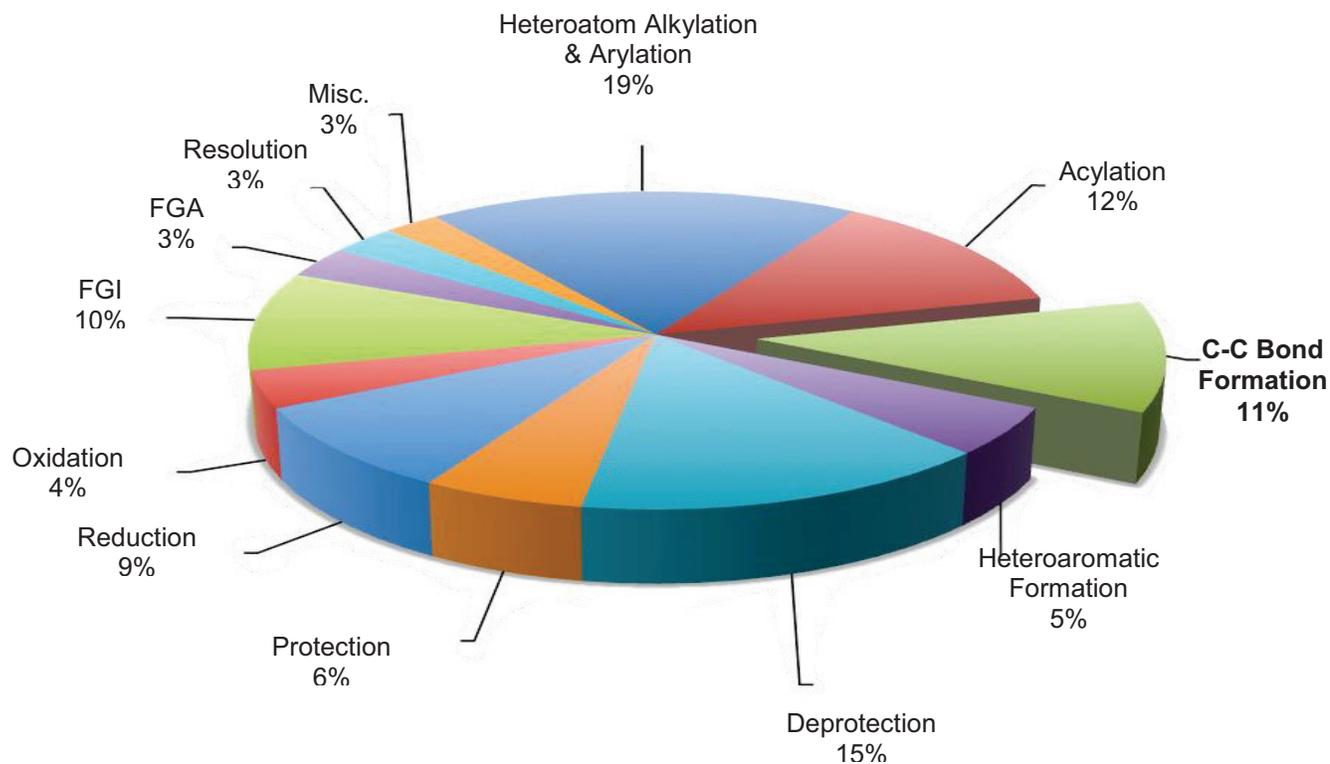
Figure 3 - Breakdown of reactions used in industry

While 11% may seem like a low value, many of the reactions were modifying reactions for example, protections, reductions, and oxidations which do not contribute to the skeletal framework of the molecule. Of the carbon-carbon bond forming reactions, 22% were made through the use of palladium-catalyzed reactions (**Figure 4**).
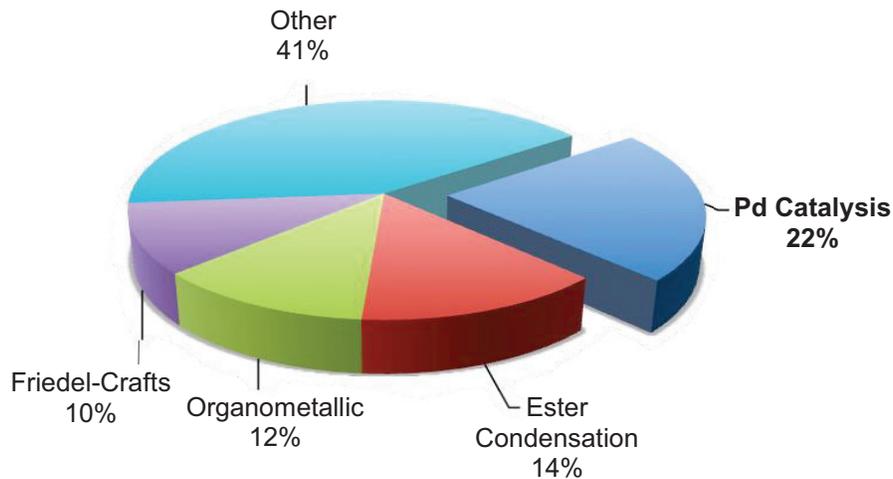
Figure 4 - Carbon-carbon bond forming reaction breakdown

The importance of palladium cross-couplings was further recognized in 2010 by the Nobel committee which awarded Richard F. Heck, Akira Suzuki, and Ei-ichi Negishi the Nobel Prize in chemistry for their revolutionary work in palladium-catalyzed cross-couplings.[8]

1.2.1 - The Mizoroki-Heck Reaction

Palladium was discovered in 1802 by Wollaston; however, its potential as a catalyst wouldn't be known for another 150 years.[9] Interest was gained in palladium's use as a catalyst in the 1950's when a German chemical company, Wacker Chemmie AG, used palladium for the conversion of ethylene (**5**) to acetaldehyde (**6**) in what is known today as the Wacker Process (**Figure 5**).[10]

- 4 -
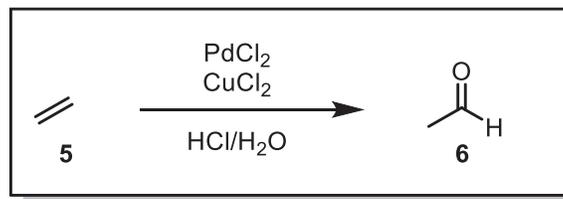
Figure 5 - The Wacker process (1959)

Around the same time, the young and eager Richard F. Heck had just accepted a position working for an American chemical company, Hercules Powder Co, following his post-doctoral studies. Heck was tasked with "doing something with transition metals" and found inspiration in the recently developed Wacker process.[11] Heck began investigating the use of palladium as a catalyst, and eventually was able to form a key carbon-carbon bond using palladium with organomercurial compounds (7) with alkenes (8) (**Figure 6**).[12]
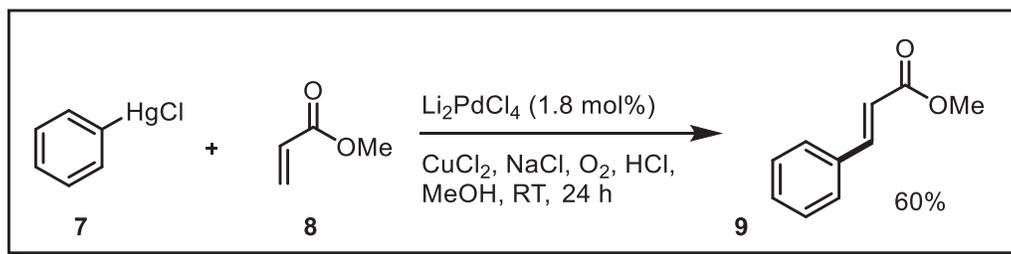
Figure 6 - Heck 1968: Cross-Coupling of Organomercurial Reagents with Olefins

At the same time a Japanese chemist by the name of Tsutomu Mizoroki reported on the arylation of olefin (**11**) with aryl iodides (**12**) catalyzed by palladium (**Figure 7**).[13] Only a few examples of aryl iodides were reported and was limited to coupling with ethylene.
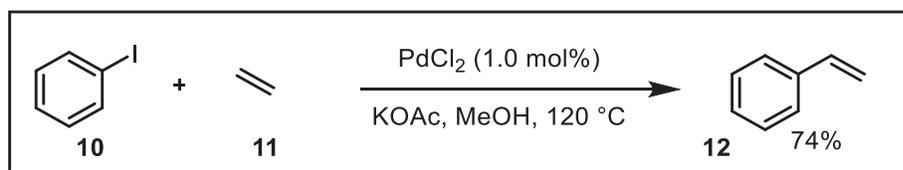
Figure 7 – The Mizoroki reaction 1971

Due to the high toxicity of organomercurial compounds Heck began working with aryl iodides. After further development, this reaction became known as the Mizoroki-Heck reaction (**Figure 8**).[14] With this work, Mizoroki and Heck gave birth to the palladium-catalyzed cross-coupling era.
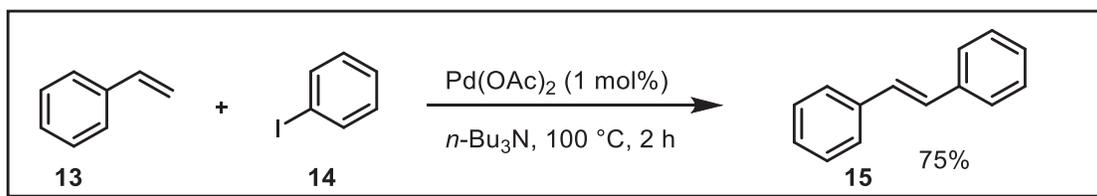
Figure 8 - The Mizoroki-Heck reaction 1972

The Mizoroki-Heck reaction proceeds via a different mechanism from what nowadays are referred to as the typical palladium-catalyzed cross-coupling mechanisms (**Figure 9**). The mechanism begins with the oxidative addition of palladium (**16**) into the aryl halide (**17**) bond generating complex (**18**). The olefin (**19**) then coordinates to the palladium (**20**) and adds over a syn-migratory insertion which forms intermediate (**21**). β-hydride elimination releases the product (**22**) and generates a palladium (**II**) hydride complex (**23**). This complex then undergoes a reductive elimination eliminating HX (**24**) and regenerating the palladium(0) catalyst (**16**).
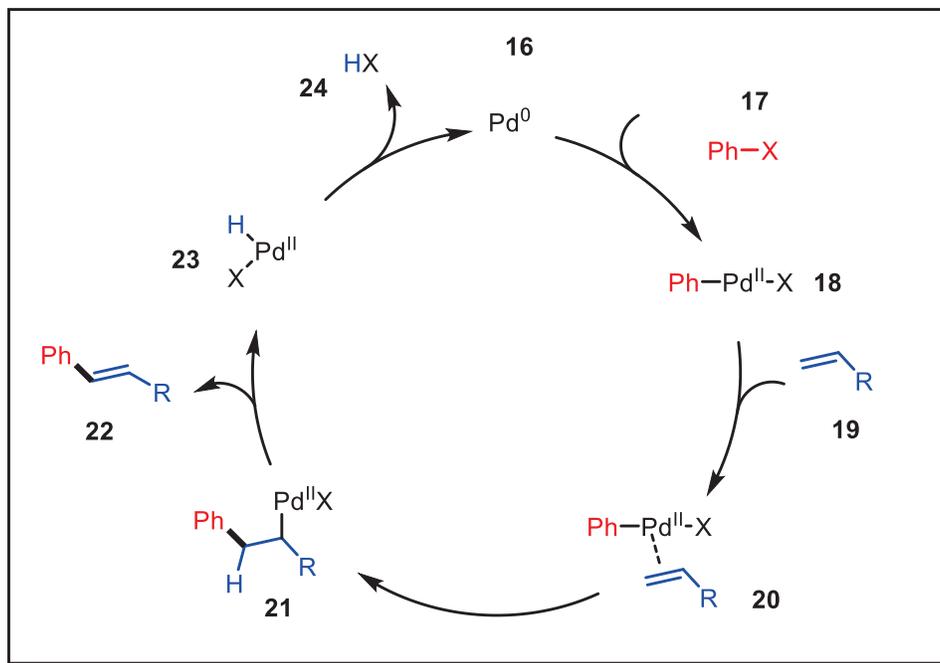
Figure 9 - Mechanism for the Mizoroki-Heck reaction

1.2.2 - The Corriu-Kumada Reaction

Around the same time that Heck was developing his reaction, Corriu,[15] and Kumada[16] independently developed a cross-coupling reaction between Grignard reagents (**25, 28**) and aryl-halides (**26, 29**) catalyzed by nickel (**Figure 10**). Soon after they released a set of improved conditions utilizing palladium over nickel. Palladium was found to result in less side-products and resulted in a much more controllable reaction.[17] More significantly, Kumada was able to introduce the use of phosphine-based ligands to control the reactivity of the metal center; a development that would have a great impact on the future of cross-coupling research.[18]
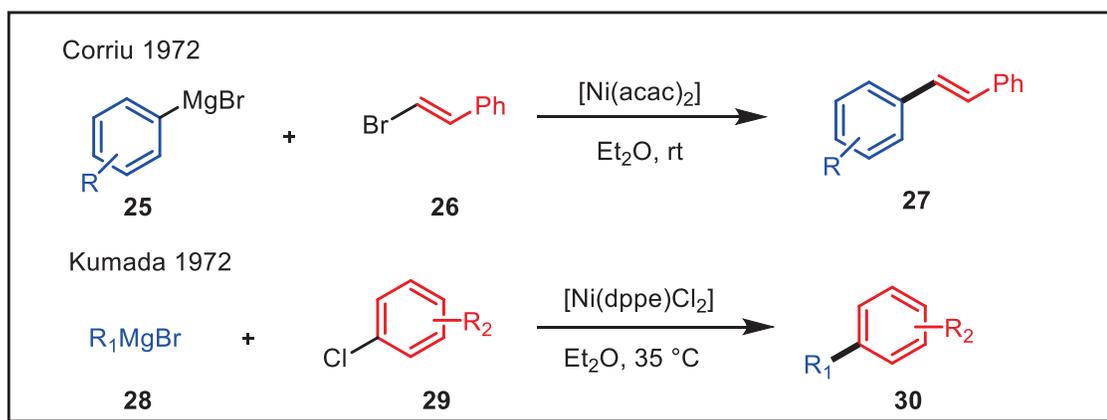
Figure 10 - Nickel catalyzed cross-coupling reactions of Grignard reagents

1.2.3 The Negishi Coupling

In 1976, Negishi reported on the cross-coupling between organoaluminum reagents with aryl-halides under catalytic amounts of nickel (**Figure 11A**).[19] Similar to Kumada, Negishi decided to replace the use of a nickel catalyst with palladium.[20] They observed while using palladium a superior stereo-specificity and reduced homocoupling. The success of these reactions lead to the development of an alternative reaction replacing organoaluminum with organozinc reagents (**Figure 11B**). Organozinc reagents proved superior over organoaluminum, resulting higher yields, higher catalytic turnovers, and higher selectivity, however, at the same time maintaining a wide scope and tolerating a variety of functional groups. The replacement of magnesium with other metals was an important milestone in the development of palladium-catalyzed cross-couplings as Negishi was able to demonstrate that other compounds were able to participate as coupling reagents.[21] This attracted many researchers leading to a continued search for an improved organometallic coupling partner.

A. Negishi 1976

Bu—$AliBu_2$ + Br—⟨⟩ $\xrightarrow[\text{THF, 50 °C, 3 h}]{\text{[Ni(PPh}_3)_4]}$ Bu—⟨⟩

31   **32**   **33**   85%

B. Negishi 1977

$\xrightarrow[\text{THF, RT, 2 h}]{\substack{\text{[PdCl}_2\text{(PPh}_3)_2\text{] (5 mol\%)} \\ i\text{Bu}_2\text{AlH (10 mol\%)}}}$

34   **35**   **36**   74%
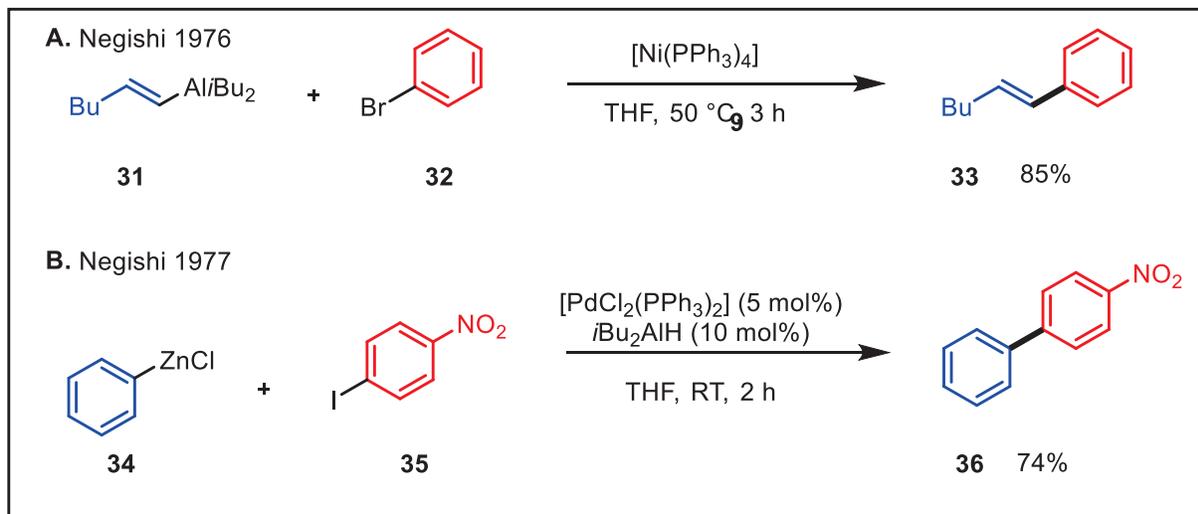
Figure 11 - The Negishi cross-couplings

1.2.4 The Stille Reaction

Organostannanes were first used in a palladium-catalyzed cross-coupling by Eaborn in 1976 (**Figure 12**).[22] Here they employed the use of aryl halides with organo-distanannes (**37**) to generate aryl-organostannanes (**39**).

R_3Sn—SnR_3 + X—Ar $\xrightarrow{\text{Pd[PPh}_3]_4}$ R_3Sn—Ar

37   **38**   R = Me or Bu   **39**
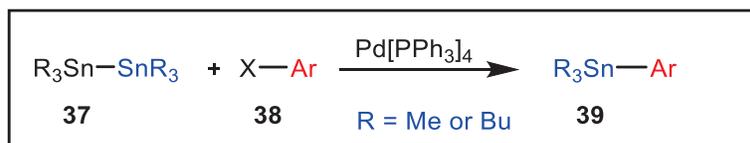
Figure 12 – First examples of organostannes in palladium-catalyzed cross-couplings

Milstein and Stille followed up on this reactivity by applying it towards the coupling of organostannanes with a variety of electrophiles to form C—C bonds (**Figure 13**).[23] The Stille reaction became one of the most versatile cross-couplings as organostannane reagents tolerated a variety of different functional groups, were readily available, and fairly air and moisture stable.[24] The use of the Stille reaction in complex reactions and in total synthesis of natural products not only made it one of the most popular C-C bond forming reactions, but also attracted awareness to

the field of palladium-catalyzed cross-coupling reactions. This reaction is currently the fourth most

published named C-C coupling reaction since its discovery.[25] The use of organostannanes proved

to be excellent cross-coupling partners, however, were also responsible for the major drawback of

this reaction, the toxicity of stannanes. This toxicity prompted further research in the hunt of the

ideal organometallic coupling partner.
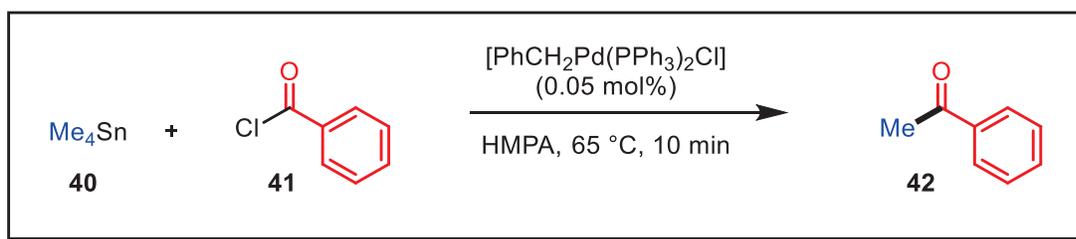
Figure 13 - Stille 1978: Cross-coupling with organostannanes

1.2.5 The Suzuki-Miyaura Reaction

One of the most powerful palladium-catalyzed cross-coupling reactions used today is the

Suzuki-Miyaura reaction. This reaction uses boronic acids with aryl-halides to form the cross-

coupling product in the presence of palladium (**Figure 14**).[26]
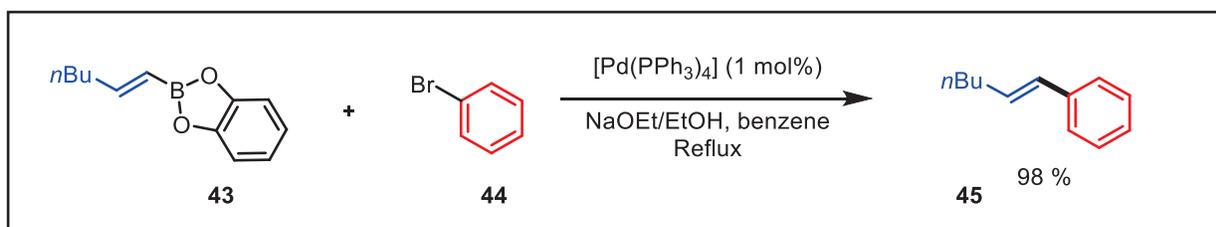
Figure 14 - The Suzuki-Miyaura reaction 1979

The Suzuki-Miyaura reaction has become one of the most useful cross-coupling reactions

today. The several thousand publications in literature highlight the impact the Suzuki reaction has

had in chemistry over the past few decades.[27] It has become extremely useful for industrial

applications, which can be attributed to certain advantageous features of the reaction such as the

use of stable and easy to handle organoboron reagents, mild and convenient reaction conditions, the high scalability, and the commercial availability of organoboron reagents. In addition, boronic acids are environmentally safer than other organometallic reagents and their by-products are easy to remove making it very attractive for large-scale synthesis.[28]

1.2.6 General Palladium-Catalyzed Cross-Coupling Mechanism

Most palladium-catalyzed cross coupling reactions have similar mechanisms, and only vary slightly depending on the nature of the reactants (**Figure 15**). Palladium (0) is typically the active species for most cross-couplings, however, the *in situ* generation of a catalytic species is quite common. Typically this occurs by the reduction of a palladium (II) species (**46**) to a palladium (0) (**47**). Generally the catalytic cycle for palladium cross-coupling reactions begins with the oxidative addition of palladium (0) (**47**) into the aryl halide (or pseudo halide) (**48**) bond generating the palladium (II) species (**49**). This can then undergo a transmetalation with the nucleophilic coupling partner (**50**) generating species (**52**). Reductive elimination releases the product (**53**) and regenerates the palladium (0) species (**46**). The mechanism is highly dependent on the substrates and conditions used, but typically follow this generic mechanism.
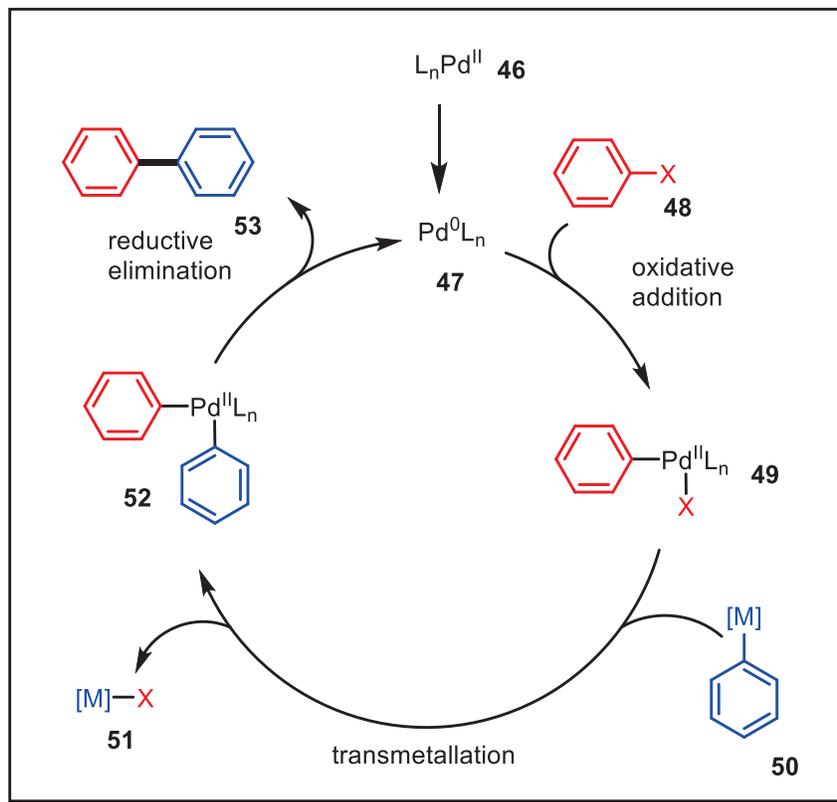
Figure 15 - Generic Palladium-Catalyzed Cross-Coupling Mechanism

1.3 Recent Advancements in Palladium-Catalyzed Cross-couplings

While the classic palladium-catalyzed reactions offer robust and versatile methods for C—C bond formation, they suffer from certain drawbacks that recent advancements have attempted to address. One of the major disadvantages to these methods is a concept that up until the 1990's wasn't a major concern for chemists, the concept of green chemistry.

1.3.1 Green Chemistry

The concept of atom economy was introduced into science in 1991 by one of the great organic chemists, Barry Trost.[29] Trost argued that those responsible for developing reactions should aim for 'elegant efficiency', where the highest possible percentage of input atoms should be incorporated in the product, ideally leaving behind no waste. The concept of atom economy

was a great start for the development of the green chemistry and is currently incorporated in the "12 principles of green chemistry", a set of principles that help define green chemistry.

A major advancement in the field of green chemistry came in 1998, when Paul Anastas and John C. Warner, who worked with the Environmental Protection Agency, published a set of principles that helped define the elusive concept of green chemistry.[30]

The 12 principles of Green Chemistry

1. It is better to prevent waste than to treat or clean up waste after it is formed.

2. Synthetic methods should be designed to maximize the incorporation of all materials used in the process into the final product.

3. Wherever practicable, synthetic methodologies should be designed to use and generate substances that possess little or no toxicity to human health and the environment.

4. Chemical products should be designed to preserve efficacy of function while reducing toxicity.

5. The use of auxiliary substances (e.g. solvents, separation agents, etc.) should be made unnecessary wherever possible and innocuous when used.

6. Energy requirements should be recognized for their environmental and economic impacts and should be minimized. Synthetic methods should be conducted at ambient temperature and pressure.

7. A raw material or feedstock should be renewable rather than depleting wherever technically and economically practicable.

8. Reduce derivatives – Unnecessary derivatization (blocking group, protection/deprotection, and temporary modification) should be avoided whenever possible.

9. Catalytic reagents (as selective as possible) are superior to stoichiometric reagents.

10. Chemical products should be designed so that at the end of their function they do not persist in the environment and break down into innocuous degradation products.

11. Analytical methodologies need to be further developed to allow for real-time, in-process monitoring and control prior to the formation of hazardous substances.

12. Substances and the form of a substance used in a chemical process should be chosen to minimize potential for chemical accidents, including releases, explosions, and fires.

These principles provide chemists with guidelines on how to develop chemistry safely while reducing the impact on the environment. They reveal some of the limitations associated with the classic palladium-catalyzed cross-couplings. One of the limitations associated with the classical methods is the poor atom economy attributed to the formation of high molecular weight by-products. For example, in the Stille reaction shown below (**Figure 16**) a cross-coupling is carried out for the formation of phenylanisol (**56**), a compound with a molecular weight of 184 g/mol however, one of the by-products generated (**57**) has a molecular weight of 417 g/mol.[31] The by-product is nearly 3 times the weight of the product. In another more industrially relevant example, a Suzuki reaction is used to generate the pharmaceutically important ABT-869 compound (**60**).[32] The molecular weight of the byproduct (**61**) (162.42 g/mol) is about half of the molecular weight of the product (**60**) (375.40 g/mol), and while significantly less than the first example, one must take into consideration that these reactions occur in large-scale synthesis.
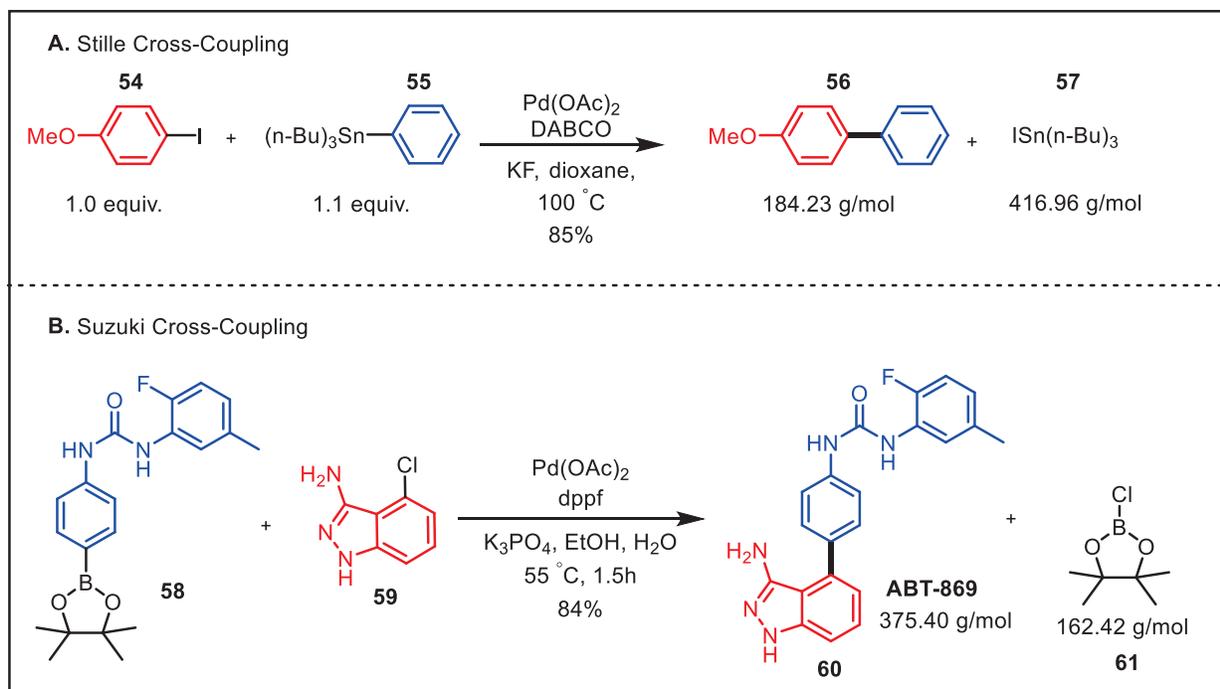
Figure 16 - Examples of Low Atom Economy Associated with Classical Methods

While these classic reactions suffer from low atom efficiency, it is not the only drawback they have. The use of organometallic coupling partners has further complications. To generate these reactive compounds it is necessary to perform a pre-functionalization, which can give rise to some problems with several sensitive functional groups. That is why in some cases the use of protective groups is required, which leads to the increase in waste generation. Organometallics also generate large amounts of metallic waste that can be toxic to the environment. These limitations prompted research to develop cross-couplings reactions that incorporate more of the green chemistry principles.

1.3.2 Palladium-Catalyzed Direct Arylations

Many attempts have been made to improve the classic palladium-catalyzed coupling reactions. One attractive approach is to replace the organometallic partner with the abundant C—

H bond, eliminating the need for stoichiometric amounts of organometallic starting materials. As one would expect, reducing the complexity of the organometallic coupling partner to a C—H bond is not without its challenges. The C—H bond is typically inert and diverse by nature resulting in difficulties associated with activation and regioselectivity.[33] Due to the high energy associated with breaking a C—H bond, transition metals are commonly used for their activation.[34]

The nature of the mechanism for the C—H bond activation is highly dependent on substrate, solvent, additives, metal, and ligands. Four classes of mechanisms are typically invoked: σ-bond metathesis, oxidative addition, electrophilic activation, and Lewis-base assisted metalation (**Figure 17**).[35] Early transition metals with high oxidation states tend to favor σ-bond metathesis; while for mid to late transition metals, oxidative addition, electrophilic metalation, and Lewis-base assisted deprotonation are more common. Following C—H activation, the resulting organometallic can then act as a nucleophilic coupling partner and proceed with the catalytic cycle.
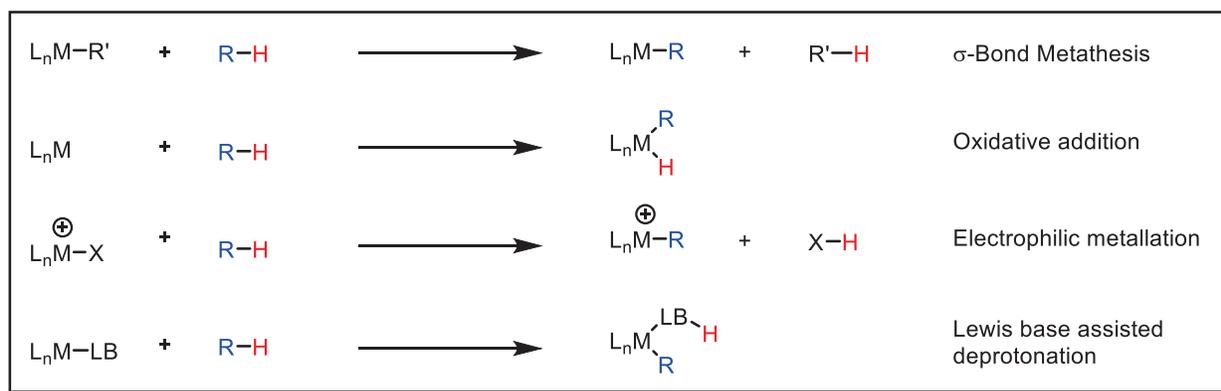
Figure 17 - General Mechanisms for Transition Metal Assisted C--H Activation

Both electron-rich and electron-poor substrates can undergo the C—H functionalization. Electron-rich substrates such as heteroaromatics are have been known to undergo C—H arylation *via* an electrophilic aromatic substitution (S$_E$Ar) pathway (**Figure 18**).[36] In this mechanism the π-system of the heteroaromatic (**62**) can act as a nucleophile and attack the palladium complex

(**63**). This complex can then undergo deprotonation releasing HX to regenerate aromaticity and to form the arylated palladium complex (**65**). The rate of this mechanism is governed by the nucleophilicity of the aromatic ring and is why electron rich 5-membered heteroaromatics are prone to these kinds of transformations.[36A]
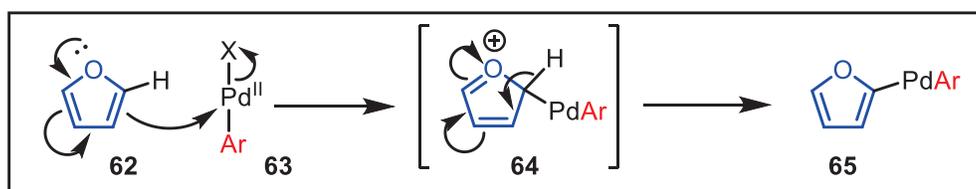
Figure 18 - Electrophilic Aromatic Substitution (S$_E$Ar) of Arylpalladium(II) Halide Complex (**63**) on Furan (**62**)

Kinetic studies performed using indolizine (**66**) support this mechanistic pathway (**Figure 19**).[37] The presence of electron-withdrawing groups (**66b**) greatly reduces the rate of not only direct arylation, but as well as Friedel-Crafts acylation, a reaction known to proceed *via* a S$_E$Ar mechanism.[38]

	Direct C-H Arylation	Friedel-Craft Acylation
—H a	1.00	1.00
—CO$_2$Et b	0.66	0.33

Relative Rates for Varying R$_1$
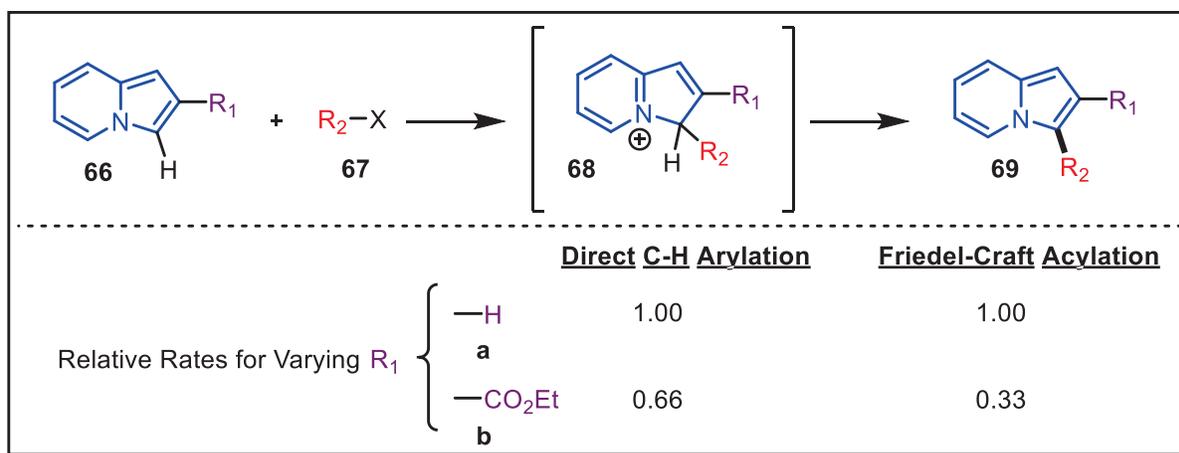
Figure 19 - Relative Rates of the Direct C-H arylation and Friedel-Crafts Acylation of Indolizines

1.3.2.1 - Regioselectivity

One of the main challenges associated with C—H arylation is in the abundant nature of the C—H bond. In cases where there are multiple reactive C—H bonds, for example in 5-membered heteroaromatics, regio-selectivity issues arise (**Figure 20**).[39] While the C2 and C5 positions of heteroaromatics are typically the most reactive for a reaction proceeding through a S_EAr mechanism, the C3 and C4 positions have also been shown to be reactive.[40] Many groups have attempted to overcome these selectivity issues.
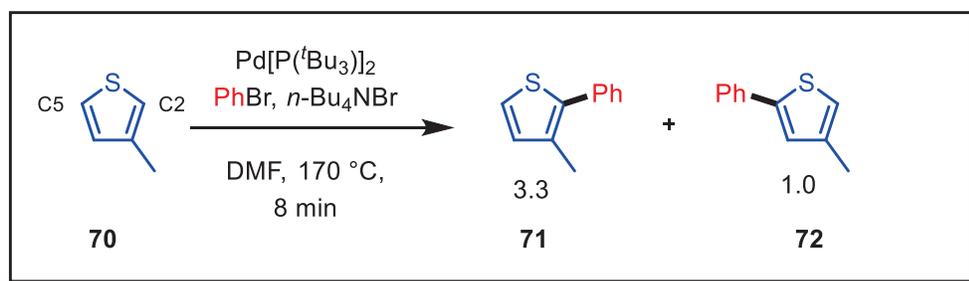
Figure 20 - Regioisomers of the C—H Arylation of 3-Methylthiophene with Bromobenzene

Sharp *et al.* developed conditions that have improved selectivity for the arylation 3-carboalkoxyfurans or thiophenes (**73**) (**Figure 21**).[36A] When using toluene with Pd(PPh₃)₄ almost absolute selectivity is achieved at the C2 position; however, when using NMP, a polar solvent, with Pd/C, high selectivity at the C5 position is observed.
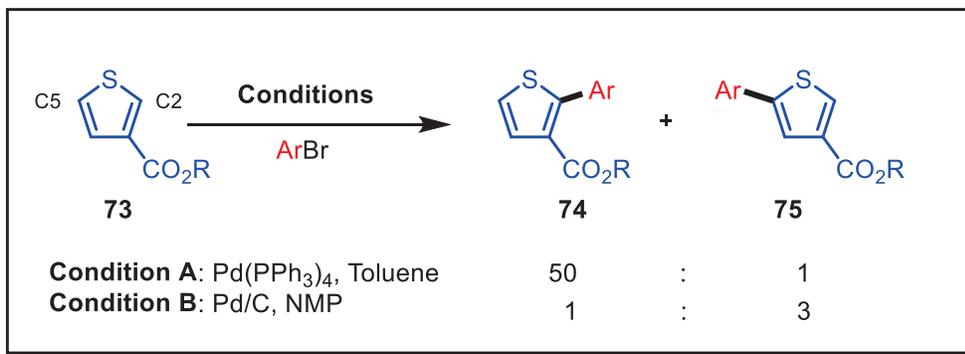
Figure 21 - Sharp's Conditions for Regio-selective Control for the Arylation of C3-Substituted Heteroaromatics with Aryl Bromides

Regio-selectivity can also be controlled using steric and electronic factors. Doucet was able to demonstrate this selectivity in C3-substituted thiophenes (**Figure 22**).[41] The coupling of 3-formylthiophene (**76**) with 4-bromobenzonitrile yields a C2-arylation in a 4:1 ratio (**77:78**). Here the selectivity is governed by the relative acidities of the protons at the C2 and C5 positions. The electron-withdrawing aldehyde increases the acidity at the C2 which leads to a favored arylation at this position (**77**). Increasing the steric bulk at the C3 position by protection of the aldehyde to a diethyl acetal (**79**) prevents the efficient coordination of palladium to the C2 position. After cross-coupling and deprotection of the acetal back to the aldehyde, the C5-arylated product (**81**) is favored.
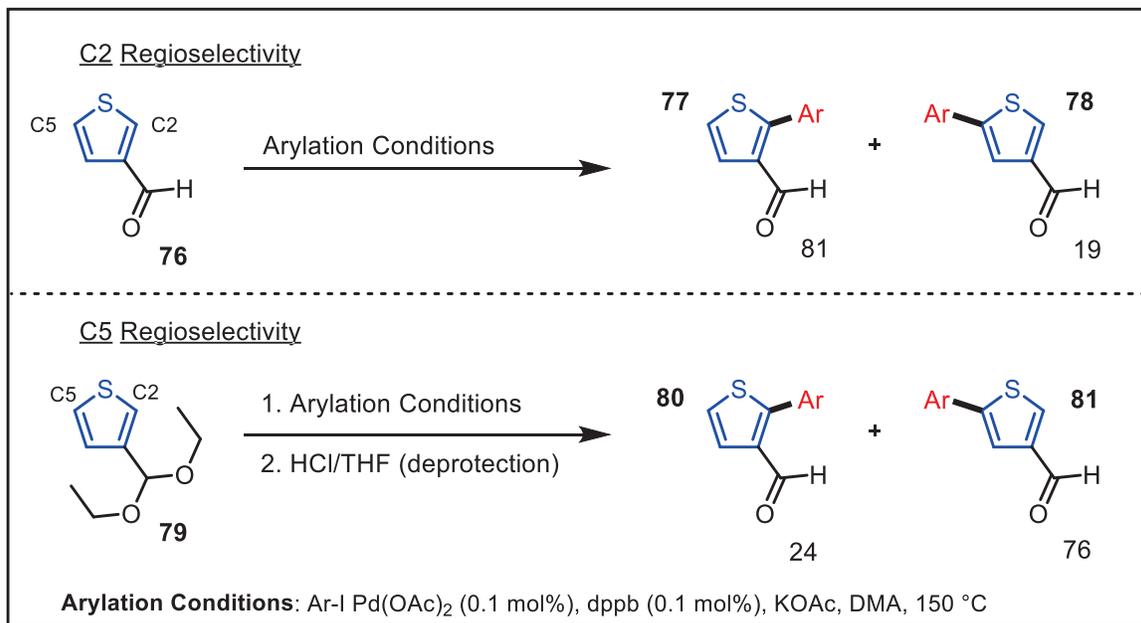
Figure 22 - Regioselective Control on The Direct Arylation of C3-Substituted Thiophenes

Recently Larrosa et al. have demonstrated almost absolute C3-regioselectivity for the arylation of thiophenes (**82**) and benzo[*b*]thiophenes (**85**) at room temperature (**Figure 23**).[42] They reported the arylation of a variety of different thiophenes (**84a-e**) with iodo-toluene in good yields with excellent selectivity for the C3 position. Almost complete regio-control was found in the presence of many challenging functional groups including halogens (**84b**), silanes (**84c**), and alcohols (**84e**). A variety of aryl iodides (**87a-e**) with different functional groups were also coupled with benzo[*b*]-thiophenes achieving excellent selectivity with good yields (**Figure 24**). Not only were they able to achieve excellent selectivity at the C3 position with a variety of different thiophenes and aryl iodides, the reaction proceeded smoothly at room temperature.
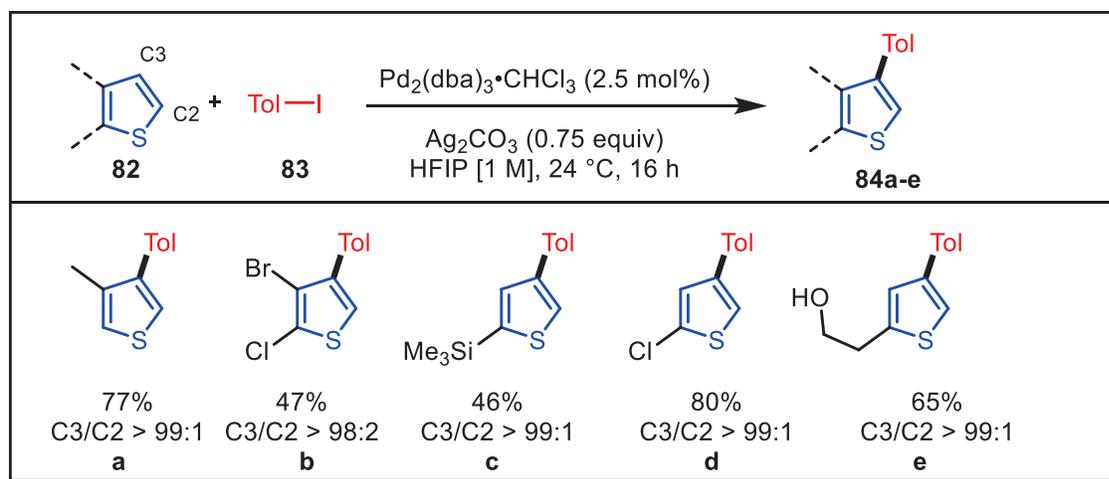
Figure 23 - Select Example for the C3-Arylation of Various Thiophenes with Iodotoluene
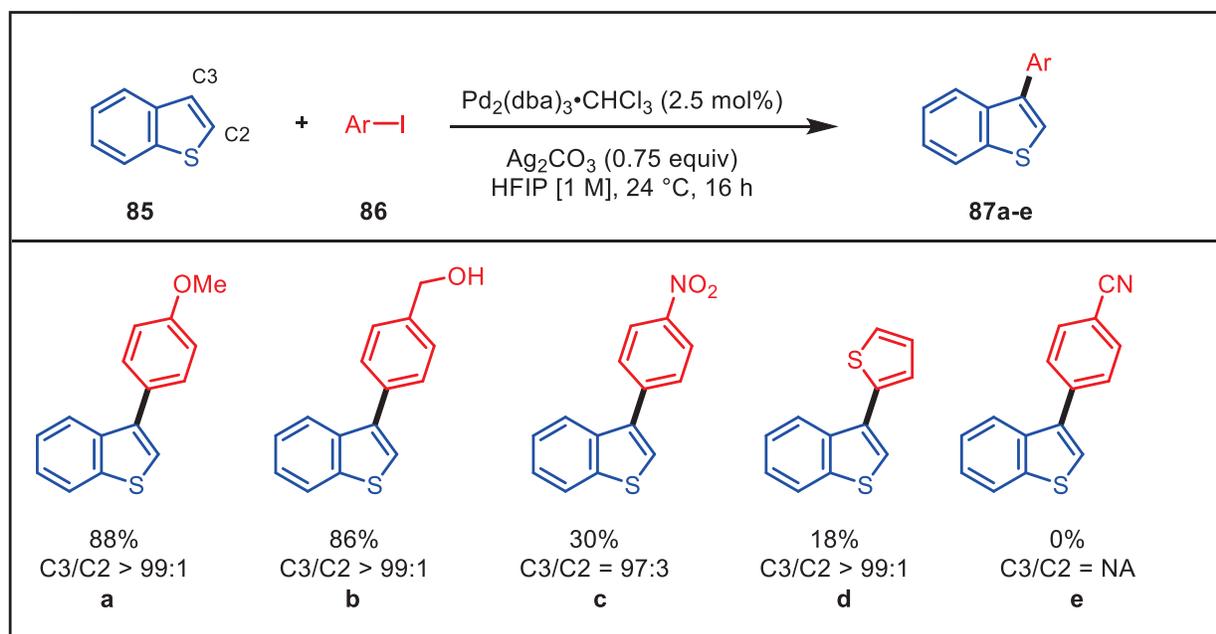
Figure 24 - Select Examples for the C3-Arylation of Benzo[b]thiophene with Aryl Iodides

1.3.2.2 The Fagnou Protocol

Over the last decade Fagnou and co-workers have had a great influence in the development of C—H arylations.[43] One of the limitations associated with direct arylation was that it was limited to electron rich systems, only electron-poor systems that were aided by a directing group could undergo this type of reactivity.[44] The Fagnou group developed a protocol capable of cross-coupling electron deficient arenes such as pentafluorobenzene (**88**) with 4-bromotoluene (**89**) in excellent yields (**Figure 25**). [43C]
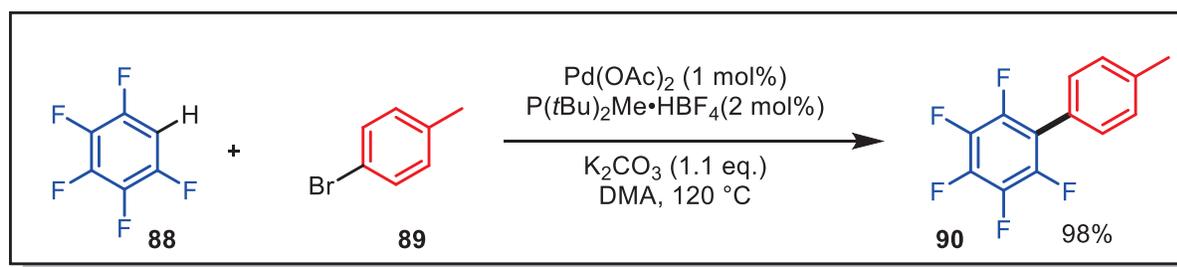
Figure 25 - Direct Arylation of Pentafluorobenzene with 4-Bromotoluene

As electron-poor systems have difficulty undergoing $S_E Ar$ mechanism, a different pathway named the concerted metalation-deprotonation was proposed by Echavarren and Maseras.[45] In this pathway after oxidative addition (**I**) a carboxylate additive (**94**) coordinates (**II**) to the palladium center displacing a halide. The palladium species (**96**) can then, assisted by the carboxylate ligand, deprotonate the arene (**95**) and concertedly coordinate to the palladium releasing the newly formed carboxylic acid (**97**) and generate the biaryl-palladium complex (**98**) (**III**). The catalytic cycle is closed after release of the product (**99**) by reductive elimination (**IV**). This mechanism offers a possible explanation for the reactivity of electron-deficient arenes undergoing C—H activation.
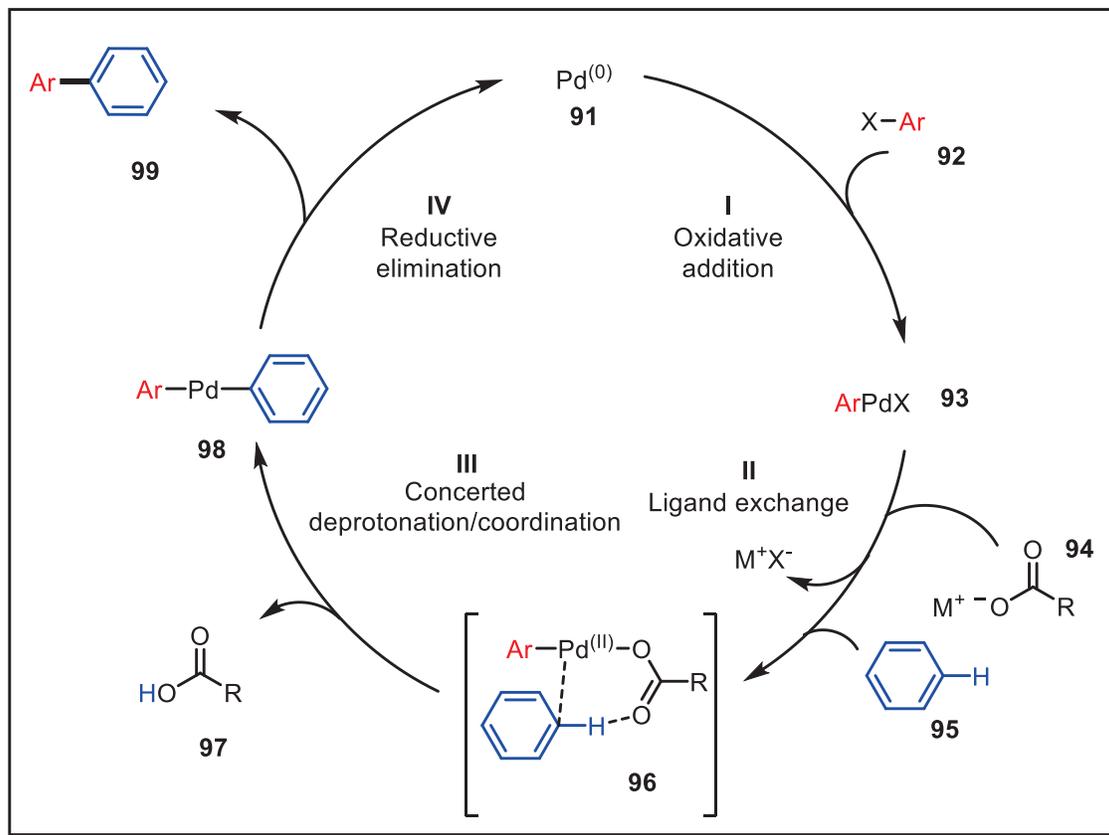
Figure 26 - Concerted Metalation-Deprotonation (CMD) mechanistic pathway

This mechanistic pathway was further supported with the coupling of differently fluorinated polybenzenes with 4-bromotoluene.[46] The reactants with the least electron density or those greater fluorinated had the highest yields while the more electron rich substituents had lower yields.

1.3.3 Decarboxylative Cross-Couplings

To address the common limitations associated with the classical methods such as the stoichiometric production of metallic waste, modern alternatives were developed. Direct functionalization of a C—H bond addressed these limitations by eliminating the need for an organometallic coupling partner; however, the challenges involved in controlling regioselectivity and activation difficulties have hindered its application and versatility.[47] In recent years a novel protocol was developed overcoming the limitations of the classical methods as well as addresses

the lack of regioselectivity present in the C—H activation. Decarboxylative cross-coupling reactions have emerged as a powerful alternative to the classic carbon-carbon bond forming protocols. Due to the availability, low cost, and the ease of handling and storage of carboxylic acids, they have become highly interesting coupling partners.[48]

Decarboxylative coupling reactions can be roughly divided into 5 categories: (**I**) cross-coupling of aryl, vinyl, or allyl electrophiles, (**II**) conjugate additions, (**III**) carbon-heteroatom bond formation, (**IV**) Heck-type vinylations, and (**V**) direct arylations reactions (**Figure 27**). These reactions can be broken down into two mechanistic categories, redox-neutral coupling and oxidative couplings. The metalated carboxylate can also undergo a proto-decarboxylation (**VI**) if treated with acid, or heated at sufficiently high temperatures. In redox-neutral coupling reactions, the carboxylic acid provides the nucleophilic coupling partner while for the oxidative coupling reactions they provide the electrophile coupling partner.[48]
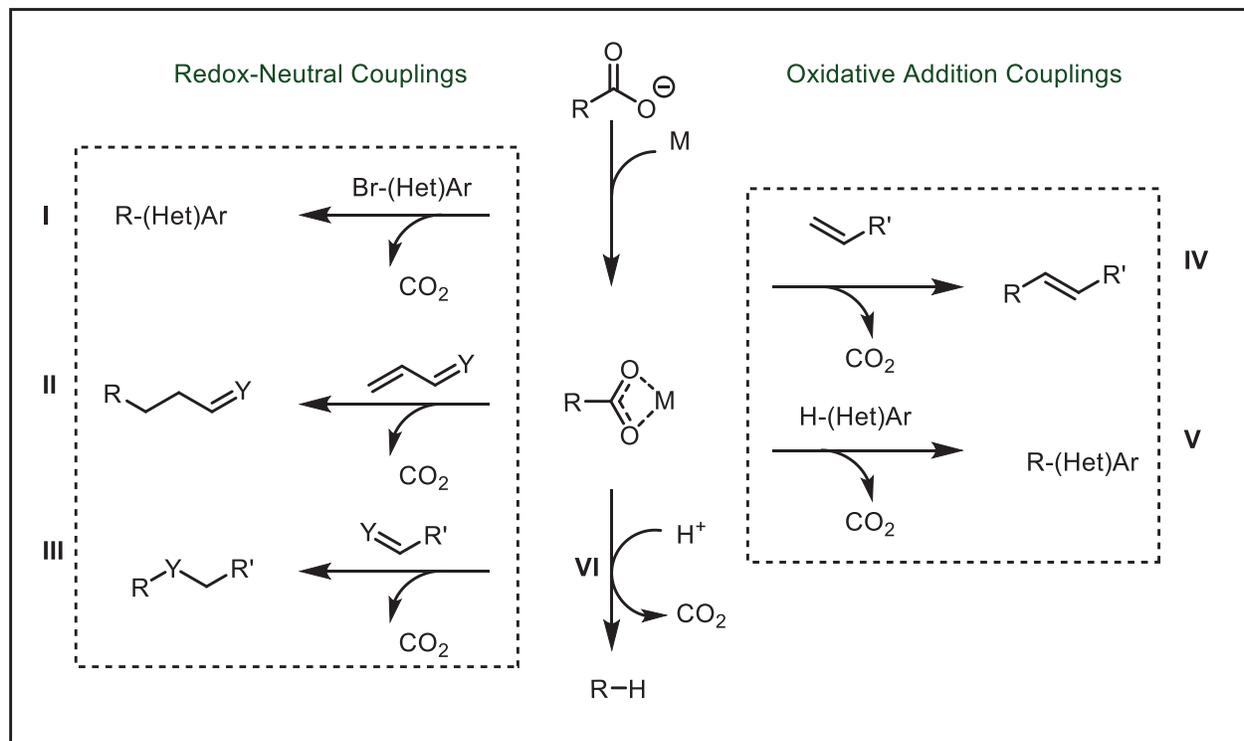
Figure 27 - General Types of Decarboxylative Cross-Couplings

The key step in all decarboxylative cross-coupling reactions is the decarboxylative carbometalation. The challenge in this transformation is the harsh conditions required for CO_2 extrusion.[48] High temperatures and harsh conditions can result in proto-decarboxylation (**VI**) as well as render the process intolerant of sensitive functional groups.[49] Furthermore the high temperatures and long reaction times result in large energy consumption which yields the reaction less green. In recent years much focus has been applied towards improving the catalytic system of these reactions and with the hopes of reducing the need for harsh conditions.

1.3.3.1 The Goossen Protocol

Goossen *et al.* initially reported the cross-coupling of 2-nitrobenzoic acids (**100**) with aryl bromides under a bimetallic system involving stoichiometric amounts of copper carbonate, potassium fluoride, and an excess of powdered molecular sieves in the presence of a palladium

catalyst at 120 °C (**Figure 27**).[50] The role of the molecular sieves is to trap the water formed during the *in situ* deprotonation with carbonate bases. One of the interesting aspects of this system was the low temperature at which decarboxylation could occur. Typically temperatures greater than 160 °C are required for decarboxylation, however, their system was able to generate the cross-coupling product at the low temperature of 120 °C. They proposed that $ArCO_2CuF$ salts were formed which facilitated this transformation reducing the temperature needed. Even with the low temperature for their system, the use of a bimetallic system requiring stoichiometric amounts of copper was a downside.
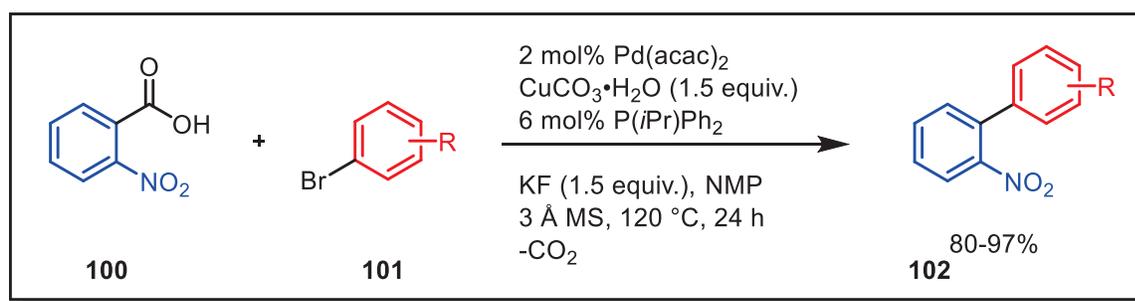
Figure 28 – Goossen Protocol 2011: Decarboxylative Cross-Coupling of 2-nitrobenzoic acids with aryl bromides

Following this protocol, a system was developed using a copper (I)/phenanthroline complex which was used to mediate the decarboxylation (**Figure 29**).[51] In this new protocol, they were able to regenerate the copper allowing for the process to be catalytic in both copper and palladium. While this new system had the benefit of being catalytic with respect to copper, the temperature needed to achieve high yields was slightly increased to 160 °C. Even though the scope of the reaction was fairly broad with respect to aryl halides, the reaction was limited to only *ortho* substituted carboxylic acids with electron-withdrawing groups. This limitation was overcome by replacing aryl halides with aryl triflates or aryl tosylates.[52]
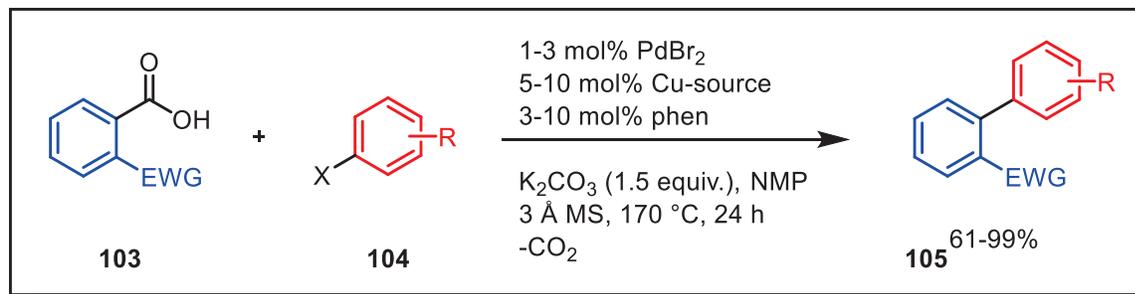
Figure 29 - Goossen Improved Protocol: Biaryl Synthesis using Catalytic Amounts of Copper

In 2014 Goossen *et al*. published a paper investigating the mechanism for their decarboxylative cross-coupling using density functional theory (DFT) methods (**Figure 30**).[53] The Goossen protocol involves a cooperative catalytic system, where a separate cycle for copper and palladium are joined by a single transmetalation step. Starting with the copper cycle, copper(I) bromide/1,10-phenanthroline (**106**) undergoes a anion exchange (**I**) between the bromide and the entering carboxylate (**107**). They proposed two possible pathways in which this could occur: (1) through the generation of an anionic copper species or (2) *via* a neutral copper species. They compared energy levels of each pathway using DFT, and determined that the most favorable pathway proceeded *via* a neutral copper complex (**108**) rather than an anionic copper species. The next step for the catalytic cycle of copper is decarboxylation (**II**) generating the organocuprate complex (**109**). This copper species can then undergo transmetalation (**III**) with palladium (**110**) regenerating the copper catalyst (**106**) and forming the organopalladium species (**111**). The palladium species (**110**) that underwent transmetalation, had been formed by the oxidative addition (**IV**) of the palladium catalyst (**113**) into an aryl halide (**114**). After transmetalation, the palladium species (**111**) undergoes reductive elimination (**IV**) regenerating the palladium catalyst (**113**) and releasing the biaryl product (**112**). From their computation studies they determined that the rate limiting step is either transmetalation (**III**) or decarboxylation (**II**) depending on the substrate.

From these results they were able to design a ligand that facilitated the decarboxylative cross-coupling which lowered the temperature by 70 °C.
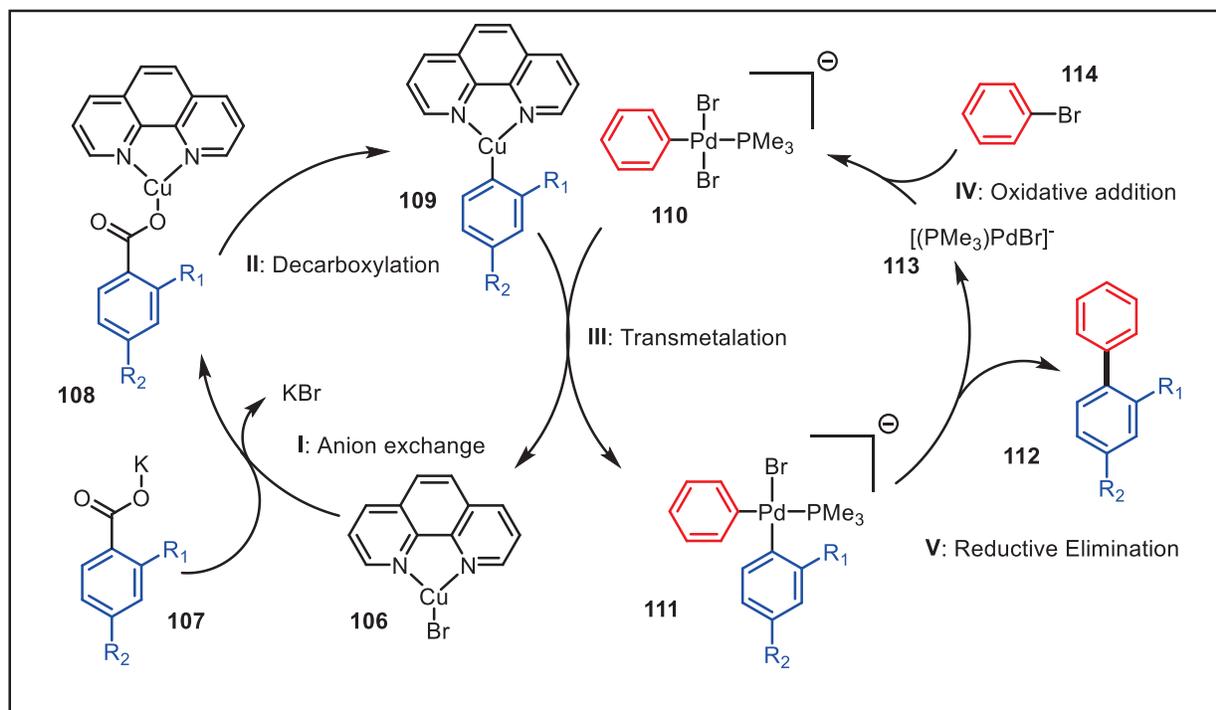
Figure 30 - Proposed mechanism for the Goossen decarboxylative cross-coupling

1.3.3.2 The Palladium-catalyzed Heteroaromatic Decarboxylative Cross-Coupling

The palladium-catalyzed decarboxylative cross-coupling of heteroaromatics with aryl-halides and pseudohalides has also been reported by Forgione *et al.* in 2006.[47] They describe attempting to perform a C—H activation on a heteroaromatic carboxylate acid (**116**) and rather than obtaining the desired coupling at the C—H position (**115**), they found the coupling product at the carboxylate position (**118**) (**Figure 31**). This newfound reactivity proved exciting and prompted further research in the area of heteroaromatic decarboxylative cross-couplings.
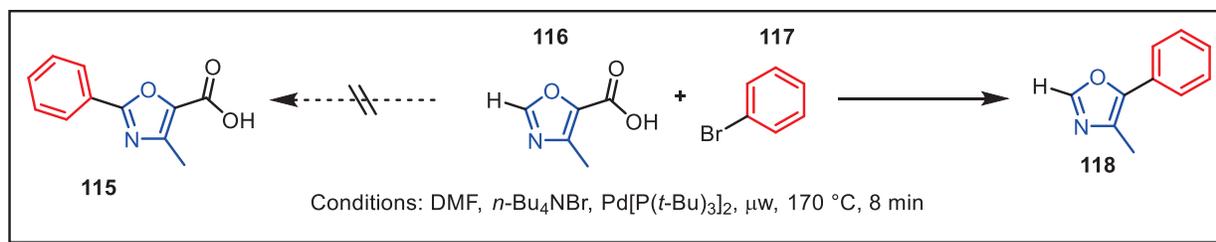
Figure 31 - The unexpected decarboxylative cross-coupling of heteroaromatics

One of the interesting features of this decarboxylative coupling is that it does not require a co-catalyst to help extrude CO_2, and therefore must proceed *via* a different mechanism than the proposed for the Goossen protocol. A few years after the initial findings, Forgione *et al*. released another paper describing a full reaction scope and a detailed assessment of possible mechanistic routes (**Figure 32**).[54]
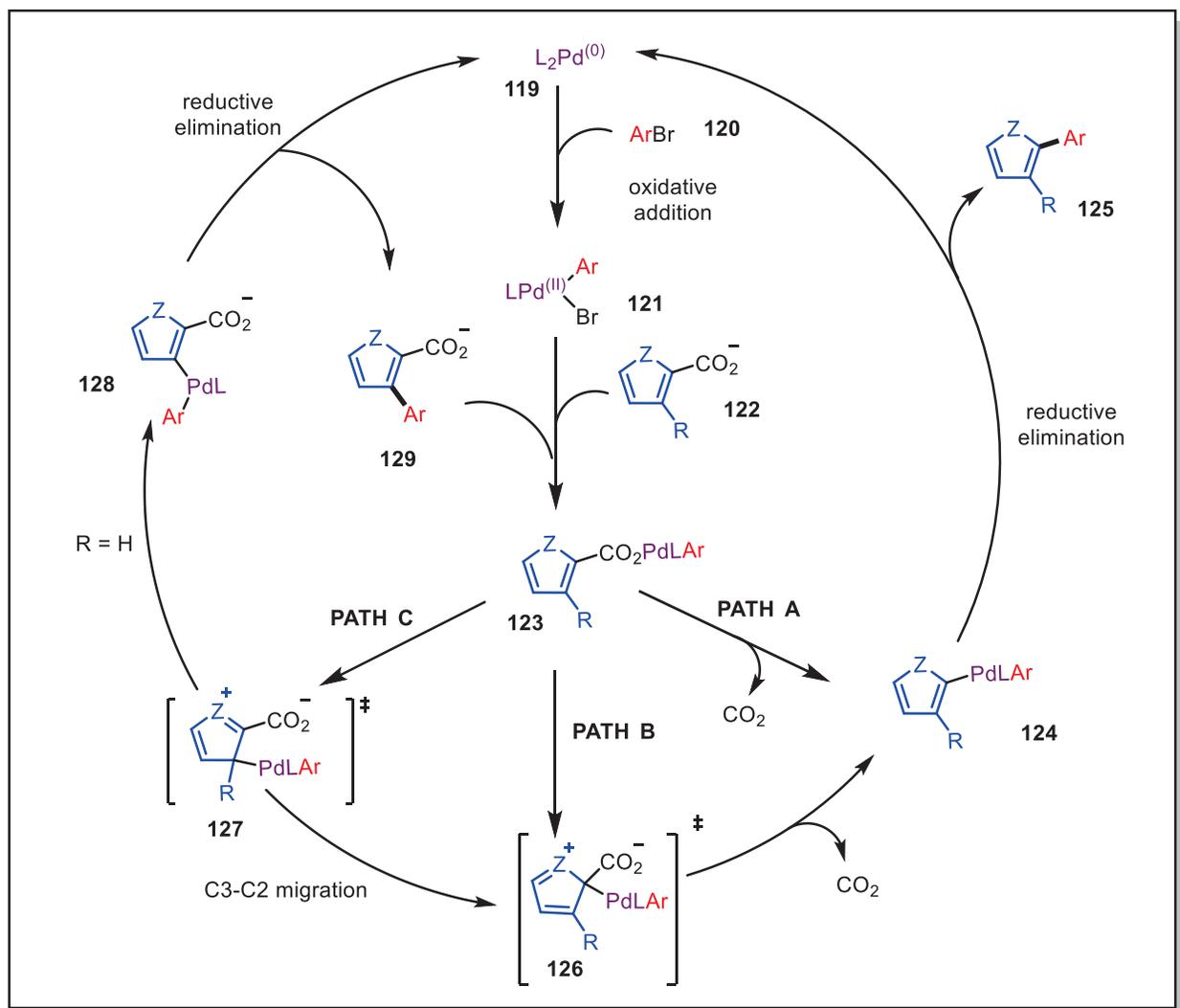
Figure 32 - Proposed mechanism for the heteroaromatic decarboxylative cross-coupling

The proposed mechanism begins as many palladium-catalyzed cross-couplings do, with the Pd (0) species (**119**) undergoing an oxidative addition into an aryl-halide (**120**) bond resulting in the formation of the Pd (II) species (**121**). Displacement of the bromide by the heteroaromatic carboxylate (**122**) forms the key intermediate (**123**). This palladated carboxylate can then undergo three possible pathways. Pathway A is a direct decarboxylation, which forms the intermediate (**124**) after CO_2 extrusion. This species then undergoes a reductive elimination releasing the product (**125**) and regenerates the Pd (0) catalyst (**119**). Pathways B and C proceed *via* an S_EAr

mechanism where the nucleophilic nature of the heteroaromatic can attack the palladium species (**123**) generating transition states (**126**) or (**127**). Pathway B proceeds *via* a nucleophilic attack from the C2 position of the heteroaromatic to the palladium complex generating the transition state (**126**). This can then re-aromatize by undergoing a decarboxylation resulting in the previously mentioned intermediate (**124**). Pathway C is similar to path B, however, was proposed to rationalize the 2,3-diarylated side product observed. In this case the nucleophilic attack occurs at the C3 position over the C2 position resulting in the transition state (**127**). In a scenario where the R group is a hydrogen, deprotonation can occur in order to regain aromaticity, generating the C3 palladated intermediate (**128**). This intermediate can then undergo a reductive elimination regenerating the catalyst (**119**) and releasing the C3 arylated-heteroaromatic carboxylate (**129**). This carboxylate can then re-enter the catalytic cycle to generate the 2,3-diarylated side-product (**125**) (R = Ar).

Many experimental observations were used to rationalize this mechanism. As previously mentioned, Path C was proposed to account for the 2,3-diarylated products observed when the R group was a hydrogen. Path A was thought to be an unlikely pathway as this mechanism does not incorporate the nucleophilic nature of the heteroaromatics. The heteroaromatic was found to be essential as Forgione demonstrated that the cross-coupling of benzoic acid (**130**) and phenylbromide (**131**) failed to form the desired cross-coupling partner (**132**) (**Figure 32A**). This could be a result of the weaker nucleophilic nature of benzene over heteroaromatics and therefore a higher energy barrier for the formation of the (**126**) transition state. Further evidence of the reaction proceeding *via* a S_EAr mechanism is obtained with the failure to generate the cross-coupling product when using furan-3-carboxylic acid (**133**) (**Figure 32B**). As previously stated, the C2 position of heteroaromatic has a greater propensity to undergo a S_EAr reaction over the C3

position. This lowered reactivity would once again lead to greater energy barrier making this transformation more challenging.
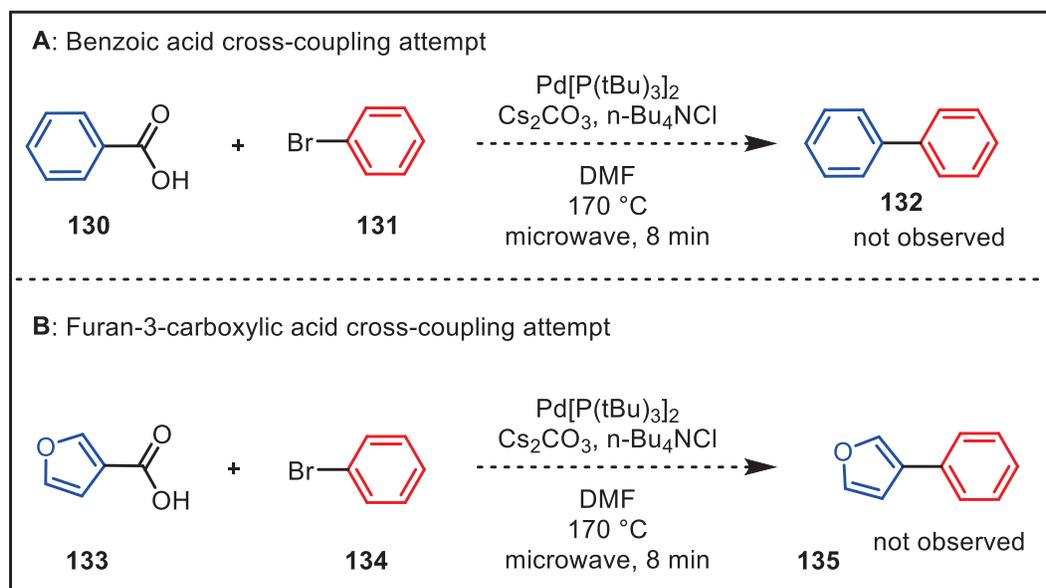
Figure 33 - (A): Benzoic acid cross-coupling attempt (B) Furan-3-carboxylic acid cross-coupling attempt

Forgione carried out competition experiments to gain more insight into the kinetics of the reaction. A competition experiment (**Figure 33**) between 3-methylfuran-2-carboxylic acid (**136**) and 3-methyl-benzofuran-2-carboxylic acid (**139**) would provide information on relative rates and therefore shed light on the decarboxylative transformation's energy barrier. As 3-methyl-benzofuran-2-carboxylic acid (**139**) proceeds with decarboxylation *via* the proposed transition state (**140**), it must break the aromaticity of the fused phenyl group and hence have a greater energy barrier than when (**136**) undergoes decarboxylation through the corresponding transition state (**137**). The ratio of products would then indicate the relative rates. The ratio of **138**:**141** was 2.2/1, representing a lower energy barrier for the decarboxylation of (**136**) over (**139**) and further supporting the proposed mechanism.

Conditions: 4-tolylBr, DMF, n-Bu$_4$NCl hydrate, Pd[P(t-Bu)$_3$]$_2$, microwave, 170 °C, 8 min
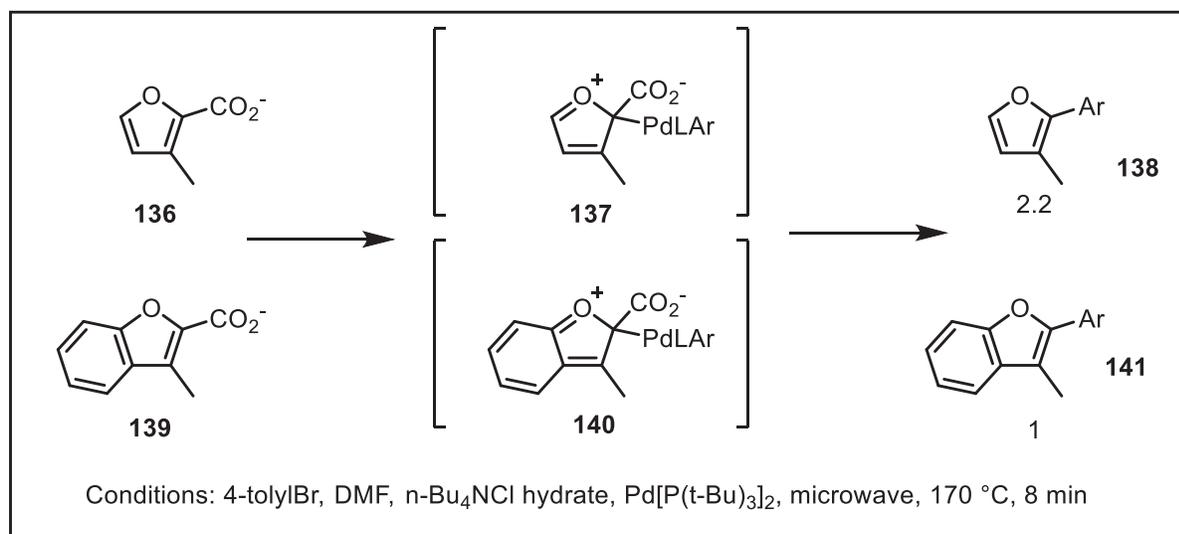
Figure 34 - Competition between the Pd-catalyzed arylation of furan-3-methyl-2-carboxylic acid and benzofuran-3-methyl-2-carboxylic acid

Another competition experiment between analogues (**142a**) and (**142b**) was designed to evaluate the electronic factors on the rate of the decarboxylation (**Figure 34**). The electron-rich (**142a**) is able to stabilize the resulting transition state though electron donation and resonance, while the more electron deficient (**142b**) cannot. The ratio of **a:b** (1.8/1) indicates that (**142a**) has a lowered energy barrier which provides further experimental support for the proposed transition state.
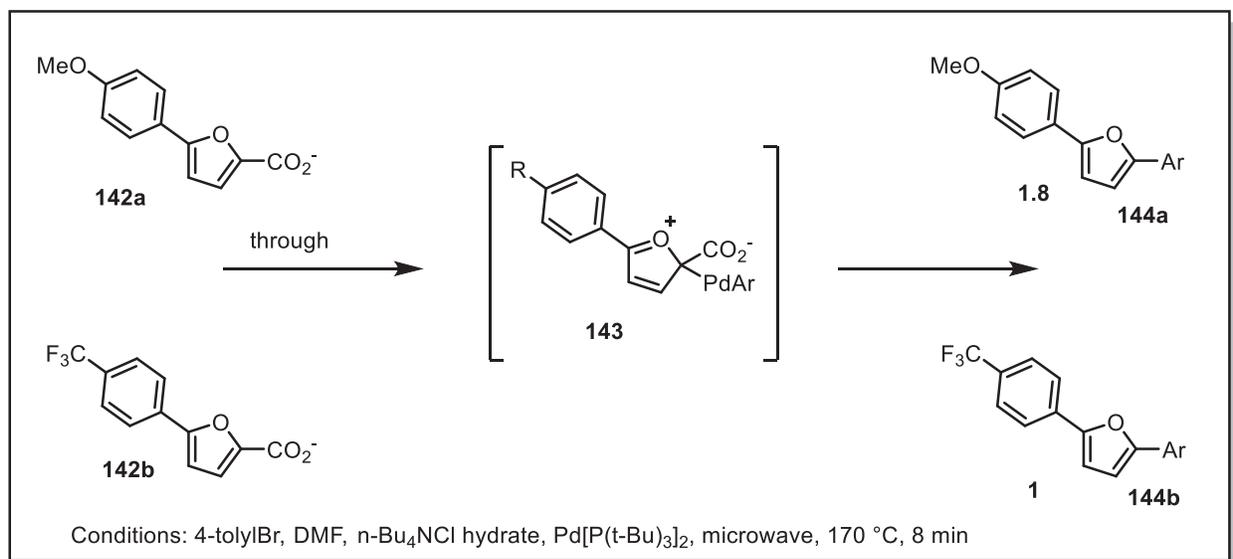
Figure 35 - Competition between the Pd-catalyzed arylation of 5-arylfuran-2-carboxylate (**142ab**) analogues

1.3.4 Palladium-Catalyzed Desulfinative Cross-Couplings

Aryl-sulfinates are versatile species in cross-coupling reactions. They can behave both as nucleophilic or electrophilic coupling partners.[55] While carboxylates coordinate via the oxygen atoms, sulfinates have been shown to coordinate to metals with additional modes of complexation (**Figure 35**).[56] Although several modes of complexation exist for sulfinates, several studies have shown that typically coordination with a palladium (II) species occurs via bonding of the sulfur atom to palladium (**145c**).[57]
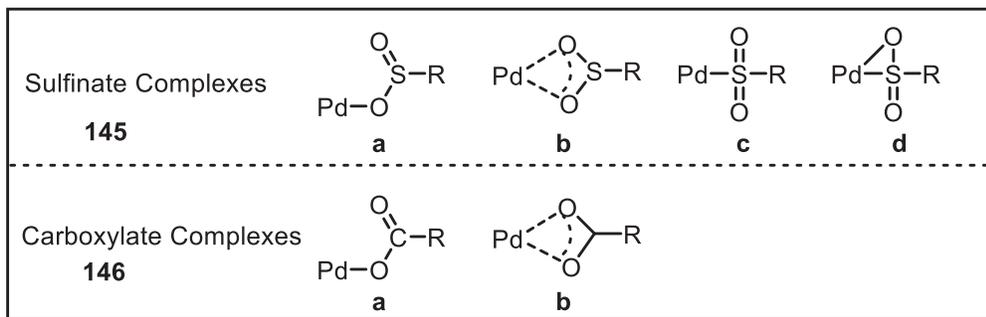
Figure 36 - Modes of complexation to palladium for sulfinates and carboxylates

Some of the first examples of sulfinates behaving as nucleophilic coupling partners were reported in the early 1970's by Garves, Selke, and Thiele.[58] Garves described the homo-coupling of aryl-sulfinates using stoichiometric amounts of sodium tetrachloropalladate (**Figure 37**).[58A] Garves also presented the first attempts at an oxidative Heck-like reaction.
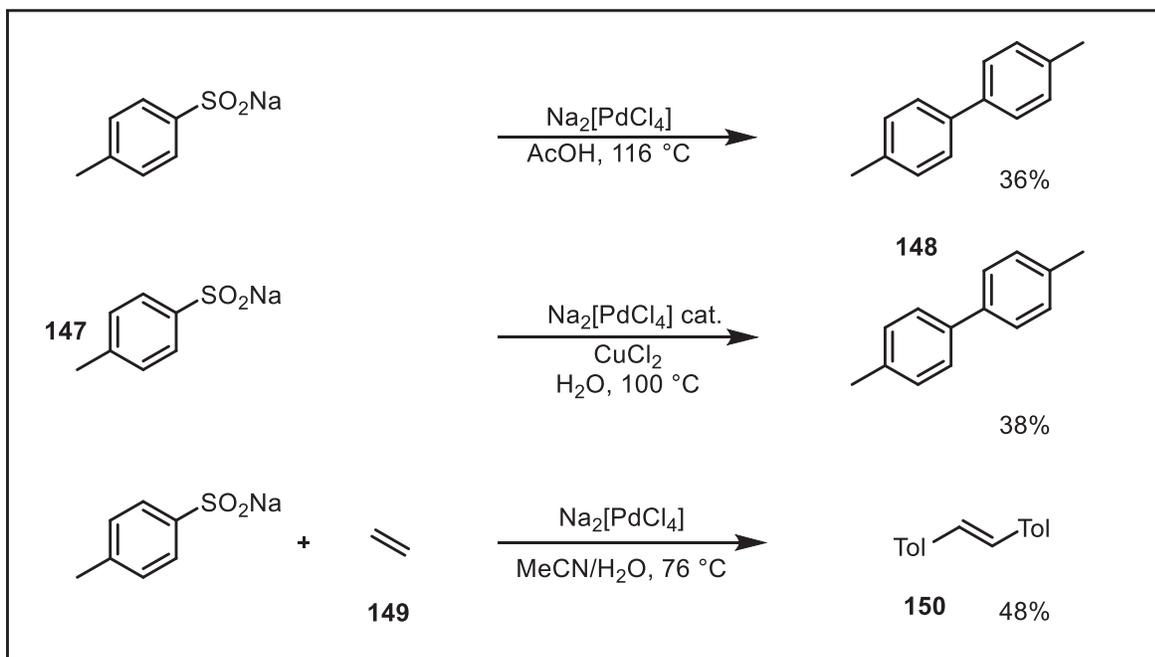
Figure 37 - Garves 1970: First examples of desulfinative cross-coupling reactions

1.3.4.1 Aryl Sulfinates as an Electrophilic Coupling Partners

        Aryl sulfinates can replace the traditional aryl halides as a coupling partner.[55] As such, the oxidative addition of Pd (0) into the aryl halide is no longer part of the reaction mechanism. The active palladium catalyst is therefore not a Pd (0) catalyst, but rather a Pd (II) species, which after the formation of Pd (0) by reductive elimination must be regenerated. Typically this is done with the use of an oxidant. As sulfinates tolerate air and moisture, the reactions can be conducted open to air allowing oxygen to behave as the oxidant. Deng and co-workers demonstrate this in a series of papers which report on the palladium-catalyzed desulfinative Mizoroki-Heck reaction, direct arylation of azoles, and the direct arylation of indoles (**Figure 38**).[59] In comparison to decarboxylative cross-couplings, the temperatures for these reactions are significantly lower. Furthermore, the direct arylation reactions do not require a ligand present unlike the direct arylations with aryl halides where typically a bulky carboxylate is required to facilitate C—H activation.
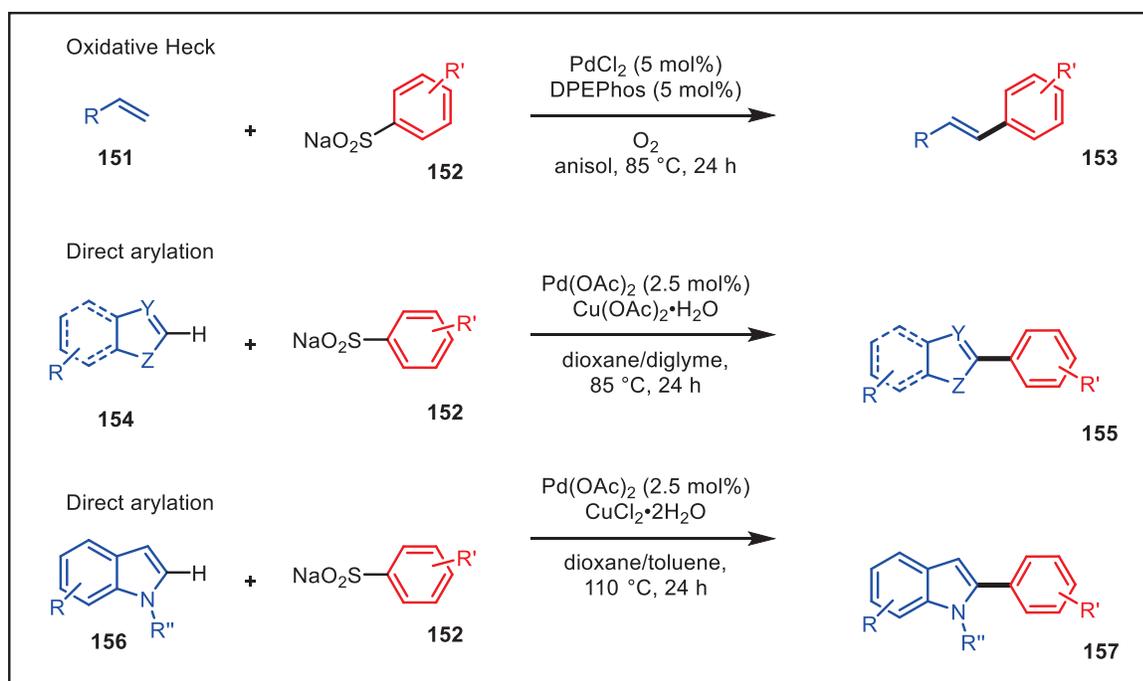
Figure 38 - Deng protocol for the oxidative Heck and direct arylations with aryl sulfinates

Aryl sulfinates have also been reported as a coupling partner for palladium-catalyzed Hiyama-like[60] cross-coupling (**Figure 39**).[61] Published in 2013 by Qi e*t al*., this reaction uses organosilanes (**158**) as the nucleophilic coupling partner with sodium sulfinates. The use of a TBAF provides a fluoride source which is necessary to activate the organosilane. As with many other palladium(II)-catalyzed reactions that use aryl sulfinates as an electrophilic partner, leaving the reaction open to air re-oxidizes palladium (0) to palladium (II) closing the catalytic cycle.[55]
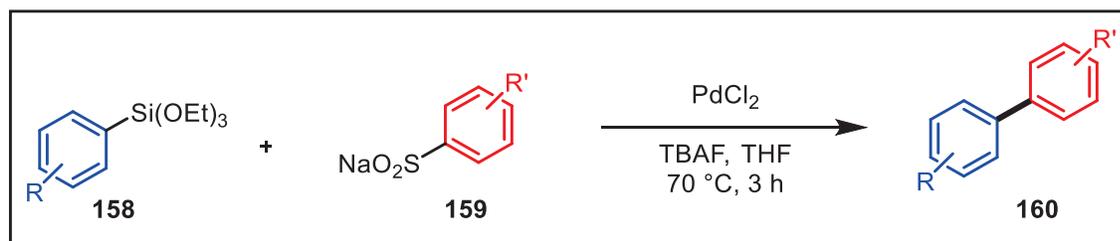
Figure 39 - Hiyama-like cross-couplings of aryl silanes with aryl sulfinates

1.3.4.2 Aryl Sulfinates as Nucleophilic Coupling Partners

Aryl sulfinates have so far been shown to be a versatile electrophilic coupling partner; in many cases exhibiting superior reactivity over their aryl halide counterpart. Nonetheless their ability to be a powerful electrophilic partner does not jeopardize their potential to act as a nucleophilic coupling partner. Up until very recently, with the exception of a few reports by Garves, Selke, and Thiele, their ability to act as a potential organometallic replacement in cross-couplings has been essentially neglected.[58]

One example of aryl sulfinates as a nucleophilic was reported in a patent published in 1992.[62] Sato and Okoshi reported the palladium-catalyzed cross-coupling of aryl sulfinates with aryl bromides (**Figure 40**). They described heating the reaction mixtures for 6-8 hours at 150 °C, obtaining yields between 25-91% by HPLC analysis.
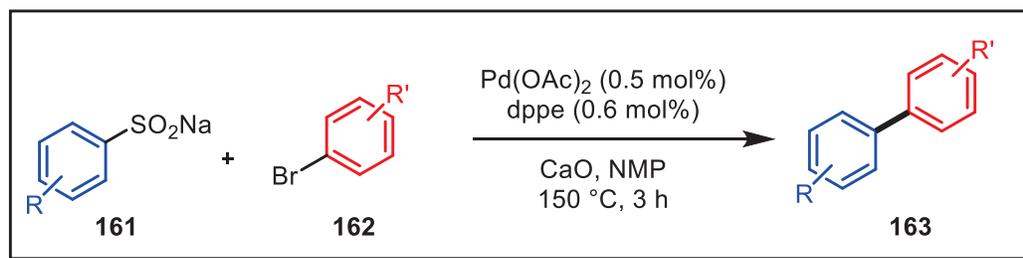
Figure 40 - Sato and Okoshi 1992: Desulfinative cross-coupling reported in a patent

In recent years, several publications have emerged describing aryl sulfinates as nucleophilic coupling partners. Duan and co-workers described the cross-coupling of aryl sulfinates and aryl triflates (**165**) (**Figure 41**).[63] The reaction employs Pd(OAc)$_2$ as the palladium source in an low catalyst loading of 2 mol% using XPhos as a ligand. The reaction proceeds at 120 °C for 24 hours in toluene. As sulfinates are not soluble in apolar solvents such as toluene, the reaction mixture is heterogeneous. Poor yields were obtained using nitro-substituted sulfinates and triflates, possibly due to an even lower solubility of nitro compounds in toluene as the author of

the paper suggests. The highest yields were obtained using electron-deficient *ortho*-substituted aryl triflates, a normally sterically challenging reaction.
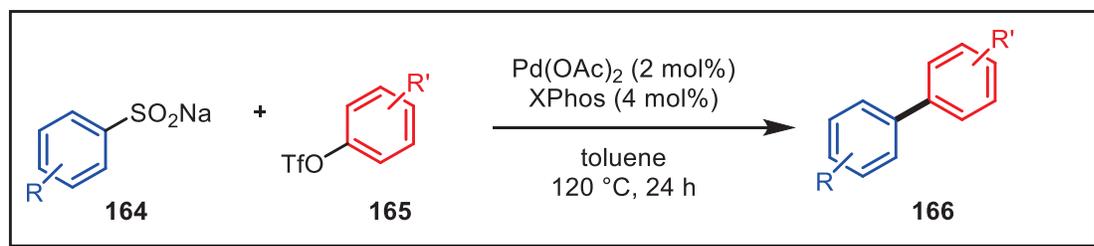
Figure 41 - Duan 2012: Cross-coupling of aryl sulfinates and aryl triflates

The cross-coupling of aryl sulfinates with aryl bromides was extended by the Forgione group.[64] The conditions developed allowed for a broad range of aryl sulfinates and aryl bromides. In these conditions the best yields were obtained using electron deficient aryl bromides and electron rich sulfinates, which was proposed to be due to facilitating oxidative addition and SO_2 extrusion. It was noticed that a common by-product of was the homo-coupling of the aryl sulfinate and when using electron rich aryl halides the formation of a sulfone via a S_NAr reaction. They were able to determine that sulfone formation was not an intermediate in the reaction and were able to propose a mechanism involving a direct desulfination (**Figure 42**).
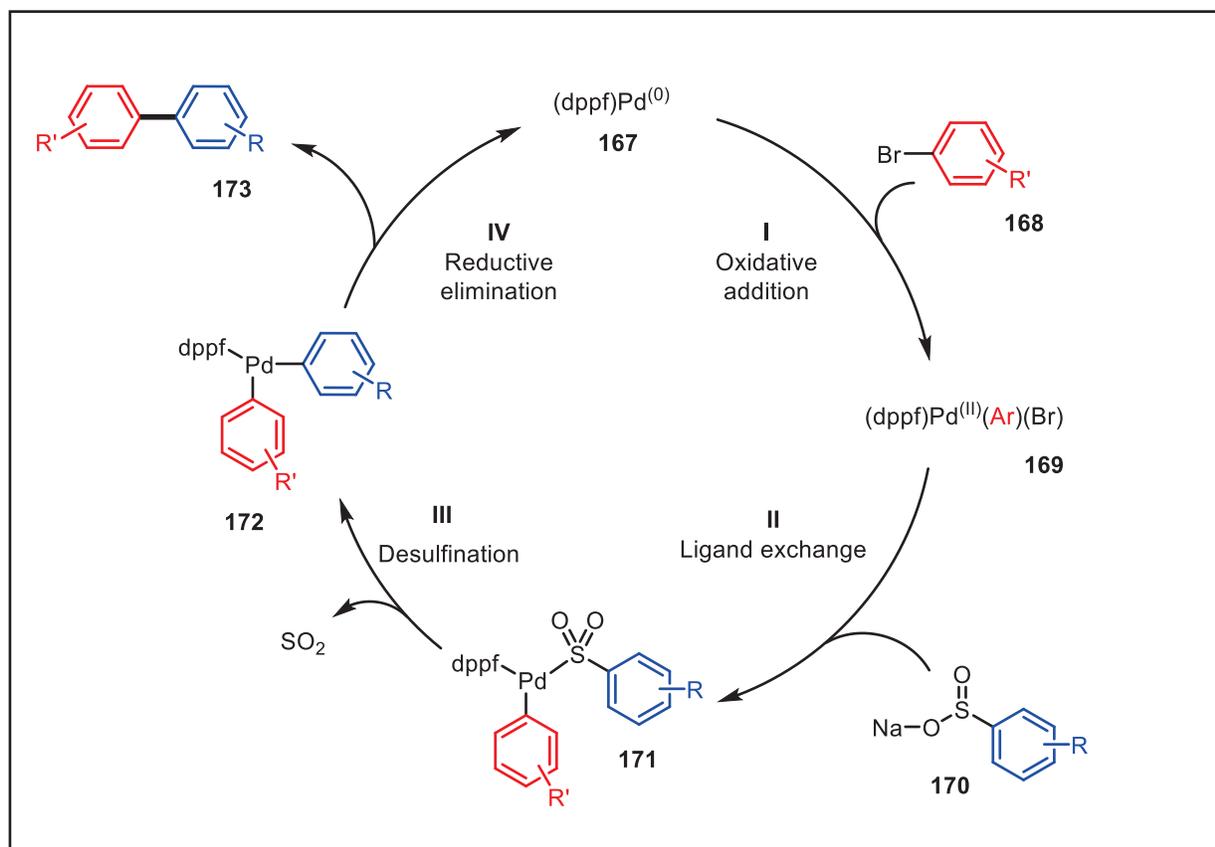
Figure 42 - Proposed mechanism for the palladium-catalyzed desulfinative cross-coupling of aryl sulfinates with aryl bromides

Similar to their decarboxylative cross-couplings, the reaction begins with the oxidative addition (**I**) of palladium (**167**) into the aryl halide (**168**) bond. This is followed by displacement (**II**) of the halide on the palladium species generating intermediate (**171**). The sulfonated palladium species (**171**) then undergoes a direct SO_2 extrusion (**III**) generating the biarylated palladium (**172**). Reductive elimination (**IV**) regenerates the palladium (0) catalyst (**167**) and releases the product (**173**). Further studies on the reaction revealed that the reaction was feasible without the need for a phosphine based ligand, therefore, improving the atom economy.[65]

1.3.4.1 Desulfinative Cross-Couplings of Heteroaromatic sulfinates with Aryl Halides

The desulfinative cross-coupling application was greatly expanded by Sévigny and Forgione by developing a method to couple heteroaromatic sulfinates with aryl halides.[66] This work parallels the work of Forgione in the decarboxylative cross-couplings. The work was able to reveal certain advantages of using sulfinates over their carboxylic acid counterpart. They demonstrated that the reaction could proceed in good to excellent yields without the use of additives, base, and could be performed in the presence of water.[67] Furthermore, the desulfinative reaction could be performed using unsubstituted 2-thiophenesulfinate salts, which was a challenge for the decarboxylative counter-part.
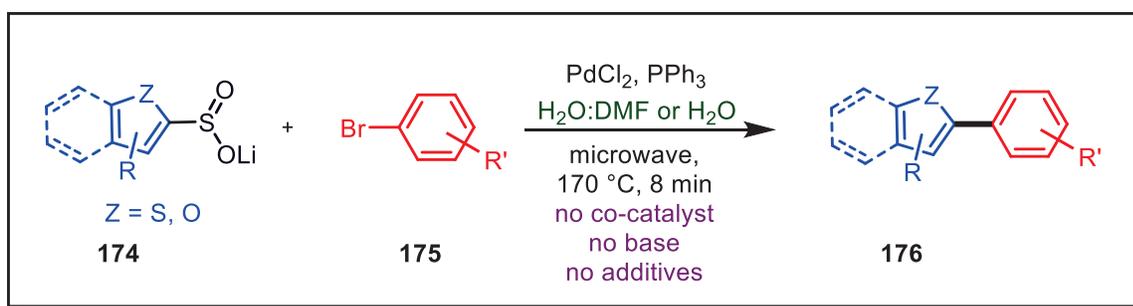
Figure 43 - Heteroaromatic desulfinative cross-coupling

The ability of the heteroaromatic desulfinative cross-coupling to tolerate aqueous conditions does not only greatly expand the versatility of the reaction, but as well, decreases the environmental impact. The environmental impact was also reduced as the solvent mixture would cause for immediate precipitation of the product, removing the need for extraction and the solvent waste associated with this step. Furthermore the precipitation of the product in the solvent could prove useful in large scale synthesis.

A possible mechanism was proposed for the palladium-catalyzed cross-coupling of heteroaromatics with aryl bromides (**Figure 44**). The proposed mechanism is similar to the

mechanism proposed by the decarboxylative cross-coupling of heteroaromatic carboxylic acids. As with the decarboxylation after oxidative addition (**I**), the heteroaromatic sulfinate (**180**) displaces a halide on the palladium species generating intermediate (**181**). This intermediate can then proceed via two pathways, pathway A involving a direct extrusion, or path B involving a electrophilic aromatic substitution reaction at the C2 position generating the transition state (**182**) which can then undergo desulfination to regain aromaticity. Both pathways lead to intermediate (**183**) that can undergo a reductive elimination releasing the product and regenerating the catalyst.
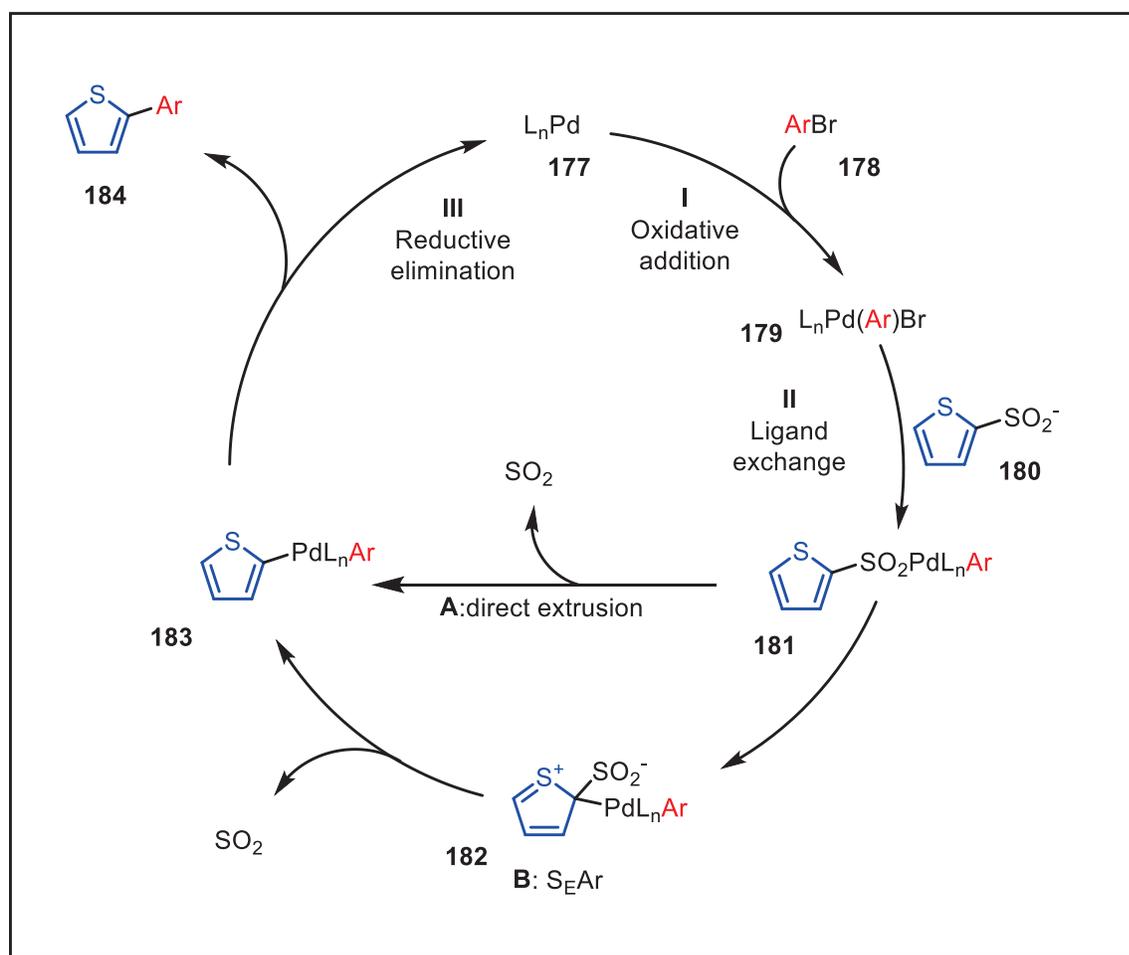
Figure 44 -Proposed mechanism for the desulfinative cross-coupling of heteroaromatics

The scope for the reaction is broad, and many sulfinates and aryl bromides are tolerated. The reaction scope was studied in both H_2O and H_2O:DMF (3:1) mixture with $PdCl_2$ and PPh_3.

Good yields were obtained with both solvent systems, however, H_2O:DMF (3:1) mixture had in general higher yields. Differently substituted methylthiophene sulfinates gave high yields. 3-methylthiophene-2-sulfinate was the most challenging substrate with a lower yield of 58 %. This was proposed to be due to steric constraints, that is, preventing efficient coordination of the sulfinates to palladium. Furan-2-sulfinate yielded the cross-coupling product in moderate yields for both solvent systems; however, benzofuran-2-sulfinate provided very good yields.

The aryl bromide scope was also evaluated. *ortho*, *meta*, and para aryl nitrile all gave high yields in both solvents. The weaker activating groups trifluoromethyl and ethyl esters resulted in a lowered yield. Electron neutral 4-bromonapthalene gave moderate yields while the electron rich 4-bromoanisol demonstrated poor yields under both conditions.

1.4 Thesis Organization

Chapter 1 of the thesis introduces the background in C-C bond formation via palladium-catalyzed cross coupling reactions. It outlines the history, importance, and development behind these cross-coupling reactions.

Chapter 2 discusses the palladium-catalyzed desulfinative cross-coupling of heteroaromatic sulfinates with aryl triflates in green solvents. These results were resultantly publish in The Journal of Heteroaromatic Chemistry.

Chapter 3 of the thesis analyses the palladium-catalyzed decarboxylative heteroaromatic cross-coupling mechanism. Here we investigate the different possible pathways for the mechanism and propose a mechanism based on experimental and DFT methods. This is a manuscript in progress.

Chapter 4 will summarize the work described in chapter 2 and 3 of the thesis. It will also describe future directions and applications.

Chapter 2 – Efficient Desulfinative Cross-Coupling of Heteroaromatic Sulfinates with Aryl Triflates in Environmentally Friendly Protic Solvents

2.1 Abstract

Aryl-substituted heteroaromatics were synthesized via desulfinative cross-coupling reactions using aryl triflate and heteroaromatic sulfinate coupling partners (**Figure 45**). This method uses synthetically versatile aryl triflates to access aryl-substituted heteroaromatics in good yields employing aqueous and alcoholic media without the use of base, additives or co-catalysts.
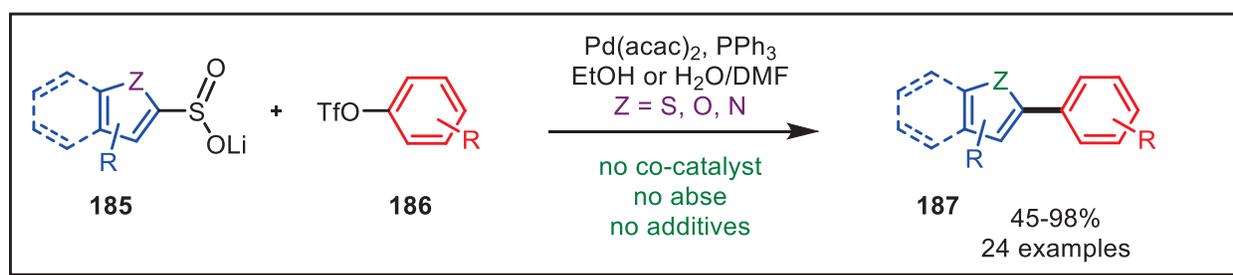
Figure 45 - Desulfinative cross-coupling of heteroaromatics with aryl triflates in green solvents

2.2 Introduction

Aryl-substituted heteroaromatics are a key motif in a variety of applications including medicinal chemistry,[68] natural products,[69] advanced materials,[70] and the agrochemical industry.[71] As a consequence of this versatility, these structures have attracted much attention of the scientific community in developing novel, efficient, methods for accessing these scaffolds. One method towards these structures is *via* desulfinative cross-couplings. This relatively new cross-coupling was shown to be an attractive alternative to the popular decarboxylative cross-couplings[72] and direct arylations[73] due to its more facile gas extrusion, chemoselectivity, and environmentally benign nature. Sulfinates can be readily synthesized from recycling the large amounts of SO_2 waste that is generated industrially.[74] The facile extrusion of SO_2 does not require a co-catalyst or extensive reaction times thus making the desulfinative cross-coupling[75]a-c of aryl

sulfinates[8d] an interesting alternative to classical methods. There are a few methods involving aryl sulfinates as nucleophilic coupling partners for palladium cross-coupling reactions.[76] Billard's group demonstrated desulfinative cross-couplings of haloquinolines with aryl-sufinates[76A] and Duan's group developed the desulfinative coupling of sodium aryl sulfinates with aryl bromides and chlorides (**Figure 46A**).[76B] Recently, we reported a cross-coupling protocol for the synthesis of aryl-substituted heteroaromatics utilizing heteroaromatic sulfinate salts and aryl bromides.[77] The cross-coupling was shown to proceed in good yields without the need of additives or base in H_2O/DMF (3:1) with $PdCl_2$ and PPh_3 (**Figure 46B**). Recently, Duan has developed conditions for the arylation of aryl sulfinates using aryl triflates in good yields (**Figure 46C**).[78] Similarly, many other groups have shown the successful use of aryl triflates in arylation processes,[79] however, there are only limited examples in aqueous solvents.[80] Replacing organic solvents by aqueous solutions is an asset for economic and environmental reasons. Nevertheless, most organic compounds and especially organometallic catalysts are not soluble in water. To further diversify our method, aryl triflates have been applied as the electrophilic desulfinative cross-coupling partner, an alternative to the aryl halide counterpart (**Figure 46D**).

These aryl triflates are attractive coupling partners due to their availability, low cost, and high yielding production. The phenol group is very common in organic synthesis and can be used to insert a new functional group on the aromatic ring as well as be converted into a new carbon-carbon bond. Due to the high abundance of the phenol functionality and the ease for its transformation into an aryl triflate, the versatility of the desulfinative palladium-catalyzed cross-coupling is increased tremendously.
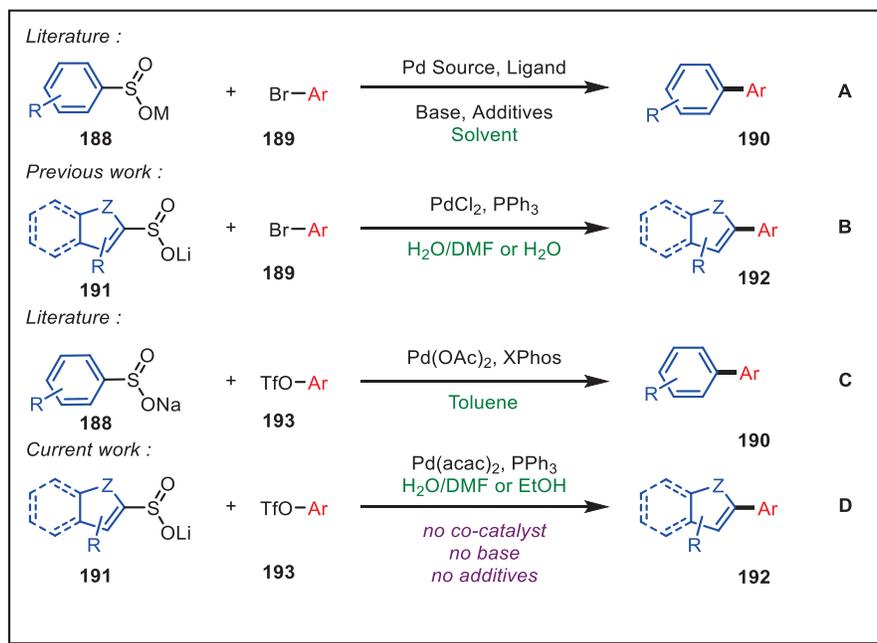
Figure 46 - Desulfinative cross-coupling reactions

2.3 Results and Discussion

Optimization of the desulfinative cross-coupling reaction began with the screening of different catalytic systems. The palladium source was first screened under the optimal conditions previously reported, H$_2$O:DMF (3:1) at 170 °C for 8 min under microwave irradiation.[77A] Lithium thiophene-2-sulfinate (**194a**) and 4-cyanophenyl triflate (**195b**) were chosen as coupling partners for the optimization of the reaction conditions (**Table 1**).

Table 1. Palladium Source and Ligand Screening
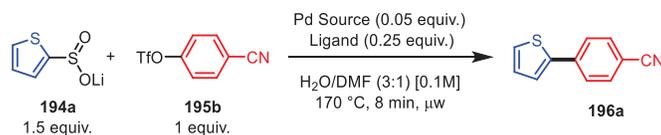
entry	Pd Source	Ligand	% Yield
1	Pd[P(^{t}Bu)$_3$]$_2$	-	trace[a]
2	PdCl$_2$	HP(^{t}Bu)$_3$BF$_4$	20[b]
3	PdCl$_2$	HP(^{t}Bu)$_2$MeBF$_4$	38[b]
4	PdCl$_2$	dppf	53
5	PdCl$_2$	HPCy$_3$BF$_4$	15[b]
6	PdCl$_2$	XPhos	39[c]
7	PdCl$_2$	^{t}BuXPhos	0[c]
8	PdCl$_2$	JohnPhos	42
9	PdCl$_2$	Me-DalPhos	0[c]
10	PdCl$_2$	Mor-DalPhos	0[c]
11	PdCl$_2$	PTh$_3$	70
12	PdCl$_2$	DPEphos	76
13	PdCl$_2$	TFP	80
14	PdCl$_2$	PPh$_3$	81
15	PdI$_2$	PPh$_3$	77
16	Pd(OAc)$_2$	PPh$_3$	79
17	Pd(acac)$_2$	PPh$_3$	86
18	Pd(TFA)$_2$	PPh$_3$	87
19	Petey[d]	PPh$_3$	88

[a]in DMF using 0.05 equiv. Pd[P(^{t}Bu)$_3$]$_2$; [b]using 0.25 equiv. Cs$_2$CO$_3$. [c]0.15 equiv. ligand; [d]Petey = Pd($\eta 3 - PhC_3H_4$)($\eta 5 - C_5H_5$).

The highly reactive Pd[P(^{t}Bu)$_3$]$_2$ only yielded a trace amount of the expected product (**Table 1, entry 1**). Promisingly, the generation of this catalyst *in situ* employing PdCl$_2$ and HP(^{t}Bu)$_3$BF$_4$ (**entry 2**) showed improved yield of the desired product that led us to screen a range of phosphine ligands (**entry 3-14**). The optimal yield was obtained using the inexpensive and readily available PPh$_3$ as the ligand (**entry 14**).

Table 2. Solvent Screening

Entry	Solvent	% Yield
1	H_2O:DMF (3:1)	86
2	H_2O	33
3	EtOH	72
4	iPrOH	56
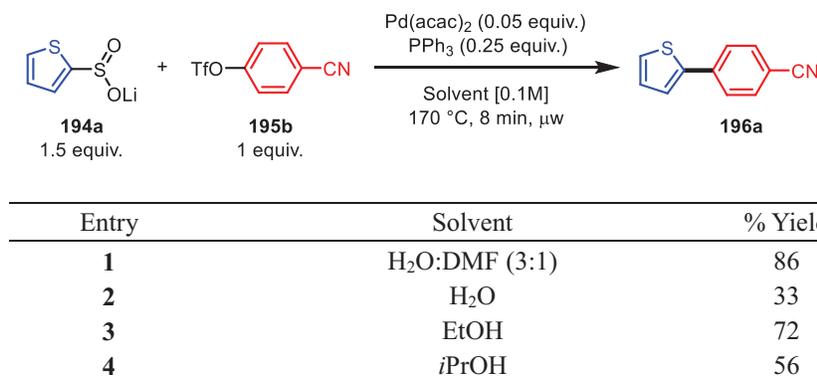
Having determined the optimal ligand, a range of palladium sources were also evaluated. Although slight variations in yield were observed (**entries 14-19**), Pd(acac)$_2$ and Pd(TFA)$_2$ were found to be the optimal palladium sources when used in conjunction with PPh$_3$. Further optimization would be carried out using the less expensive Pd(acac)$_2$.

Although the H_2O/DMF yielded the desired product in good yield (**Table 2, entry 1**), the presence of significant amounts of DMF makes the water more difficult to purify and consequently recycle.[81] Unfortunately, the coupling in pure water occurs in moderate yield (**entry 2**), which indicates that DMF may play a role in solubilizing all reagents. The use of alcoholic solvents (**entries 3-4**) is attractive, because they are biodegradable[82] and readily available from biomass.[83] There are a variety of applications of alcoholic solvents in synthetic organic chemistry,[84] many involving cross-coupling reactions.[85] Despite their potential attractiveness as a solvent, no significant work has been carried out on decarboxylative or desulfinative palladium-catalyzed cross-coupling reactions. In order to develop the desulfinative cross-coupling employing a green solvent system, that may improve the solubility of reagents when compared to pure water, protic solvents EtOH and iPrOH were selected for evaluation.[82] The preliminary results

employing EtOH (**entry 3**) and *i*PrOH (**entry 4**), although lower than those obtained in the H₂O/DMF solvent mixture, provided encouraging yields and the benefit of being single solvent systems that would be easier to subsequently purify. As such, further optimizations were carried out with both these solvents.

Table 3. Screening of Reaction Conditions in Alcoholic Solvents
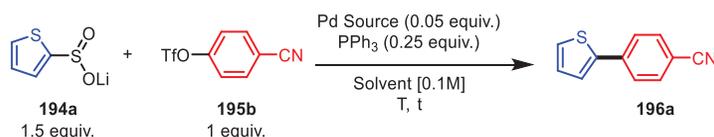
Entry	T (ºC)	Pd Source	t	Solvent	% Yield
1	170 µw	Pd(acac)₂	8 min	*i*PrOH	56
2		Pd(acac)₂	8 min	EtOH	72
3		Pd(acac)₂	15 min	*i*PrOH	68
4		Pd(acac)₂	30 min	*i*PrOH	41
5	150 µw	Pd(acac)₂	26 min	EtOH	74
6		Pd(acac)₂	1 h	EtOH	89
7		Pd(acac)₂	2 h	EtOH	80
8	120 µw	Pd(acac)₂	4 h	EtOH	71
9	120 Δ	Pd(acac)₂	19 h	EtOH	89
10	150 Δ	Pd(TFA)₂	2 h	EtOH	56
11	150 Δ	Pd(TFA)₂	3 h	EtOH	54

Employing Pd(acac)₂ in conjunction with PPh₃ in EtOH or *i*PrOH, the temperature, time, and heating method were optimized. Although increasing reaction times to 170 ºC in the microwave did not prove beneficial (**Table 3, entries 1-4**), when the reaction temperature was reduced to 150 ºC (**entries 5-7**), an important improvement in cross-coupling yield to 89% was observed (**entry 6**). Further reducing the reaction temperature to 120 ºC while increasing the reaction time to 4 h did not prove beneficial when performed in the microwave (**entry 8**). However when performed thermally and extending the reaction time to 19 h, an excellent yield of 89% was

obtained   (**entry 9**). Other attempts at thermal conditions (**entries 10-11**) using Pd(TFA)$_2$ did not show any increased yield. Having determined the optimal heating conditions in EtOH using the microwave at 150 ºC for 1 h, and using H$_2$O/DMF (3:1) at 170 °C for 8 min, these two conditions were applied in a study of heteroaromatic sulfinate substrate scope.

While employing the H$_2$O/DMF solvent system, good to excellent yields were obtained (**Table 4**), however, in all cases, equal or better yields were obtained when using ethanol as the solvent. As demonstrated in the table, benzo[*b*]thiophene-2-sulfinate (**194b, entry 2**) and benzo[*b*]furan-2-sulfinate (**194g, entry 7**) provided the corresponding product in the highest yield. Interestingly, the unsubstituted sulfinate (**194a, entry 1**) led to a reduced yield. Methyl-substituted thiophenes (**194c-e, entries 3-5**) provided the corresponding cross-coupling product in good yields in EtOH, however, 2-methylthiophene (**entry 5**) provided much better yields in EtOH in comparison with the H$_2$O/DMF mixture, highlighting the significant advantage of EtOH in certain cases. Furan-2-sulfinate (**194f, entry 6**) also provided the corresponding product in very good yields, but the pyridine-2-sulfinate gave only moderate yield (**194g, entry 8**). Although EtOH generated the cross-coupling products with consistently higher yields, using the H$_2$O/DMF system also proved to be efficient, highlighting the complementary nature of these solvents systems. Other aryl triflate coupling partners bearing electron donating groups were investigated to emphasize the versatility of this methodology. Electrophilic coupling partners with electron donating groups have been known to undergo palladium-mediated cross-couplings less efficiently.[10] This was also observed under our modified conditions, especially when considering the most challenging 4-methoxyphenyl triflate (**195d, entries 9 and 10**). However, thiophene-2-sulfinate (**194a**) underwent cross-coupling with 3-methoxyphenyl triflate (**195c, entry 11**) in a very good yield of the corresponding product. In both cases, the yields observed were moderate to very good, further

demonstrating that the method can be efficient with both electron-donating groups and electron-withdrawing groups on the aromatic ring of the triflate coupling partner

Table 4. Heteroaromatic Sulfinate Scope

Entry	Product		Solvent	
			EtOH[a]	H$_2$O/DMF[b] (3:1)
1	196a		86%	86%
2	196b		95%	71%
3	196c		77%	53%
4	196d		85%	70%
5	196e		79%	10%
6	196f		82%	74%
7	196g		89%	75%
8	196h		61%	20%
9	196i		45%	-
10	196j		50%[c]	-
11	196k		80%	-
12	196l		58%[c]	-

[a]150 °C, 1 h, microwave irradiation; [b]170 °C, 8 min, microwave irradiation; [c] 2.0 equiv. of sulfinate, 1.0 equiv. of aryl triflate; 0.1 equiv. of Pd(acac)$_2$, 0.5 equiv. of PPh$_3$.

To summarize, the reported conditions generate industrially interesting aryl-susbsituted heteroaromatic products using versatile aryl triflates as a coupling partners in alcoholic and

aqueous media. The use of biodegradable EtOH as the solvent proved to be efficient by providing a range of heteroaromatic bi-aryls in moderate to excellent yields. This green solvent system provided improved results overall than the H_2O/DMF mixture. This process provides an economical and green alternative to other available methods using aryl triflates for palladium-catalyzed cross-coupling reactions of heteroaryl sulfinates with aryl triflates and has potential for further development.

2.4 Experimental

All anhydrous flasks were flame-dried while under high-vacuum and purged with argon unless otherwise stated. Solids were weighed on a balance open to air and added to a round-bottom flask or microwave vial unless otherwise noted. Liquids were transferred using a glass syringe with a stainless steel needle or a micropipette for µL volumes unless noted otherwise. Manual flash chromatography columns were carried out using 40-63 µm silica gel from Silicycle. All reagents purchased are from Sigma-Aldrich or Alfa Aesar and used without further purification unless otherwise noted. All solvents were purchased as ACS grade from Fischer Scientific or JT Baker unless otherwise noted. Anhydrous solvents were dried and stored in a flame-dried Schlenk flask using 3 Å molecular sieves, which were activated by heating at 150 ºC under high vacuum overnight. Distilled water was obtained from an in-house distillery. Unless otherwise noted, reactions were performed using a Biotage Initiator 2.3 build 6250 microwave. Purifications by flash column chromatography were performed using a Teledyne Isco CombiFlash® Rf unless mentioned otherwise. Proton nuclear magnetic resonance spectra (^{1}H NMR) were measured at 500 MHz using a Varian VNMRS-500 in CDCl3 unless stated otherwise. Carbon nuclear magnetic resonance spectra (^{13}C NMR) were measured at 125 MHz using the Varian VNMRS-500 in CDCl3 unless stated otherwise. The chemical shifts are reported in parts per million (ppm) and referenced

from either residual solvent or the tetramethylsilane (TMS) signal. The multiplicity is represented as; s = singlet, d = doublet, t = triplet, q = quartet and m = multiplet which is indicated in parentheses along with the number of protons and coupling constants (in Hz). Gas chromatograph-mass spectral analyses (GC-MS) were obtained using an Agilent 7890A GC system and Agilent 5975C VL MSD with Triple-Axis MS Detector with a HP-588 column coated with (5%-phenyl)-methylpolysiloxane.

2.4.1 General procedure for the synthesis of heteroaromatic lithium sulfinates

To a dried, rubber septum capped flask, under an argon stream, equipped with a magnetic stir bar and cooled to -78 ºC was added the heteroaromatic (1.0 equiv.) with anhydrous Et_2O (0.3 M). After 20 min, with stirring, *tert*-butyllithium (0.9 equiv.) was added slowly with a glass syringe over 5 min. The reaction was stirred for 2 h while maintaining a temperature of -78 ºC. The reaction was then quenched by bubbling SO_2 produced from general procedure (B) for the generation of anhydrous sulfur dioxide for 1 h, while warming to 23 ºC, precipitating the sulfinate salt. The salt was isolated *via* vacuum filtration, washed thoroughly with Et_2O followed by acetone, and dried under vacuum. The solid was then ground to a fine powder, to which Et_2O was added, and sonicated for 10 min, followed by vacuum filtration and drying under high vacuum. Heteroaromatic lithium sulfinates 194a-1g[10] and 194h[22] correspond to what was reported previously in the literature.

2.4.2 General procedure for the generation of anhydrous sulfur dioxide

To a three-neck flask equipped with a magnetic stir bar, sodium sulfite or sodium metabisulfite (1.0 equiv.) and water were added. Concentrated sulfuric acid (1.0 equiv.) was added

drop-wise, with stirring, from a capped pressure-equalized addition funnel. The gas generated was then scrubbed twice *via* diffusion through concentrated sulfuric acid.

2.4.3 General procedure for the arylation of heteroaromatic lithium sulfinates with aryl triflate

To a 5 mL conical microwave vial equipped with a spin-vein was added heteroaromatic sulfinate (0.30 mmol, 1.5 equiv.), aryl triflate (0.20 mmol, 1.0 equiv.), Pd(acac)$_2$ (0.01 mmol, 0.05 equiv.) and PPh$_3$ (0.05 mmol, 0.25 equiv.). 2 mL of either EtOH or 3:1 H$_2$O:DMF were added and the vial was pre-stirred for 30 sec at 23 ºC followed by appropriate heating (see Table 4). The crude cross-coupling solution was diluted with EtOAc (5 mL). The organic layer was washed with a saturated NaCl aqueous solution (2x 5 mL), saturated NaHCO$_3$ aqueous solution (2x 5 mL), distilled H$_2$O (1x 5 mL), and saturated NaCl aqueous solution (1x 5 mL). The combined aqueous phases were washed with EtOAc (3x 5 mL). The combined organic phases were dried over Na$_2$SO$_4$ and after filtration the solvent evaporated under reduced pressure and the solid residue was purified by flash column chromatography.

2.4.4 Characterization

4-(Thiophen-2-yl)benzonitrile (196a). The above compound was prepared from general procedure (C) on a 0.20 mmol (37.05 mg) scale. ^{1}H NMR (500 MHz, CDCl$_3$) δ 7.69 (d, J = 8.4 Hz, 2H), 7.65 (d, J = 8.4 Hz, 2H), 7.42 (dd, J = 3.5, 0.9 Hz, 1H), 7.40 (dd, J = 5.1, 1.0 Hz, 1H), 7.13 (dd, J = 5.0, 3.7 Hz, 1H) ppm. ^{13}C NMR (126 MHz, CDCl$_3$) δ 142.2, 138.8, 132.9 (2C), 128.7, 127.2, 126.2 (2C), 125.2, 119.0, 110.7 ppm.

4-(Benzo[*b*]thiophen-2-yl)benzonitrile (196b). The above compound was prepared from general procedure (C) on a 0.20 mmol (47.06 mg) scale. ^{1}H NMR (500 MHz, CDCl$_3$) δ 7.84 (dd, *J* = 6.4, 2.1 Hz, 1H), 7.81 (dd, *J* = 6.6, 2.4 Hz, 1H), 7.77 (d, *J* = 8.2 Hz, 2H), 7.64 (s, 1H), 7.42 – 7.35 (m, 2H) ppm. ^{13}C NMR (126 MHz, CDCl$_3$) δ 141.8, 140.4, 140.1, 138.7, 132.8 (2C), 126.8 (2C), 125.5, 125.1, 124.3, 122.5, 121.9, 118.7, 111.5 ppm.

4-(5-Methylthiophen-2-yl)benzonitrile (196c). The above compound was prepared from general procedure (C) on a 0.20 mmol (39.85 mg) scale. ^{1}H NMR (300 MHz, CDCl$_3$) δ 7.61 (s, 4H), 7.22 (d, *J* = 3.6 Hz, 1H), 6.78 (dd, *J* = 3.6, 1.1 Hz, 1H), 2.53 (d, *J* = 0.8 Hz, 3H) ppm. ^{13}C NMR (126 MHz, CDCl$_3$) δ 142.3, 139.7, 139.0, 132.8 (2C), 126.9, 125.6 (2C), 125.2, 119.1, 110.0, 15.7 ppm.

4-(4-Methylthiophen-2-yl)benzonitrile (196d). The above compound was prepared from general procedure (C) on a 0.20 mmol (39.85 mg) scale. ^{1}H NMR (300 MHz, CDCl$_3$) δ 7.64 (d, *J* = 1.8 Hz, 4H), 7.23 (d, *J* = 1.1 Hz, 1H), 6.99 – 6.96 (m, 1H), 2.30 (d, *J* = 0.8 Hz, 3H) ppm. ^{13}C NMR (126 MHz, CDCl$_3$) δ 141.8, 139.3, 138.9, 132.8 (2C), 127.5, 125.9 (2C), 122.7, 119.0, 110.5, 15.9 ppm.

4-(3-Methylthiophen-2-yl)benzonitrile (196e). The above compound was prepared from general procedure (C) on a 0.20 mmol (39.85 mg) scale. ^{1}H NMR (500 MHz, CDCl$_3$) δ 7.70 – 7.67 (m, 2H), 7.59 – 7.55 (m, 2H), 7.30 (d, *J* = 5.1 Hz, 1H), 6.96 (d, *J* = 5.1 Hz, 1H), 2.36 (s, 3H) ppm. ^{13}C

NMR (126 MHz, CDCl$_3$) δ 139.6, 135.8, 135.1, 132.4 (2C), 131.8, 129.3 (2C), 125.3, 119.0, 110.6, 15.3 ppm.

4-(Furan-2-yl)benzonitrile (196f). The above compound was prepared from general procedure (C) on a 0.20 mmol (33.64 mg) scale. ^{1}H NMR (300 MHz, CDCl$_3$) δ 7.74 (d, J = 8.7 Hz, 2H), 7.65 (d, J = 8.8 Hz, 2H), 7.54 (dd, J = 1.8, 0.6 Hz, 1H), 6.81 (dd, J = 3.4, 0.6 Hz, 1H), 6.53 (dd, J = 3.5, 1.8 Hz, 1H) ppm. ^{13}C NMR (126 MHz, CDCl$_3$) δ 152.1, 143.8, 134.78, 132.72 (2C), 124.0 (2C), 119.1, 112.4, 110.4, 108.3 ppm.

4-(Benzo[b]furan-2-yl)benzonitrile (196g). The above compound was prepared from general procedure (C) on a 0.20 mmol (43.85 mg) scale. ^{1}H NMR (500 MHz, CDCl$_3$) δ 7.95 – 7.92 (m, 2H), 7.73 – 7.70 (m, 2H), 7.63 (ddd, J = 7.7, 1.2, 0.6 Hz, 1H), 7.54 (dd, J = 8.3, 0.8 Hz, 1H), 7.36 (ddd, J = 8.4, 7.3, 1.3 Hz, 1H), 7.30 – 7.26 (m, 1H) ppm. ^{13}C NMR (126 MHz, CDCl$_3$) δ 155.4, 153.7, 134.6, 132.7 (2C), 128.8, 125.7, 125.2 (2C), 123.6, 121.6, 118.9, 111.65, 111.56, 104.5 ppm.

4-(Pyridin-2-yl)benzonitrile (196h). The above compound was synthesized following general procedure (C) on a 0.20 mmol (45 mg) scale. ^{1}H NMR (500 MHz, CDCl$_3$) δ 7.57 – 7.54 (m, 4H), 6.93 – 6.89 (m, 4H) ppm. ^{13}C NMR (126 MHz, CDCl$_3$) δ 159.7, 152.0, 134.3 (2C), 122.6, 119.2, 117.1, 116.3 (2C), 112.8, 103.7, 29.7 ppm.

2-(4-Methoxyphenyl)thiophene (196i). The above compound was synthesized following general procedure (C) on a 0.20 mmol (46 mg) scale ale. ^{1}H NMR (500 MHz, CDCl$_3$) δ 7.55 – 7.54 (m, 1H), 7.54 – 7.52 (m, 1H), 7.20 (ddd, J = 4.7, 4.3, 1.2 Hz, 2H), 7.05 (dd, J = 5.1, 3.6 Hz, 1H), 6.95 – 6.89 (m, 2H), 3.84 (s, J = 2.8 Hz, 3H) ppm. ^{13}C NMR (126 MHz, CDCl$_3$) δ 159.2, 143.2, 128.1, 127.4, 127.4, 124.0, 122.49, 122.21, 115.2, 114.4, 55.9 ppm.

2-(4-Methoxyphenyl)benzo[b]thiophene (196j). The above compound was synthesized following general procedure (C) on a 0.20 mmol (61 mg) scale. ^{1}H NMR (500 MHz, CDCl$_3$) δ 7.82 – 7.79 (m, 1H), 7.74 (dd, J = 7.7, 1.1 Hz, 1H), 7.66 – 7.63 (m, 2H), 7.43 (d, J = 0.5 Hz, 1H), 7.35 – 7.32 (m, 2H), 7.30 – 7.28 (m, 1H), 6.98 – 6.94 (m, 2H), 3.86 (s, 3H) ppm. ^{13}C NMR (126 MHz, CDCl$_3$) δ 127.8 (2C), 124.93, 124.80, 124.44, 123.94, 123.73, 123.25, 122.2, 121.4, 118.2, 114.4 (2C), 55.4 ppm.

2-(3-Methoxyphenyl)thiophene (196k). The above compound was synthesized following general procedure (C) on a 0.20 mmol (46 mg) scale. ^{1}H NMR (500 MHz, CDCl$_3$) δ 7.31 (dd, J = 3.6, 1.2 Hz, 1H), 7.29 (s, 1H), 7.28 – 7.27 (m, 1H), 7.21 (ddd, J = 7.7, 1.7, 1.0 Hz, 1H), 7.15 – 7.14 (m, 1H), 7.08 (dd, J = 5.1, 3.6 Hz, 1H), 6.84 (ddd, J = 8.2, 2.5, 0.9 Hz, 1H), 3.86 (s, 3H) ppm. ^{13}C NMR (126 MHz, CDCl$_3$) δ 160.1, 144.4, 135.9, 130.0, 128.1, 125.0, 123.4, 118.7, 113.1, 111.8, 55.4 ppm.

2-(3-Methoxyphenyl)benzo[b]thiophene (196l). The above compound was synthesized following general procedure (C) on a 0.20 mmol (61 mg) scale. ^{1}H NMR (500 MHz, CDCl$_3$) δ 7.84 – 7.81

(m, 1H), 7.79 – 7.76 (m, 1H), 7.54 (d, J = 0.6 Hz, 1H), 7.37 – 7.29 (m, 4H), 7.26 – 7.24 (m, 1H), 3.89 (d, J = 1.9 Hz, 3H) ppm. ^{13}C NMR (126 MHz, CDCl$_3$) δ 160.01 144.2, 140.7, 139.6, 135.8, 130.10 124.6, 124.5, 123.7, 122.4, 119.8, 119.2, 113.9, 112.3, 55.5 ppm.

2.5 Acknowledgements

Chapter 3: Towards the Understanding of the Mechanism for the Decarboxylative Cross-Coupling of Heteroaromatics

3.1 Abstract

The mechanism for the palladium-catalyzed decarboxylative cross-coupling of heteroaromatics with aryl halides was investigated using DFT studies. The initial, transitional, and final states of all transformations in the catalytic system were evaluated for several model reactions. It was determined that the rate-limiting step was the decarboxylation and the energy barrier for this transformation was dependent on the carboxylic acid substrate and ligand system. The decarboxylation is proposed to proceed *via* an electrophilic aromatic substitution reaction where using the nucleophilic nature of the heteroaromatic to coordinate with the palladium at the C2-position forms a transition state that can then undergo decarboxylation. The proposal was validated by comparing computational results with experimental data.

3.2 Introduction

Palladium-catalyzed decarboxylative couplings have become a powerful alternative to the more traditional methods for the formation of carbon-carbon bonds.[86] In particular, the last decade has seen the development of a multitude of catalytic transformations utilizing the carboxylic acid moiety to generate a variety of interesting scaffolds.[48] In these transformations a carboxylic acid (**197**) (**Figure 47**) can be coupled with an electrophilic aromatic partner (**198**) in the presence of a palladium catalyst.
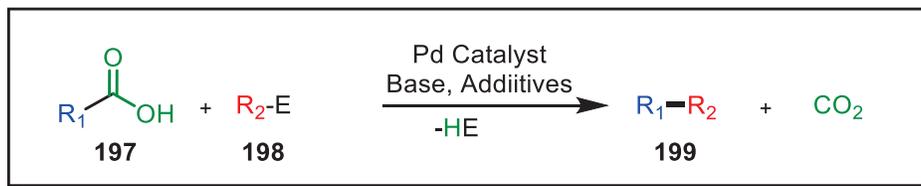
Figure 47 - General Decarboxylative Cross-Coupling

These reactions have generated significant interest in the scientific community mainly due to the inexpensive nature, broad availability, and long-term stability of carboxylic acids.[87] The replacement of the organometallic coupling partner with a carboxylic acid allows for several synthetic advantages such as greater functional group tolerance, a reduction in toxic metallic by-products, and an increase in atom efficiency. However, the difficulty connected to the use of carboxylic acids as coupling partners is in the high energy required for the decarboxylative transformation. Typically, carboxylates require rather forcing conditions in order to achieve CO_2 extrusion; however, various groups have developed approaches to overcome this limitation. Methods to overcome the high energy barrier involve the use of co-catalyst,[51] harsh conditions,[88] and the use of activated substrates such as electron deficient benzoic acids[89] or heteroaromatic carboxylic acids, which will be the focus of this paper.[47]

Several groups have been able to model their palladium-catalyzed decarboxylative cross-coupling systems using computational techniques (**Figure 48**).[90] In 2010 Liu reported on the decarboxylation of polyflurobenzoates (**200**) with aryl halides, and studied the mechanism using DFT (**Figure 48A**).[91] Here, the use of electron-deficient polyfluorobenzoic acids activates the carboxylic acid sufficiently to overcome the energy barrier for decarboxylation. Using DFT to model their system, they determined the rate-limiting step is the decarboxylation with an energy

barrier of 24.1 kcal/mol. The decarboxylative transition state geometry 201 proceeded *via* a concerted mechanism with all of the atoms on the arene carboxylate coplanar 201.
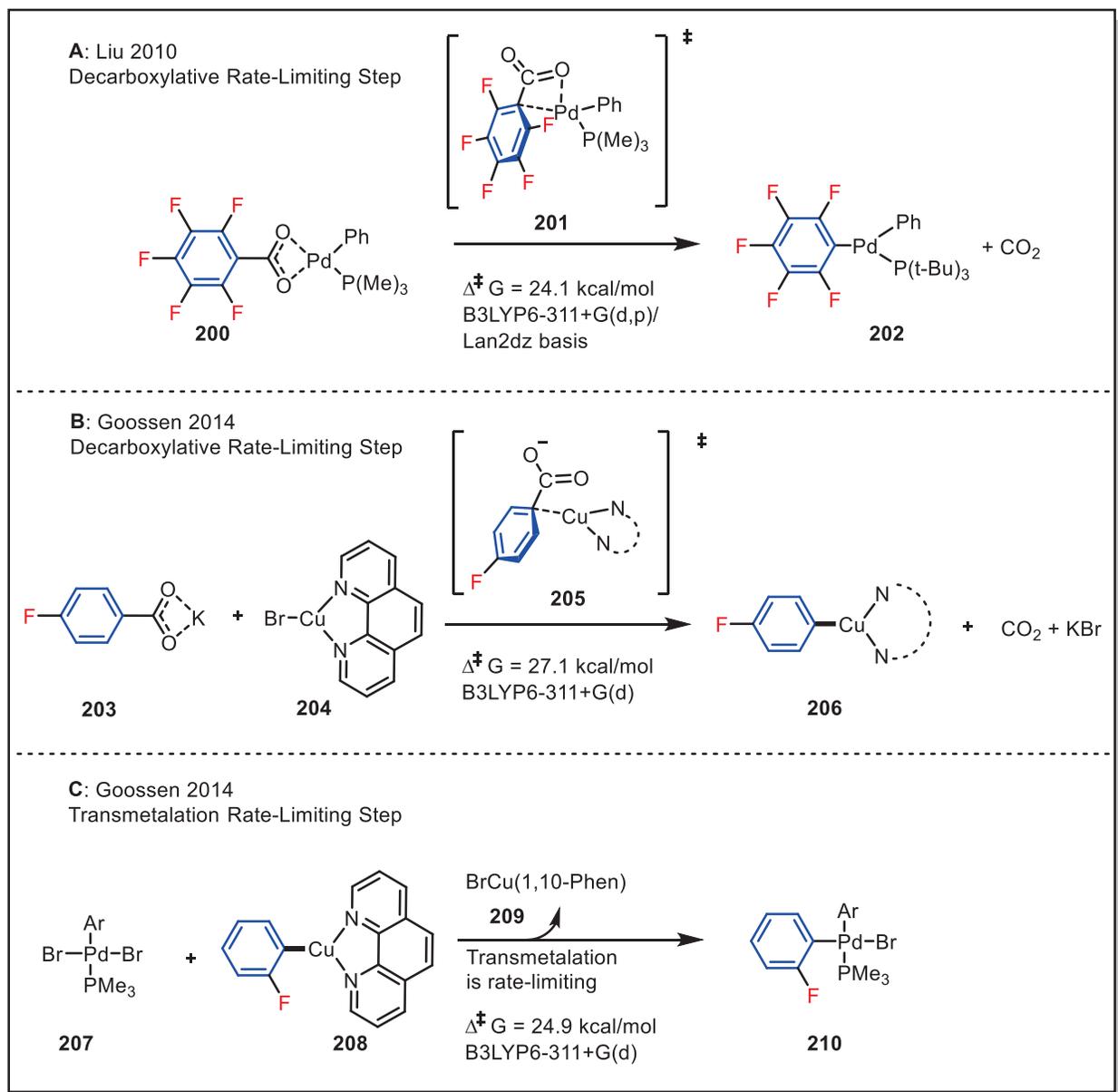
Figure 48 - DFT investigations on the rate limiting step for decarboxylative cross-couplings

Goossen *et al.* were able to propose a plausible mechanism for the Cu/Pd-catalyzed decarboxylative cross-coupling of potassium 2- and 4-fluorobenzoate (**203, 207**) with

bromobenzene.[53] Mechanistic studies on these copper/palladium bimetallic systems have shown that copper promotes CO_2 extrusion to generate an organocuprate species (**206**), which acts as the nucleophilic species to attack the palladium catalyst. They proposed that the decarboxylation and the transmetalation have rather similar activation energies that depends on the individual substrates for which of these steps will be rate-determining (**Figure 48B-C**).

Heteroaromatics carboxylic acids can also be used in palladium-catalyzed couplings with extrusion of CO_2 where the heteroaromatic facilitates the decarboxylative step. In 2009, Forgione proposed possible mechanisms that take into consideration the involvement of the heteroaromatic in the decarboxylative step.[54] Herein, we discuss the mechanism of the palladium-catalyzed decarboxylative cross-coupling of heteroaromatics carboxylic acids with aryl halides through the use of DFT (**Figure 49**).
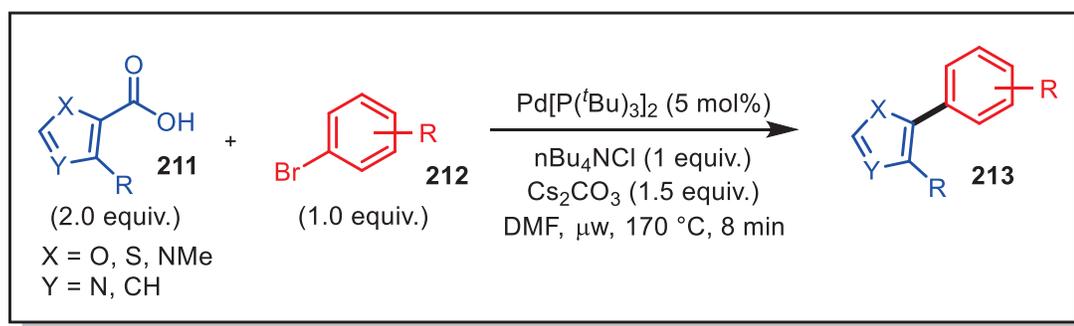
Figure 49 - Palladium-catalyzed heteroaromatic decarboxylative cross-couplings

3.3 Model Systems

In this investigation, several catalytic systems were modeled. All transformations of the catalytic cycle was modeled using the substrates furan-2-carboxylic acid and bromobenzene in the presence of Pd(PMe₃)₂. Experimentally furan-2-carboxylic acid is a difficult substrate that typically results in moderate yields, therefore can reveal some of the difficulties of this reaction.

The key step in the catalytic cycle is the decarboxylation, therefore a variety of different carboxylic acids were investigated to gain insight into the mechanism for this transformation. For computational simplification the PMe$_3$ ligand was used to model all the catalytic steps in order to reduce the complexity, while for the decarboxylation transformation additional studies were performed using the experimentally used P(t-Bu)$_3$ ligand. Further studies were performed for the decarboxylation using a variety of different carboxylic acids.

The catalytic cycle (**Figure 50**) was used as a starting point based on the mechanism previously proposed by Forgione. Several groups have shown that this is a typical mechanism for a decarboxylative cross-coupling.[49, 53] While the majority of the steps are similar to other palladium-catalyzed cross-coupling reactions, the mechanism for the decarboxylation is highly dependent on the substrates and reactants used. The proposed mechanism begins with the Pd(0) species (**214**) undergoing an oxidative addition into an aryl-halide bond resulting in the formation of the Pd (II) species (**216**). Displacement of the bromide by the heteroaromatic carboxylate (**217**) forms the key intermediate (**218**). This palladated carboxylate can then undergo three possible pathways. Pathway A is a direct decarboxylation, which forms the intermediate (**219**) after CO$_2$ extrusion. This species then undergoes a reductive elimination releasing the product (**220**) and regenerating the Pd (0) catalyst. Pathways B and C proceed *via* an electrophilic aromatic substitution reaction (S$_E$Ar) where the nucleophilic nature of the heteroaromatic can attack the palladium species. Pathway B proceeds *via* a nucleophilic attack from the C2 position of the heteroaromatic to the palladium complex generating the transition state (**221**). This can then re-aromatize by undergoing a decarboxylation resulting in the previously mentioned intermediate (**219**). Pathway C is similar to path B, however, was proposed to rationalize the 2,3-diarylated side product observed (**220** R = Ar). In this case the nucleophilic attack occurs at the C3 position over

generating the transition state (**222**). In a scenario where the R group is a hydrogen, deprotonation can occur in order to regain aromaticity, generating the C3 palladated intermediate (**223**). This intermediate can then undergo a reductive elimination regenerating the catalyst and releasing the C3 arylated-heteroaromatic carboxylate (**224**). This carboxylate can then re-enter the catalytic cycle to generate the 2,3-diarylated side-product.
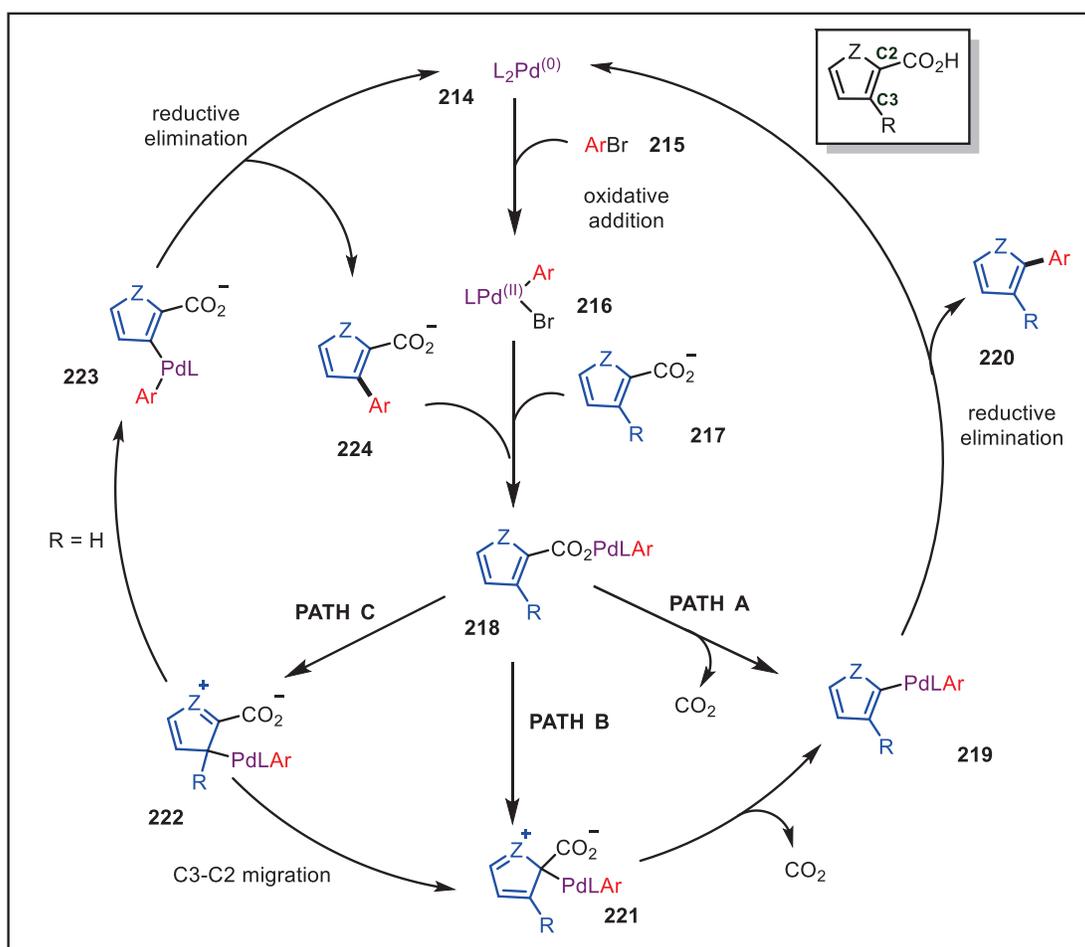
Figure 50 - Original mechanism proposed by Forgione

The primary focus in modeling the catalytic cycle will be placed on the decarboxylation, as a large amount of research has already been reported on oxidative addition,[92] ligand exchange,[93] and reductive elimination.[94]

3.4 Computational Methods

Calculations were carried out with the use of two software packages, FHI-aims[95] was used for all transition state searches and VASP was used to calculate implicit solvation energies. Transition state searches were performed using the aimsChain code included in the FHI-aims package. All geometries for initial and final states were optimized for isolates gas-phase molecules using the B3LYP exchange-correlation functional with the tight basis set included with FHI-aims. Transition states were located using the Nudged Elastic Band (NEB) method with a minimum of 6 images per transformation. All final transition states were calculated using the climbing image method with a tight convergence setting having a force threshold below 0.03 eV.

3.5 Modeling the Catalytic Cycle with DFT

3.5.1 Oxidative Addition and Ligand Exchange
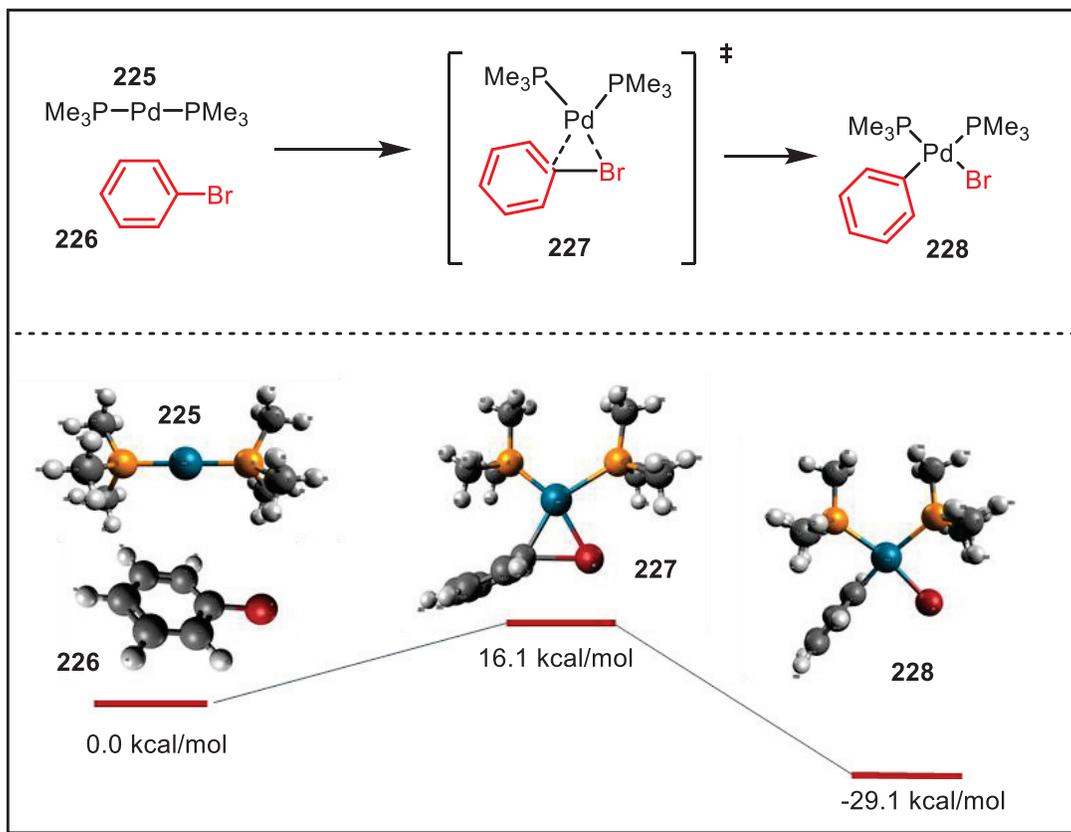
Figure 51 - Energy profile for the oxidative addition of bromobenzene and Pd(PMe3)2

The catalytic cycle begins with oxidative addition of Pd(PMe$_3$)$_2$ (**225**) into the halogen-carbon bond in bromobenzene (**226**). This proceeds *via* the Pd(0) species approaching the carbon-bromine bond to form a bridged complex (**227**) that represents the transition state. As the Pd-Br and the Pd-C bond begin to form, the phosphine ligands are pushed away forming a square planar geometry about the palladium center (**228**). The activation barrier (16.1 kcal/mol) for this reaction is relatively low and is in agreement to values previously reported.[96] The overall process is

strongly exothermic (-29.1 kcal/mol) and under the typical reaction conditions, oxidative addition would be expected to proceed with relative ease.

The next step in the catalytic cycle is the ligand exchange, where the cesium heteroaromatic carboxylate salt (**229**) displaces a bromide on the palladium species (**230**). The coordination of the heteroaromatic cesium carboxylate to the palladium species is highly favorable (-22.4 kcal/mol). From this intermediate (**231**), the carboxylate coordinates to the palladium (**233**) releasing CsBr (**232**). Evidence for the formation of the palladium carboxylate (**233**) has been observed using NMR techniques.[93]
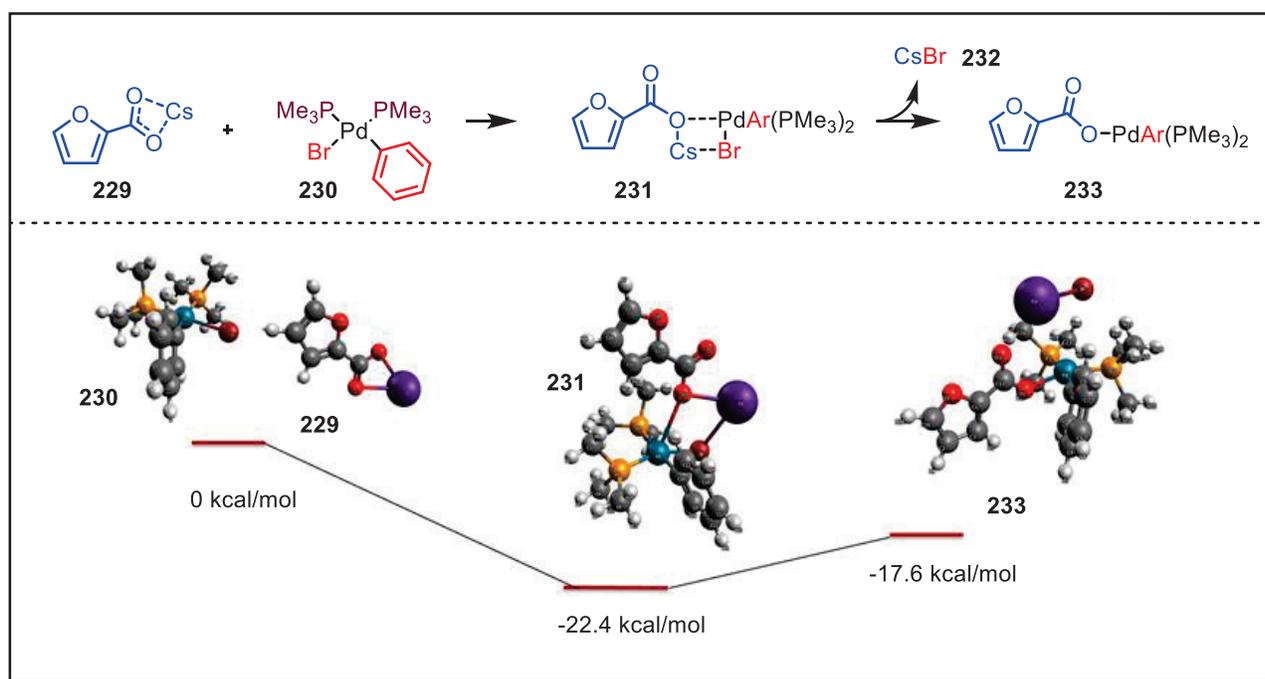
Figure 52 - Energy profile for the ligand exchange

3.5.1 Decarboxylation

The decarboxylation step for a cross-coupling reaction has been the subject of previous DFT studies however, no study has been performed on the decarboxylative cross-coupling of heteroaromatics with aryl halides.[51] We set out to compare the energies of possible pathways for the heteroaromatic decarboxylative cross-coupling, as well as compare computational data to experimental results.

3.5.1.1 Decarboxylation with PMe₃ as Ligand
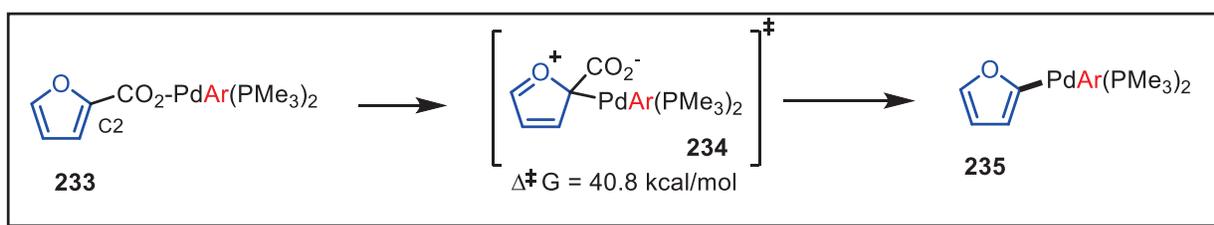
Figure 53 - Decarboxylation of furan-2-carboxylate by PdAr(PMe₃)₂

Exhaustive transition state searches found that the lowest energy pathway proceeded *via* an S_EAr-like transition state where palladium would migrate from coordinating to the carboxylate to coordinating to the C2 position of the furan-2-carboxylic acid (**234**). The activation energy in this transition (40.8 kcal/mol) was relatively high, however, still feasible for a reaction performed at 170 °C. The reaction is endothermic by 7.7 kcal/mol (**Figure 54**).
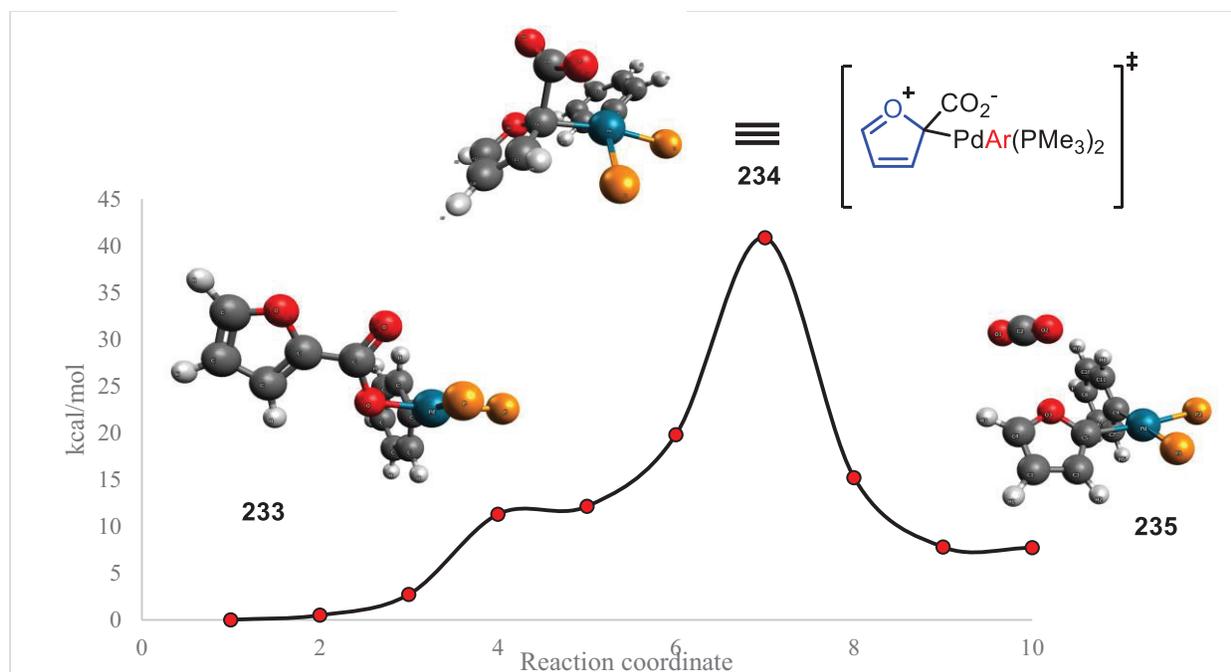
Figure 54 - Energy profile for the decarboxylation of furan-2-carboxylate by PdAr(PMe₃)₂. Ligand groups have been omitted for clarity.

In the transition state (**234**) both the palladium and the carboxylate are bonded to the C2 position of the furan ring. The C2 carbon appears to have a sp^3 hybridization further supporting the $S_E Ar$ mechanism. While this system provided a reasonable energy and geometry, it does not represent the conditions used experimentally. In order to model a system that more closely resembles those obtained experimentally, PMe₃ ligands were modified to the P(*t*-Bu₃) ligand.

3.5.1.2 Decarboxylation with monocoordinated P(t-Bu)$_3$

$\Delta^{\ddagger}G = 36.5$ kcal/mol
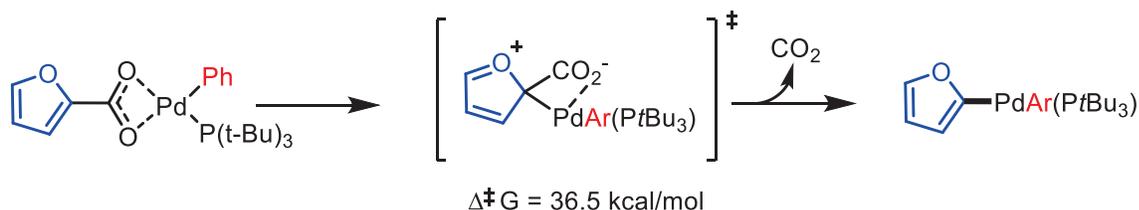
Figure 55 - Decarboxylation of furan-2-carboxylate with PdAr(P*t*Bu$_3$)

The use of PMe$_3$ as a starting point for our calculations proved useful in understanding the mechanism in a simplified system and in reducing the computational load associated with these calculations minimizing the total amount of atoms in the system. While a good starting point, it does not provide us with a precise representation of the system as decarboxylative cross-couplings typically use large bulky ligands that provide the highest yields. As ligands greatly effect experimental yields, this is important to take into consideration when looking for transition states. The ligand of choice for the heteroaromatic decarboxylative cross-coupling is P(*t*-Bu)$_3$.

While for the smaller PMe$_3$ system, the decarboxylation was modeled with two phosphine ligands, for the bulky P(*t*-Bu)$_3$ ligand it was modeled with only one phosphine ligand. A number of experimental and computational studies on systems that utilize bulky phosphine ligands, such as P(*t*-Bu)$_3$, have shown that the most relevant catalytically active species for these systems is the mono-ligated palladium.[97] The ligand loss is thought to occur during oxidative addition resulting in a tri-coordinated palladium (**Figure 56**).
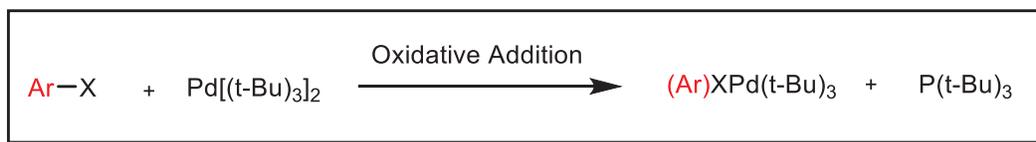
Figure 56 - Ligand loss during oxidative addition

Transition state searches starting from species (**236**) resulted in a similar transition state geometry (**237**) to that found for the Pd(PMe$_3$)$_2$ species (**233**) (**Figure 54**). The C2 position of the furan (**237**) has a distorted sp^3 geometry. The C-C bond between the C2 position and the carboxylate carbon has elongated from 1.47 Å to 1.87 Å while the C2-Pd bond begins to form at a distance of 2.21 Å and finishes at 1.99 Å. The Pd-C-C angle is 89.5 °, distorted from an idealized 109.5 °. The energy barrier for the transformation is 36.5 kcal/mol, which as expected, is lower than the transition state using PMe$_3$ (40.8kcal/mol).
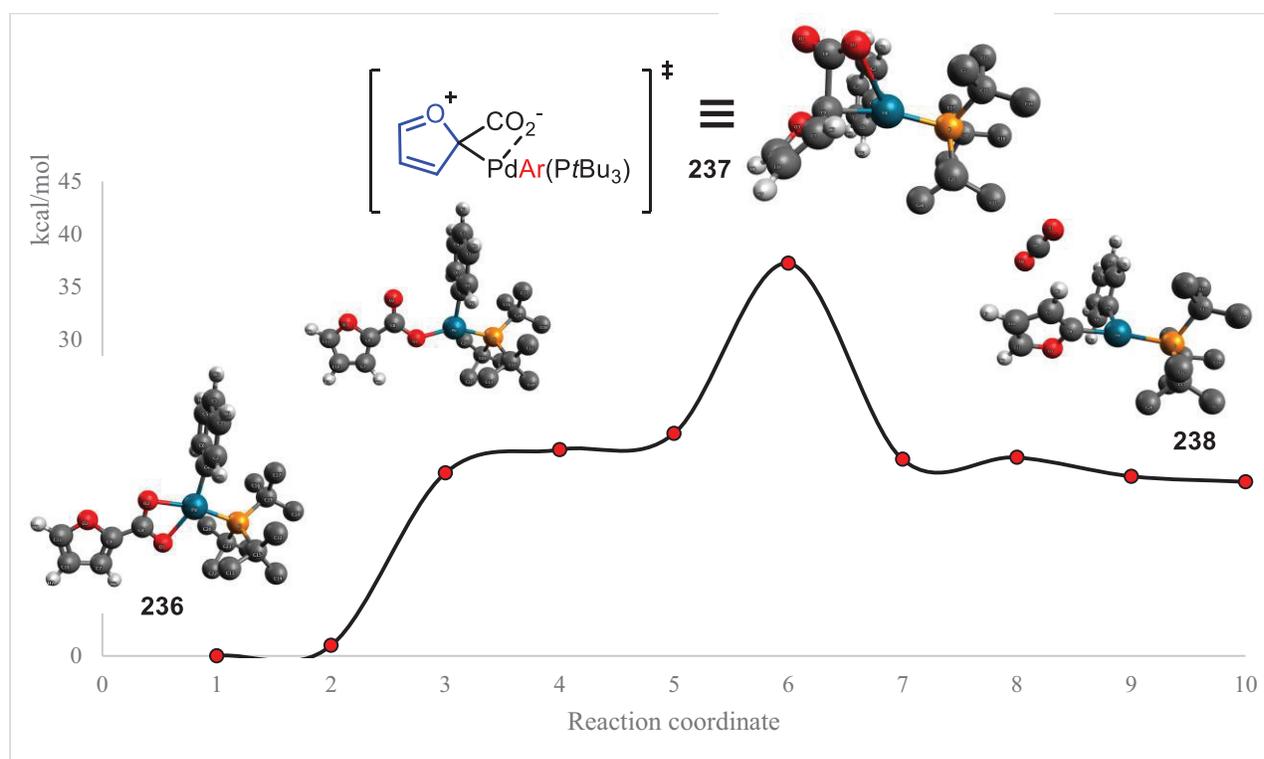
Figure 57 - Profile for the decarboxylation of furan-2-carboxylate catalyzed by Pd(P*t*-Bu$_3$)$_3$

In the catalyst system with PMe$_3$ the carboxylate coordinates *via* a single oxygen to the palladium, however, when using the P(*t*-Bu)$_3$ catalyst, the open coordination site on the palladium allows for both oxygens of the carboxylate to coordinate to the palladium (**Figure 58**). Furthermore

the open coordination site allows for carboxylate to continue to coordinate with the palladium in the transition state **(237)**
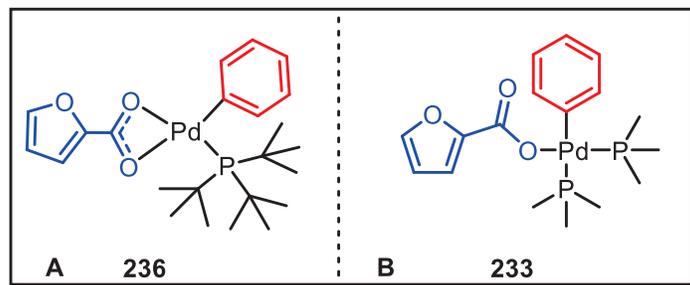
Figure 58 - (A) Coordination of carboxylate to mono-ligated PdPh(P*t*-Bu₃) (B) Coordination of carboxylate to di-ligated PdPh(PMe₃)

The first step in the mechanism is breaking the coordination of one of the oxygens and the rotation of the furan ring to allow for decarboxylation (**Figure 57**). Following this, the complex can access the transition state and undergo decarboxylation to form **(237)**. The transformation occurs as an endothermic process, where the product **(238)** is 16.3 kcal/mol higher in energy than the starting material. The reaction is considered an irreversible reaction since CO_2 is extruded from the mixture. Even though these reactions are typically carried out in a sealed reaction vessel, at 170 °C the effective concentration of CO_2 dissolved in DMF is negligible.[98]

3.5.1.3 Decarboxylation of 1-Methyl-2-Pyrrolecarboxylate
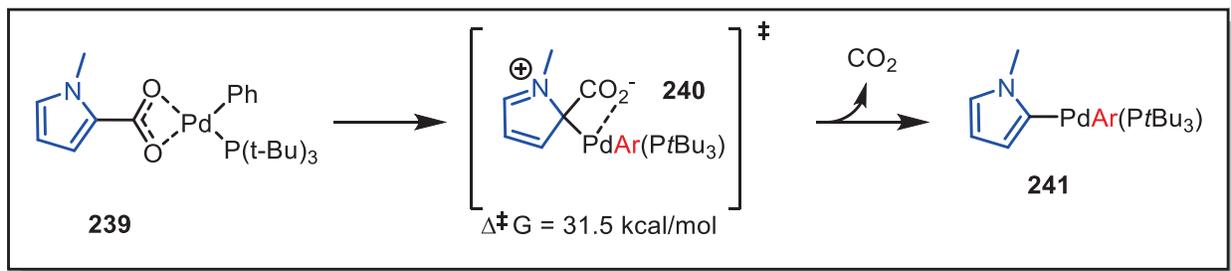
Figure 59 - Decarboxylation of 1-methyl-2-pyrrolecarboxylate by PdPh(Pt-Bu$_3$)

Initial results were focused on the decarboxylation of furan-2-carboxylic acid, which experimentally is challenging as the yields are quite low. Investigating different heteroaromatic carboxylic acids allows us to paint a more complete picture of the mechanism. 1-Methyl-2-pyrrolecarboxylate (**239**) is the ideal reactant as typically yields are high. The energy barrier for the decarboxylation of (**239**) was calculation to be 31.5 kcal/mol, which is lower than the barrier for furan-2-carboxylic acid (**236**) (36.5 kcal/mol). This can explain the differences in yields observed experimentally between these substrates.
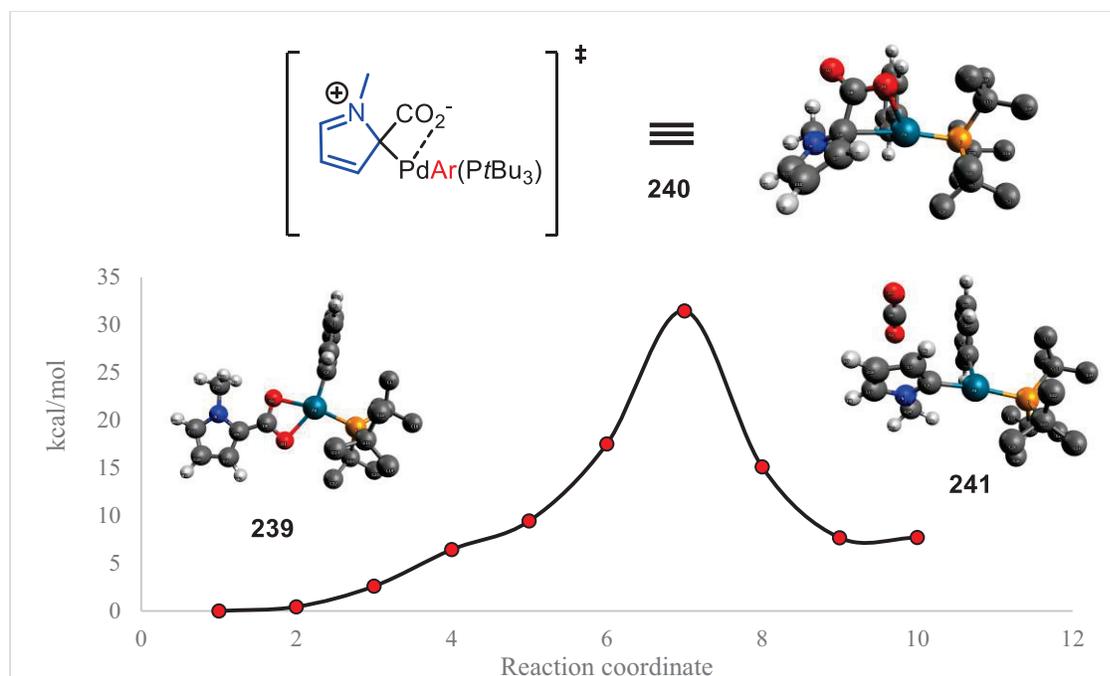
Figure 60 - Energy profile decarboxylation of 1-methyl-2-pyrrolecarboxylate by PdPh(P*t*-Bu₃)

The lowered energy barrier for the pyrrole carboxylic acid versus the furan carboxylic acid may be explained by the relative reactivity of these heteroaromatics towards electrophiles. It has been shown that pyrroles are more reactive towards electrophiles than furans.[99] This would affect the ability of the heteroaromatic carboxylic acid to form the S_EAr transition state (**240**). The more nucleophilic the heteroaromatic is, the more accessible the transition state will be. To further test this theory, the transition state energy for benzoic acid was calculated as benzoic acid is known to react slower than heteroaromatics with electrophiles in the absence of a co-catalyst.

3.5.1.4 Benzoic Acid
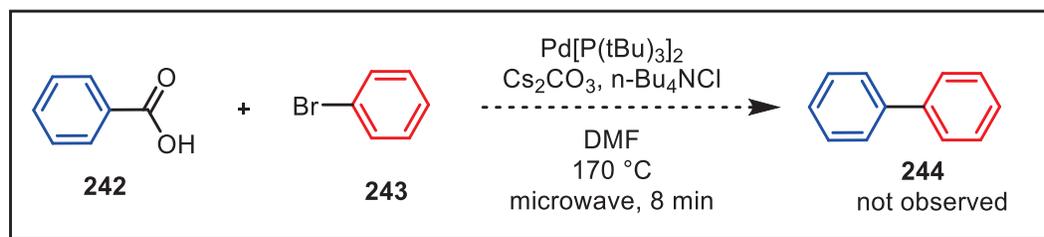
Figure 61 - Attempted decarboxylative cross-coupling of benzoic acid with bromobenzene

Under the standard reactions conditions benzoic acid does not form the intended cross-coupling product (**Figure 61**). This lack of reactivity exhibited by benzoic acid provides insight into the reaction mechanism. As previously mentioned, the proposed mechanism for heteroaromatic carboxylic acids undergoes a $S_E Ar$ type mechanism which takes advantage of the nucleophilicity of heteroaromatic rings at the C2 position. The nucleophilicity of benzene has been shown to be substantially lower than that of a heteroaromatic.[100] To further support our postulated mechanism, the reaction profile of benzoic acid decarboxylation was investigated using DFT (**Figure 62**).
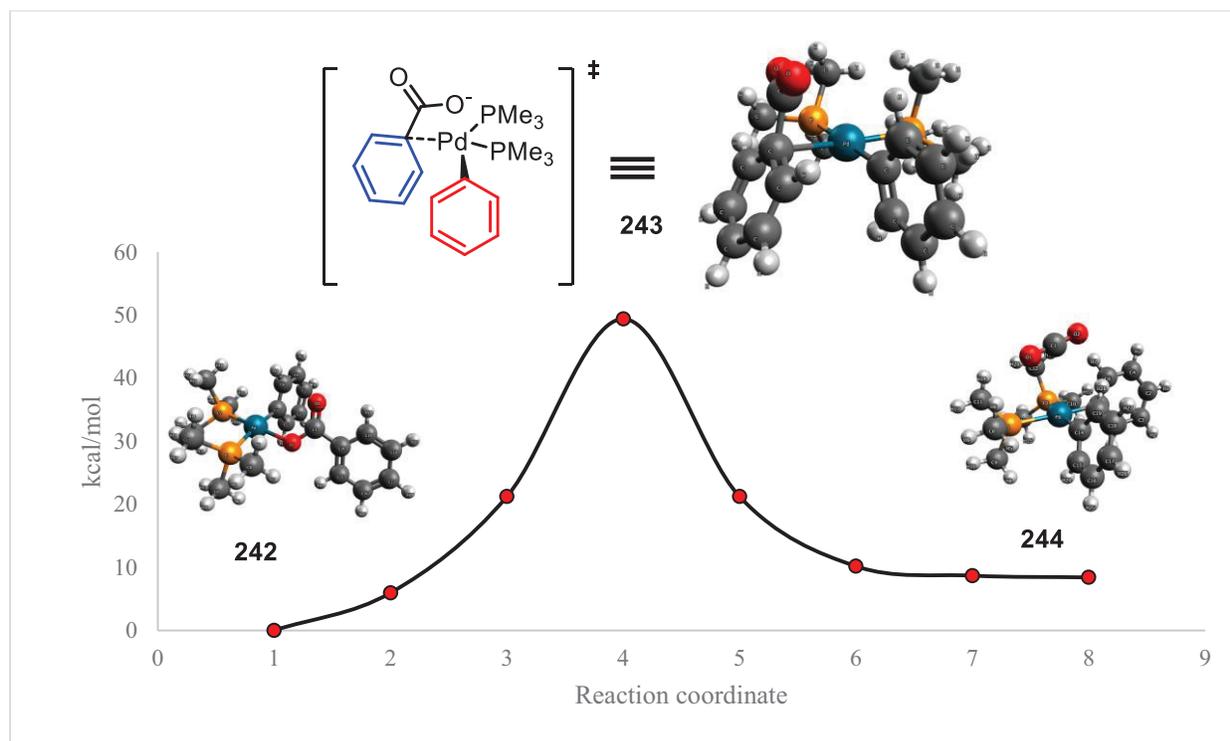
Figure 62 - Energy profile for decarboxylative cross-coupling of benzoic acid with bromobenzene

The reaction profile for the decarboxylation of benzoic acid is shown above. The energy barrier (49.4 kcal/mol) is substantially higher than that of the heteroaromatic counter parts (31.5 kcal/mol for **239**). Interestingly, the transition state (**243**) for this reaction proceeds *via* a different geometry than the heteroaromatic transition states. Unlike the transition states for the

heteroaromatics, the geometry of the ring remains planar and only upon decarboxylation does the Pd-C bond form. This is more indicative of a direct CO_2 extrusion rather than a S_EAr mechanism.

3.5.1.5 Furan-3-carboxylic acid

The inability of benzoic acid to behave as a coupling partner demonstrates the importance of the heteroatom under these conditions, however, the presence of a heteroatom alone does not guarantee that a cross-coupling will occur. This can be seen in the reaction between furan-3-carboxylic acid (**245**) and phenyl bromide (**246**) where under the standard conditions the intended cross-coupling product (**247**) is not observed (**Figure 63**). Similar to the benzoic acid example, significant mechanistic insight can be deduced. This demonstrates that both the presence and position of the heteroatom are important with respect to the carboxylic acid.
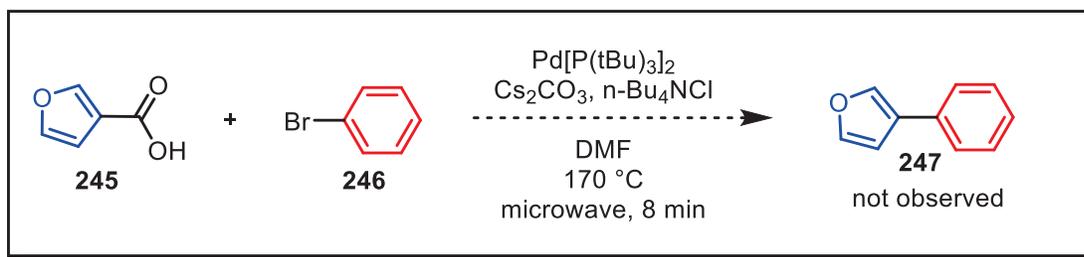
Figure 63 - Attempted decarboxylative cross-coupling of furan-3-carboxylic acid with bromobenzene

A number of studies have shown that furans have an increased propensity to undergo electrophilic aromatic substitution at the C2 position over the C3 position.[40] This is in part due to the C2 position having a greater mesomeric stabilization for the transition state (**Figure 64**).
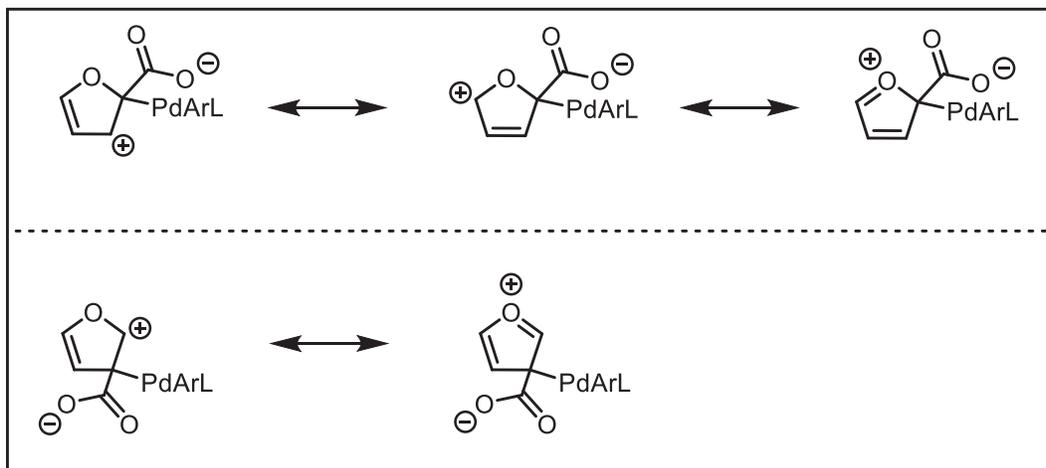
Figure 64 - Mesomeric isomers for furan carboxylic acids

As our proposed transition state requires a nucleophilic attack of the heteroaromatic to the palladium species, at the same position of the carboxylic acid, the C3 position is likely not a strong enough nucleophile. This offers an explanation as to why furan-3-carboxylic acid does not result in the cross-coupling product. Computational studies on the decarboxylation of furan-3-carboxylic acid supports this argument (**Figure 65**).
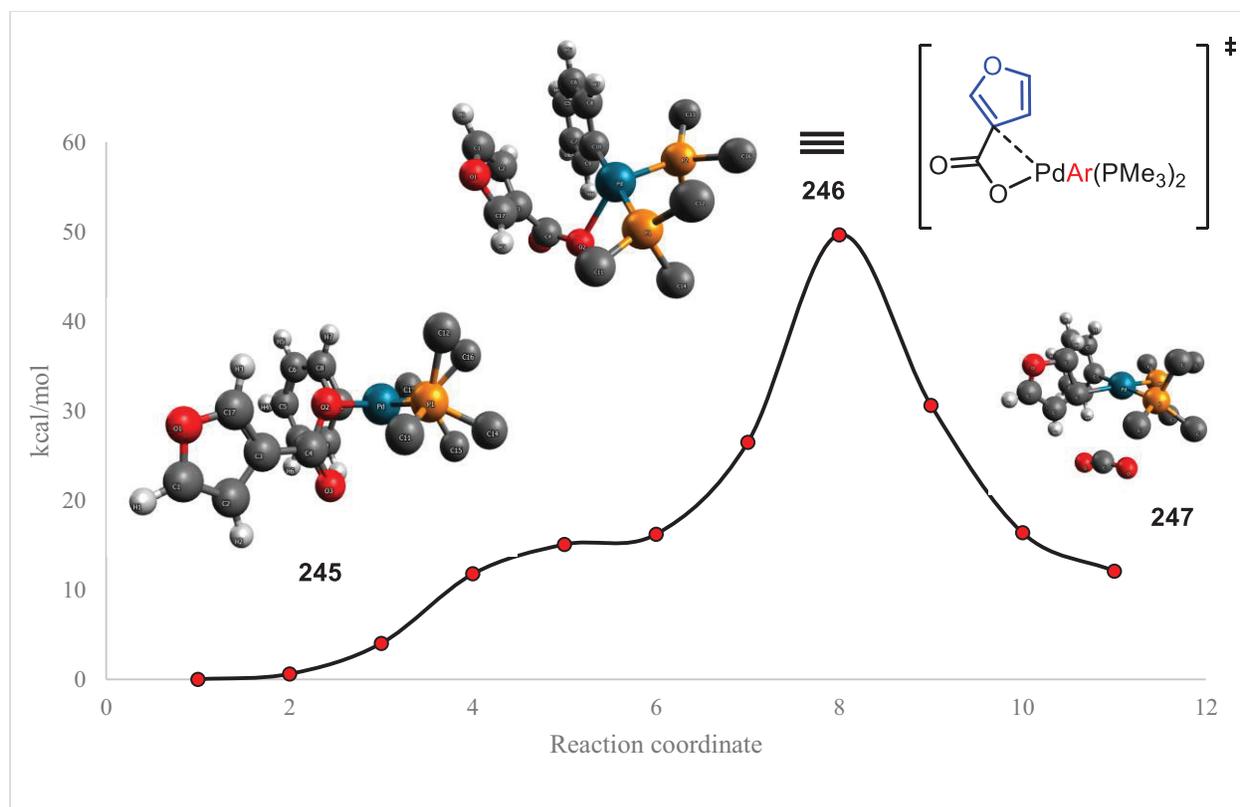
Figure 65 - Energy profile for decarboxylative cross-coupling of furan-3-carboxylic acid with bromobenzene

The energy barrier for this decarboxylation was determined to be 49.6 kcal/mol, a value, similar to the benzoic acid example, much higher than the energies for transition states involving decarboxylation at the C2 position of the heteroaromatic. This results in an energy barrier that is too great to overcome for a reaction performed at 170 °C. The transition state (**246**) does not resemble that of a S_EAr-like mechanism, but proceeds in a concerted fashion to generate (**247**).

3.5.1.6 Comparison of experimental kinetic data to theoretical

To further support our proposed mechanism, competition experiments were compared to computational data. To evaluate the effect of varying electron richness a competition experiment was carried out where electron-rich and -poor analogues of 5-arylfuran-2-carboxylic acid were subjected to the standard reaction conditions in a 1:1 molar ratio (**Figure 66A**). It was found that

a ratio of 1.8:1 favoring the electron rich substrate (**248b**) was obtained. The reaction profiles for these substrate were also calculated (**Figure 66B**).
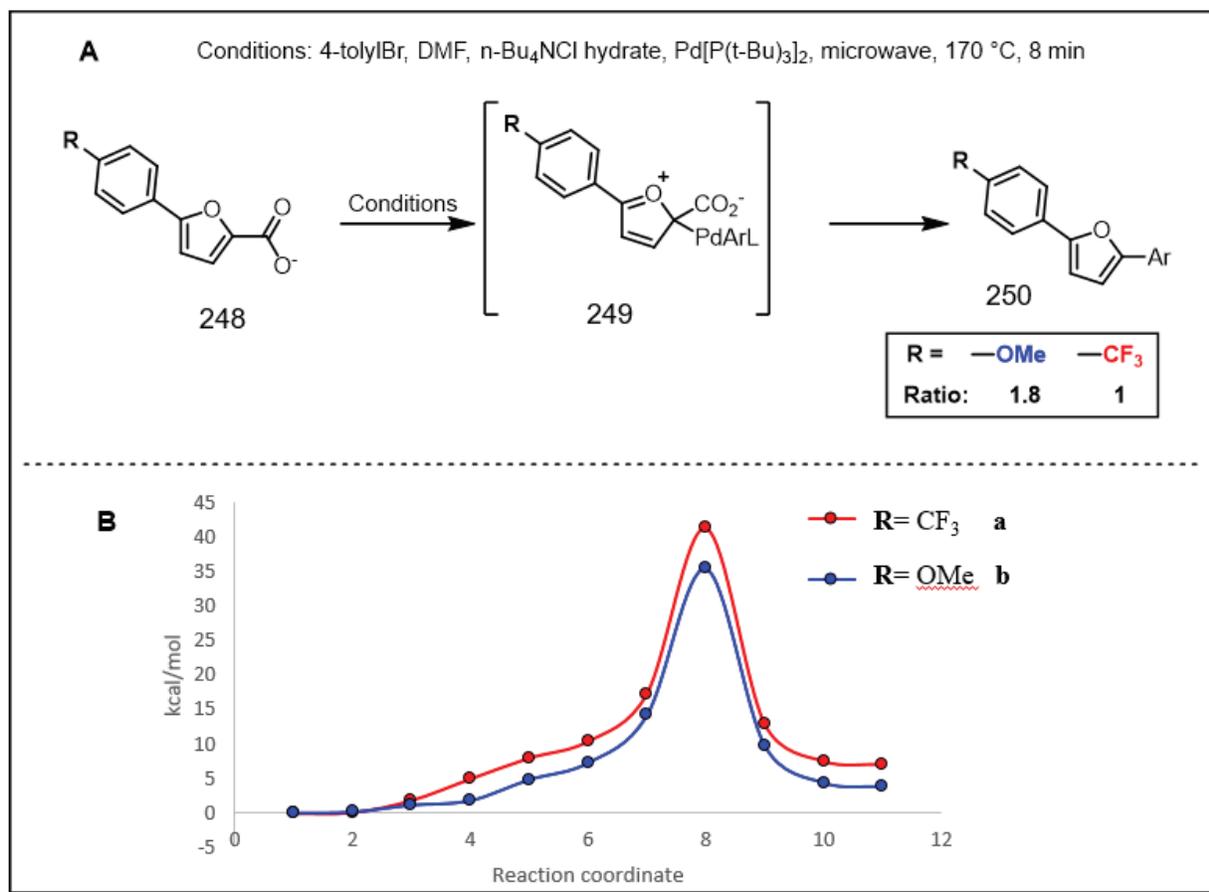
Figure 66 - (A) Competition between the Pd-catalyzed arylation of 5-arylfuran-2-carboxylic acid analogues (B) Energy profile for the decarboxylation of electron rich and poor 5-arylfuran-2-carboxylate

The energy barrier for –CF$_3$ (**248a**) and –OMe (**248b**) followed a similar trend to experimental data, with values of 41.4 kcal/mol and 35.5 kcal/mol respectively. The more electron rich substrate (**248b**) has a lower energy barrier due to the stabilization of the transition state (**249**). The inductive effect would have the opposite trend as it pulls electron density away from the furan ring, and therefore destabilizing the transition state.

3.5.1.7 CO$_2$ Direct extrusion versus an S$_E$Ar mechanism

Two possibilities were originally proposed for the mechanism for CO$_2$ extrusion in the heteroaromatic decarboxylative cross-coupling (**Figure 50**). While one of the proposed mechanisms involved the formation of the C-2 palladated intermediate that the transition state search found as described above, another mechanism was also proposed. A direct CO$_2$ extrusion involving a concerted decarboxylation where CO$_2$ is extruded simultaneously to the formation of the new C2-Pd bond. A computational model of this mechanism was created and the energies were determined *via* DFT (**Figure 67**). The transition state (**251**) activation energy 49.2 kcal/mol is greater than for the S$_E$Ar pathway (**Figure 54**, 40.8 kcal/mol) and based on these results is unlikely to be the minimal energy pathway.
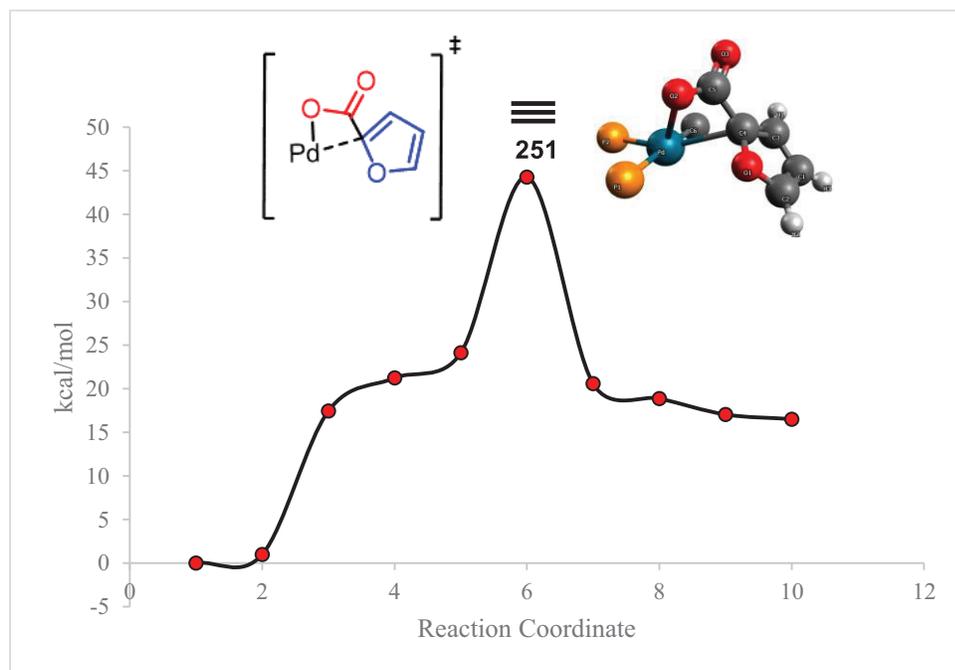
Figure 67 - Direct CO$_2$ extrusion energy profile for furan-2-carboxylate catalyzed by PdPh(PMe$_3$)$_2$ (Ligands not shown above for simplification)

3.6 Reductive Elimination

The last step in the catalytic cycle is the reductive elimination of the palladium (II) species (**235**) (**Figure 68**). This transformation proceeds *via* the transition state (**253**) with an activation energy of 10.2 kcal/mol. The biaryl heteroaromatic product (**254**) is released and the catalyst is regenerated (**225**). The reaction is exergonic by -17.4 kcal/mol. With a low energy barrier of 10.2 kcal/mol the transformation should proceed with ease under the reaction conditions.
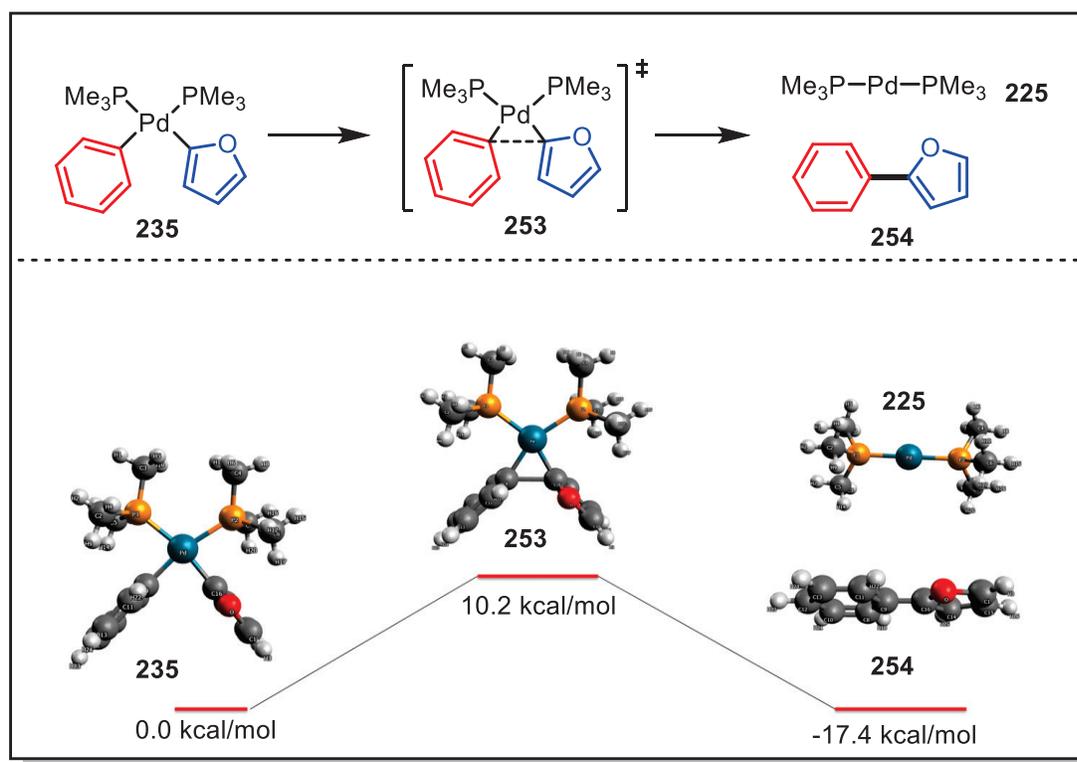
Figure 68 - Energy profile for the reductive elimination of **235**

3.7 Summary of the Catalytic Cycle

The geometries and energies for all starting materials, products and transition states were calculated for the decarboxylative cross-coupling of furan-2-carboxylic acid with bromobenzene in the presence of Pd(PMe$_3$)$_2$ (**Figure 69**).
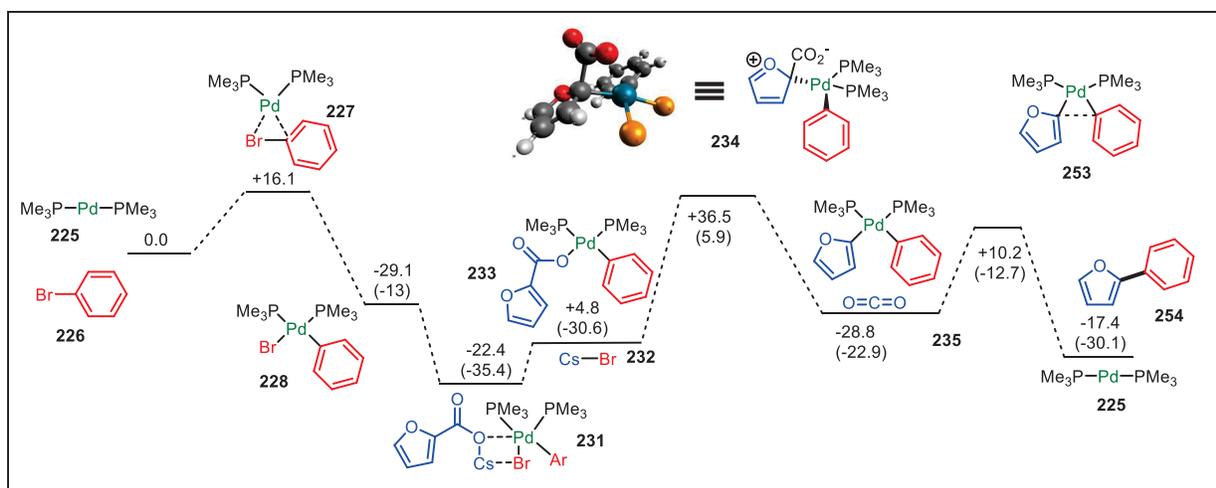
Figure 69 - Energy profile for the palladium-catalyzed heteroaromatic decarboxylation of furan-2-carboxylic acid and bromobenzene with Pd(PMe$_3$)$_2$

Furthermore, the more interesting decarboxylative mechanism was further investigated using a variety of different carboxylic acid substrates and the more experimentally relevant monocoordinated Pd(P(t-Bu$_3$)) complex. Among all the decarboxylative pathways investigated, the lowest energy pathway was found using 1-methyl-2-pyrrolecarboxylate (**239**) with the Pd(t-Bu)$_3$Ph complex with an activation energy of 31.5 kcal/mol, a value in accordance to other reported activation energies of similar transformations (**Figure 59**).

The calculations performed help support the S$_E$Ar mechanism initially proposed, and are complementary to experimental observations. Theoretical calculations on the decarboxylation of benzoic acid and furan-3-carboxylic acid show that the presence (**Figure 62**) and location (**Figure 65**) of the heteroatom is important for the decarboxylation to occur with a reasonable activation energy. Both compliment the experimentally observed lack of reactivity for these substrates under conditions that do not require a co-catalyst to facilitate decarboxylation. Furthermore, calculations support the observed increased reactivity for substrates with greater electron richness, supporting the S$_E$Ar mechanism where increasing the heteroaromatic nucleophilicity decreases the transition

state energy (**Figure 66**). The rate limiting step for the catalytic cycle was found to be the decarboxylation step (**Figure 69**). This implies that in order to further progress this reaction, development of the catalyst should aim to reduce the energy required for the decarboxylation step.

Chapter 4: Future Works and Conclusion

4.1 Desulfinative Cross-Coupling of Heteroaromatic Sulfinates with Aryl Triflates

4.1.1 – Conclusion and Summary

We were able to develop conditions that generate industrially interesting aryl-substituted heteroaromatic compounds using versatile aryl triflates as a coupling partners in alcoholic and aqueous media without the use of additives, base, or co-catalysts. The use of biodegradable ethanol as the solvent proved to be efficient by providing a range of heteroaromatic bi-aryls in moderate to excellent yields. This green solvent system yielded improved results over the H$_2$O/DMF mixture. This method provides an economical and green alternative to other available methods using aryl triflates for palladium-catalyzed cross-coupling reactions of heteroaromatic sulfinates with aryl triflates and has potential for further development.
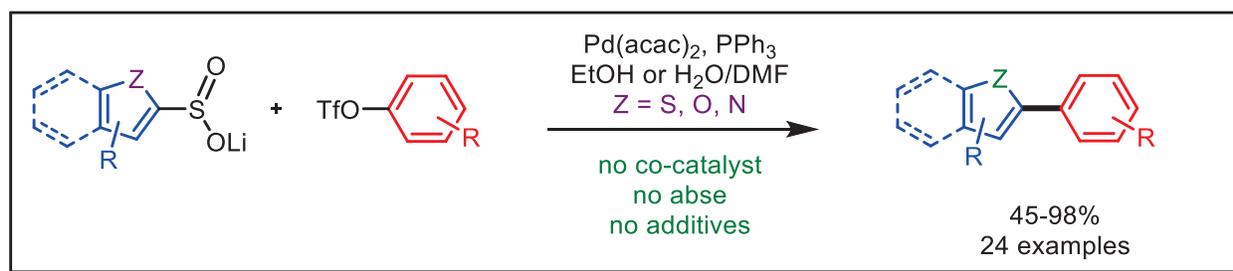
Figure 70 - Desulfinative cross-coupling of heteroaromatic sulfinates with aryl triflates in green solvents

4.1.2 – Future Work

Iodonium (III) compounds have been widely used in organic synthesis over the last few decades. These compounds have been particularly useful in palladium-catalyzed transformations. Their efficacy can be contributed to their ability to act as a strong electrophile as well as a powerful

oxidant. Therefore, we propose the application of hypervalent iodonium salts in the palladium-catalyzed heteroaromatics desulfinative cross-couplings.

Z = S, O, HC=N
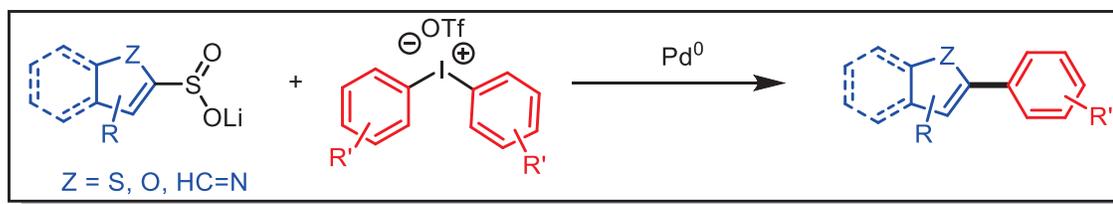
4.2 Towards the understanding of the palladium-catalyzed heteroaromatic cross-coupling reaction.

4.2.1 Conclusion and Summary

The full catalytic cycle for the palladium-catalyzed decarboxylative cross-coupling of heteroaromatics with aryl halides was investigated using DFT studies. The initial, transitional, and final states of all transformations in the catalytic system were evaluated for the cross-coupling of furan-2-carboxylic acid and bromobenzene catalyzed by $Pd(PMe_3)_2$. It was determined that the rate limiting step was the decarboxylation and the energy barrier for this transformation was dependent on the carboxylic acid substrate and ligand system. Furthermore, the decarboxylative transformation was investigated with a variety of carboxylic acids to improve our understanding of this mechanism. The decarboxylation is proposed to proceed *via* a S_EAr reaction, where the nucleophilic nature of the heteroaromatic coordinates with the palladium at the C2-position forming a transition state that can then undergo decarboxylation. The proposal was validated by comparing computational results with experimental data.

4.2.2 Future Work

The application of an implicit solvation package is useful for modeling the bulk of a solvent. However, it struggles at simulating individual interactions between the solvent and the system. For these types of interactions, an explicit model works best. In explicit solvation,

individual solvent molecules are added to the system to better explain these solvent-solute interactions. To better represent the interactions of our system with solvent, which has been shown to be critical for obtaining the cross-coupling product in high yield, an explicit solvation model will be applied.

We set out to validate the mechanism proposed by Forgione, where he rationalized the formation of a common side product, the 2,3-diarylated heteroaromatic. This pathway is currently being investigated *via* DFT methods. Furthermore, the modeling of the desulfinative cross-coupling of heteroaromatics is being investigated.

References

[1]   (A) A. S. Matharu, S. J. Cowling, G. Wright, *Liq. Cryst.* **2007**, *34*, 489-506; (B) Y. Cheng, B. K. Albrecht, J. Brown, J. L. Buchanan, W. H. Buckner, E. F. DiMauro, R. Emkey, R. T. Fremeau, Jr., J. C. Harmange, B. J. Hoffman, L. Huang, M. Huang, J. H. Lee, F. F. Lin, M. W. Martin, H. Q. Nguyen, V. F. Patel, S. A. Tomlinson, R. D. White, X. Xia, S. A. Hitchcock, *J. Med. Chem.* **2008**, *51*, 5019-5034; (C) D. J. Dale, P. J. Dunn, C. Golightly, M. L. Hughes, P. C. Levett, A. K. Pearce, P. M. Searle, G. Ward, A. S. Wood, *Organic Process Research & Development* **2000**, *4*, 17-22; (D) J. M. Brown, D. I. Hulmes, T. P. Layzell, *J. Chem. Soc., Chem. Commun.* **1993**, 1673-1674.

[2]   E. Vitaku, D. T. Smith, J. T. Njardarson, *J. Med. Chem.* **2014**, *57*, 10257-10274.

[3]   R. D. Taylor, M. MacCoss, A. D. Lawson, *J. Med. Chem.* **2014**, *57*, 5845-5859.

[4]   M. R. Kilbourn, *International journal of radiation applications and instrumentation. Part B, Nuclear medicine and biology* **1989**, *16*, 681-686.

[5]   J. T. Njaretharson, *Future Med Chem* **2012**, *4*, 951-954.

[6]   S. King, Forbes, **2013**.

[7]   J. S. Carey, D. Laffan, C. Thomson, M. T. Williams, *Organic & biomolecular chemistry* **2006**, *4*, 2337-2347.

[8]   The Nobel Foundation.

[9]   W. H. Wollaston, *Philosophical Transactions of the Royal Society of London* **1805**, *95*, 316-330.

[10]   J. Smidt, W. Hafner, R. Jira, J. Sedlmeier, R. Sieber, R. Rüttinger, H. Kojer, *Angew. Chem.* **1959**, *71*, 176-182.

[11]   R. Heck, *Synlett* **2006**, *2006*, 2855-2860.

[12]   R. F. Heck, *J. Am. Chem. Soc.* **1968**, *90*, 5518-5526.

[13]   K. Mori, T. Mizoroki, A. Ozaki, *Bull. Chem. Soc. Jpn.* **1973**, *46*, 1505-1508.

[14]   R. F. Heck, J. P. Nolley, *J. Org. Chem.* **1972**, *37*, 2320-2322.

[15]   R. J. P. Corriu, J. P. Masse, *J. Chem. Soc., Chem. Commun.* **1972**, 144a-144a.

[16]   (A) K. Tamao, Y. Kiso, K. Sumitani, M. Kumada, *J. Am. Chem. Soc.* **1972**, *94*, 9268-9269; (B) K. Tamao, K. Sumitani, M. Kumada, *J. Am. Chem. Soc.* **1972**, *94*, 4374-4376.

[17]   S. Murahashi, M. Yamamura, K. Yanagisawa, N. Mita, K. Kondo, *J. Org. Chem.* **1979**, *44*, 2408-2417.

[18]   K. S. K. Tamao, Y. Kiso, M. Zembayashi, A. Fujioka, S.-i. Kodama, I. Nakajima, A. Minato, M. Kumada, *Bull. Chem. Soc. Jpn.* **1976**, *49*, 1958-1969.

[19]   E.-i. Negishi, S. Baba, *J. Chem. Soc., Chem. Commun.* **1976**, 596b-597b.

[20]   E. Negishi, A. O. King, N. Okukado, *J. Org. Chem.* **1977**, *42*, 1821-1823.

[21]   E. Negishi, *Acc. Chem. Res.* **1982**, *15*, 340-348.

[22]   D. Azarian, S. S. Dua, C. Eaborn, D. R. M. Walton, *J. Organomet. Chem.* **1976**, *117*, C55-C57.

[23]   D. Milstein, J. K. Stille, *J. Am. Chem. Soc.* **1978**, *100*, 3636-3638.

[24]   M. Kosugi, K. Fugami, **2002**, 263-283.

[25]   Z. Wang, in *Comprehensive Organic Name Reactions and Reagents*, John Wiley & Sons, Inc., **2010**.

[26]   N. Miyaura, A. Suzuki, *J. Chem. Soc., Chem. Commun.* **1979**, 866.
[27]   S. Kotha, K. Lahiri, D. Kashinath, *Tetrahedron* **2002**, *58*, 9633-9695.
[28]   A. Suzuki, **2001**, *783*, 80-93.
[29]   B. Trost, *Science* **1991**, *254*, 1471-1477.
[30]   P. T. A. a. J. C. Warner, *Green Chemistry: Theory and Practice*, Oxford University Press, New York, **1998**.
[31]   J. H. Li, Y. Liang, D. P. Wang, W. J. Liu, Y. X. Xie, D. L. Yin, *J. Org. Chem.* **2005**, *70*, 2832-2834.
[32]   A. W. Kruger, M. J. Rozema, A. Chu-Kung, J. Gandarilla, A. R. Haight, B. J. Kotecki, S. M. Richter, A. M. Schwartz, Z. Wang, *Organic Process Research & Development* **2009**, *13*, 1419-1425.
[33]   C. Barckholtz, T. A. Barckholtz, C. M. Hadad, *J. Am. Chem. Soc.* **1999**, *121*, 491-500.
[34]   G. P. McGlacken, L. M. Bateman, *Chem. Soc. Rev.* **2009**, *38*, 2447-2464.
[35]   J. Wencel-Delord, T. Droge, F. Liu, F. Glorius, *Chem. Soc. Rev.* **2011**, *40*, 4740-4761.
[36]   (A) B. Glover, K. A. Harvey, B. Liu, M. J. Sharp, M. F. Tymoschenko, *Org. Lett.* **2003**, *5*, 301-304; (B) W. Li, D. P. Nelson, M. S. Jensen, R. S. Hoerrner, G. J. Javadi, D. Cai, R. D. Larsen, *Org. Lett.* **2003**, *5*, 4835-4837; (C) C. C. Hughes, D. Trauner, *Angew. Chem. Int. Ed. Engl.* **2002**, *41*, 1569-1572.
[37]   (A) C.-H. Park, V. Ryabova, I. V. Seregin, A. W. Sromek, V. Gevorgyan, *Org. Lett.* **2004**, *6*, 1159-1162; (B) I. V. Seregin, V. Gevorgyan, *Chem. Soc. Rev.* **2007**, *36*, 1173-1193.
[38]   C. C. Price, **2011**, 1-82.
[39]   T. Weskamp, V. P. W. Böhm, W. A. Herrmann, *J. Organomet. Chem.* **1999**, *585*, 348-352.
[40]   H. A. Benesi, J. H. Hildebrand, *J. Am. Chem. Soc.* **1949**, *71*, 2703-2707.
[41]   J. J. Dong, H. Doucet, *Eur. J. Org. Chem.* **2010**, *2010*, 611-615.
[42]   C. Colletto, S. Islam, F. Julia-Hernandez, I. Larrosa, *J. Am. Chem. Soc.* **2016**, *138*, 1677-1683.
[43]   (A) M. Parisien, D. Valette, K. Fagnou, *J. Org. Chem.* **2005**, *70*, 7578-7584; (B) J. P. Leclerc, K. Fagnou, *Angew. Chem. Int. Ed. Engl.* **2006**, *45*, 7781-7786; (C) M. Lafrance, C. N. Rowley, T. K. Woo, K. Fagnou, *J. Am. Chem. Soc.* **2006**, *128*, 8754-8756.
[44]   V. G. Zaitsev, O. Daugulis, *J. Am. Chem. Soc.* **2005**, *127*, 4156-4157.
[45]   D. García-Cuadrado, A. A. C. Braga, F. Maseras, A. M. Echavarren, *J. Am. Chem. Soc.* **2006**, *128*, 1066-1067.
[46]   S. I. Gorelsky, D. Lapointe, K. Fagnou, *J. Am. Chem. Soc.* **2008**, *130*, 10848-10849.
[47]   P. Forgione, M. C. Brochu, M. St-Onge, K. H. Thesen, M. D. Bailey, F. Bilodeau, *J. Am. Chem. Soc.* **2006**, *128*, 11350-11351.
[48]   N. Rodriguez, L. J. Goossen, *Chem. Soc. Rev.* **2011**, *40*, 5030-5048.
[49]   D. Tanaka, S. P. Romeril, A. G. Myers, *J. Am. Chem. Soc.* **2005**, *127*, 10323-10333.
[50]   L. J. Goossen, G. Deng, L. M. Levy, *Science* **2006**, *313*, 662-664.
[51]   L. J. Goossen, N. Rodriguez, B. Melzer, C. Linder, G. Deng, L. M. Levy, *J. Am. Chem. Soc.* **2007**, *129*, 4824-4833.
[52]   L. J. Goossen, N. Rodríguez, C. Linder, *J. Am. Chem. Soc.* **2008**, *130*, 15248-15249.
[53]   A. Fromm, C. van Wullen, D. Hackenberger, L. J. Goossen, *Journal of American Chemical Society* **2014**, *136*, 10007-10023.
[54]   F. Bilodeau, M. C. Brochu, N. Guimond, K. H. Thesen, P. Forgione, *J. Org. Chem.* **2010**, *75*, 1550-1560.
[55]   D. H. Ortgies, A. Hassanpour, F. Chen, S. Woo, P. Forgione, *Eur. J. Org. Chem.* **2016**, *2016*,

408-425.

[56]   G. n. Vitzthum, E. Lindner, *Angewandte Chemie International Edition in English* **1971**, *10*, 315-326.

[57]   B. Chiswell, L. M. Venanzi, *Journal of the Chemical Society A: Inorganic, Physical, Theoretical* **1966**, 1246-1248.

[58]   (A) K. Garves, *J. Org. Chem.* **1970**, *35*, 3273-3275; (B) R. Selke, W. Thiele, *Diarylbildung und Arylierung von Olefinen durch Reakionen von Arylsulfinaten und Palladiumsalzen, Vol. 313*, **1971**.

[59]   (A) R. Chen, S. Liu, X. Liu, L. Yang, G.-J. Deng, *Organic & Biomolecular Chemistry* **2011**, *9*, 7675-7679; (B) X. Zhou, J. Luo, J. Liu, S. Peng, G.-J. Deng, *Org. Lett.* **2011**, *13*, 1432-1435; (C) M. Wu, J. Luo, F. Xiao, S. Zhang, G.-J. Deng, H.-A. Luo, *Adv. Synth. Catal.* **2012**, *354*, 335-340.

[60]   Y. Hatanaka, T. Hiyama, *J. Org. Chem.* **1988**, *53*, 918-920.

[61]   K. Cheng, S. Hu, B. Zhao, X.-M. Zhang, C. Qi, *J. Org. Chem.* **2013**, *78*, 5022-5025.

[62]   T. O. K. Sato, *Vol. 5159082 A*, US, **1992**.

[63]   C. Zhou, Q. Liu, Y. Li, R. Zhang, X. Fu, C. Duan, *J. Org. Chem.* **2012**, *77*, 10468-10472.

[64]   D. H. Ortgies, A. Barthelme, S. Aly, B. Desharnais, S. Rioux, P. Forgione, *Synthesis* **2013**, *45*, 694-702.

[65]   D. H. Ortgies, P. Forgione, *Synlett* **2013**, *24*, 1715-1721.

[66]   S. Sévigny, P. Forgione, *Chemistry – A European Journal* **2013**, *19*, 2256-2260.

[67]   S. Sevigny, P. Forgione, *New J. Chem.* **2013**, *37*, 589-592.

[68]   (A) E. Bey, S. Marchais-Oberwinkler, M. Negri, P. Kruchten, A. Oster, T. Klein, A. Spadaro, R. Werth, M. Frotscher, B. Birk, R. W. Hartmann, *J. Med. Chem.* **2009**, *52*, 6724; (B) N. W. Y. Wong, P. Forgione, *Org. Lett.* **2012**, *14*, 2738.

[69]   S. Nakamura, K. Mitsuyoshi, K. Goto, M. Nakamura, Y. Tsuda, K. Shishido, *Heterocycles* **1996**, *43*, 2747.

[70]   (A) J. Ohshita, S. Kangai, Y. Tada, H. Yoshida, K. Sakamaki, A. Kunai, Y. Kunugi, *J. Organomet. Chem.* **2007**, *692*, 1020; (B) J. Ohshita, S. Kangai, H. Yoshida, A. Kunai, S. Kajiwara, Y. Ooyama, Y. Harima, *J. Organomet. Chem.* **2007**, *692*, 801; (C) T. Beryozkina, V. Senkovskyy, E. Kaul, A. Kiriy, *Macromolecules* **2008**, *41*, 7817; (D) D. J. Schipper, K. Fagnou, *Chem. Mater.* **2011**, *23*, 1594; (E) J. H. Seo, E. B. Namdas, A. Gutacker, A. J. Heeger, G. C. Bazan, *Adv. Funct. Mater.* **2011**, *21*, 3667; (F) Fan Zhang, D. Wu, Y. Xua, X. Feng, *J. Mater. Chem* **2011**, *21*, 17950; (G) K. Beydoun, J. Boixel, V. Guerchais, H. Doucet, *Catal. Sci. Technol.* **2012**, *2*, 1242; (H) R. J. Ono, S. Kang, C. W. Bielawski, *Macromolecules* **2012**, *45*, 2321.

[71]   M. E. Matheron, M. Porchas, *Plant. Dis.* **2004**, *88*, 665.

[72]   (A) L. J. Gooßen, G. Deng, L. M. Levy, *Science* **2006**, *313*, 662; (B) J.-M. Becht, C. L. Drian, *Org. Lett.* **2008**, *10*, 3161; (C) F. Bilodeau, M.-C. Brochu, N. Guimond, K. H. Thesen, P. Forgione, *J. Org. Chem.* **2009**, *75*, 1550.

[73]   (A) D. Alberico, M. E. Scott, M. Lautens, *Chemical Revue* **2007**, *107*, 174; (B) Y. Li, J. Wang, M. Huang, Z. Wang, Y. Wu, Y. Wu, *J. Org. Chem.* **2014**, *79*, 2890.

[74]   S. J. Smith, J. V. Aardenne, Z. Klimont, R. J. Andres, A. Volke, S. D. Arias, *Atmos. Chem. Phys.* **2011**, *11*, 1101.

[75]   (A) K. Garves, *J. Org. Chem.* **1970**, *35*, 3273; (B) G. Vitzthum, E. Lindnerl, *Angew. Chem. Int. Ed.* **1971**, *10*, 315; (C) V. R. Selke, W. Thiele, *J. Prakt. Chem.* **1971**, *313*, 875; (D) K. Sato, T. Okoshi, *Patent US5159082* **1992**.

[76]   (A) J. Colomb, T. Billard, *Tetrahedron Lett.* **2013**, *54*, 1471; (B) C. Zhou, Y. Li, Y. Lu, R. Zhang, K. Jin, X. Fu, C. Duan, *Chin. J. Chem.* **2013**, *31*, 1269; (C) A. Barthelme, S. Aly, B. Desharnais, S. Rioux, P. Forgione, *Synthesis* **2013**, *45*, 694.

[77]   (A) S. Sévigny, P. Forgione, *New J. Chem.* **2013**, *37*, 589; (B) S. Sévigny, P. Forgione, *Chem. Eur. J.* **2013**, *19*, 2256.

[78]   C. Zhou, Q. Liu, Y. Li, R. Zhang, X. Fu, C. Duan, *J. Org. Chem.* **2012**, *77*, 10468−10472.

[79]   (A) G. W. Kabalka, L.-L. Zhou, A. Naravane, *Tetrahedron Lett.* **2006**, *47*, 6887; (B) J. Roger, H. Doucet, *Org. Biomol. Chem.* **2007**, *6*, 169–174.

[80]   (A) C. G. Blettner, W. A. König, W. Stenzel, T. Schotten, *J. Org. Chem.* **1999**, *64*, 3885; (B) C. Rabeyrin, D. Sinou, *J. Mol. Catal. A: Chem.* **2004**, *215*, 89.

[81]   D. A. Devi, B. Smitha, S. Sridhar, T. M. Aminabhavi, *Sep. Purif. Technol.* **2006**, *51*, 104.

[82]   C. Capello, U. Fischer, K. Hungerbühler, *Green Chem.* **2007**, *9*, 927.

[83]   (A) T. Chmielniak, M. Sciazko, *Applied Energy* **2003**, *74*, 393; (B) D. Pimentel, T. W. Patzek, *Natural Resources Research* **2005**, *14*, 65.

[84]   (A) D. S. Bose, L. Fatima, H. B. Mereyala, *J. Org. Chem.* **2003**, *68*, 587; (B) A. Laitinen, Y. Takebayashi, I. Kylänlahti, J. Yli-Kauhaluoma, T. Sugetab, K. Otakeb, *Green Chem.* **2004**, *6*, 49.

[85]   (A) G. W. Kabalka, E. Dadusha, M. Al-Masum, *Tetrahedron Lett.* **2006**, *47*, 7459; (B) J.-W. Wang, F.-H. Meng, L.-F. Zhang, *Organometallics* **2009**, *28*, 2334; (C) W. Ren, J. Li, D. Zou, Y. Wu, Y. Wu, *Tetrahedron* **2012**, *68*, 1351; (D) X. Le, Z. Dong, Z. Jin, Q. Wang, J. Ma, *Catal. Commun.* **2014**, *53*, 47.

[86]   (A) M. Nilsson, E. Kulonen, S. Sunner, V. Frank, J. Brunvoll, E. Bunnenberg, C. Djerassi, R. Records, *Acta Chem. Scand.* **1966**, *20*, 423-426; (B) M. Nilsson, C. Ullenius, U.-Å. Blom, N. A. Zaidi, *Acta Chem. Scand.* **1968**, *22*, 1998-2002; (C) J. Chodowska-Palicka, M. Nilsson, S. Liaaen-Jensen, S. E. Rasmussen, A. Shimizu, *Acta Chem. Scand.* **1970**, *24*, 3353-3361; (D) I. Shimizu, T. Yamada, J. Tsuji, *Tetrahedron Lett.* **1980**, *21*, 3199-3202; (E) J. Tsuji, T. Yamada, I. Minami, M. Yuhara, M. Nisar, I. Shimizu, *J. Org. Chem.* **1987**, *52*, 2988-2995; (F) A. G. Myers, D. Tanaka, M. R. Mannion, *J. Am. Chem. Soc.* **2002**, *124*, 11250-11251.

[87]   O. Baudoin, *Angew. Chem. Int. Ed. Engl.* **2007**, *46*, 1373-1375.

[88]   T. Cohen, R. A. Schambach, *J. Am. Chem. Soc.* **1970**, *92*, 3189-3190.

[89]   R. Shang, Y. Fu, Y. Wang, Q. Xu, H. Z. Yu, L. Liu, *Angew. Chem. Int. Ed. Engl.* **2009**, *48*, 9350-9354.

[90]   (A) R. Shang, Y. Fu, J.-B. Li, S.-L. Zhang, Q.-X. Guo, L. Liu, *J. Am. Chem. Soc.* **2009**, *131*, 5738-5739; (B) S.-L. Zhang, Y. Fu, R. Shang, Q.-X. Guo, L. Liu, *J. Am. Chem. Soc.* **2010**, *132*, 638-646.

[91]   R. Shang, Q. Xu, Y. Y. Jiang, Y. Wang, L. Liu, *Org. Lett.* **2010**, *12*, 1000-1003.

[92]   L. J. Goossen, D. Koley, H. L. Hermann, W. Thiel, *Organometallics* **2005**, *24*, 2398-2410.

[93]   D. Tanaka, S. P. Romeril, A. G. Myers, *J. Am. Chem. Soc.* **2005**, *127*, 10323-10333.

[94]   M. Perez-Rodriguez, A. A. Braga, M. Garcia-Melchor, M. H. Perez-Temprano, J. A. Casares, G. Ujaque, A. R. de Lera, R. Alvarez, F. Maseras, P. Espinet, *J. Am. Chem. Soc.* **2009**, *131*, 3650-3657.

[95]   V. Blum, R. Gehrke, F. Hanke, P. Havu, V. Havu, X. Ren, K. Reuter, M. Scheffler, *Comput. Phys. Commun.* **2009**, *180*, 2175-2196.

[96]   R. Shang, Y. Fu, J. B. Li, S. L. Zhang, Q. X. Guo, L. Liu, *J. Am. Chem. Soc.* **2009**, *131*, 5738-5739.

[97]   U. Christmann, R. Vilar, *Angew. Chem. Int. Ed. Engl.* **2005**, *44*, 366-374.
[98]   M. Jödecke, Á. Pérez-Salado Kamps, G. Maurer, *Journal of Chemical & Engineering Data* **2012**, *57*, 1249-1266.
[99]   P. Linda, G. Marino, *Chemical Communications (London)* **1967**, 499.
[100]   G. Marino, *Tetrahedron* **1965**, *21*, 843-848.